Metagenomic and Metatranscriptomic Insights into Wetland Plant-Microbe Interactions and Dark CO_2 Fixation

Dissertation

With the aim of achieving the degree of

Doctor rerum naturalium (Dr. rer. nat.)

At the Department of Microbiology and Biotechnology

Subdivision at the Faculty of Mathematics, Informatics and Natural Science

of the University of Hamburg

Submitted by

Clara Luise Grüterich

Hamburg, 2024

Contributions to the quoted articles

Chapter 2: "Assessing environmental gradients in relation to dark CO_2 fixation in estuarine wetland microbiomes"

L. Grüterich designed the study and conducted all field and laboratory work, including DNA and RNA isolation, plate reader assays, and physicochemical measurements of soil properties. L. Grüterich analyzed the metagenomic and metatranscriptomic data following bioinformatic processing. J. Woodhouse assisted with the bioinformatic analyses. L. Grüterich wrote the initial manuscript.

Chapter 3: "Transcriptomic response of wetland microbes to root influence"

L. Grüterich designed the sampling for microbial analyses and performed DNA and RNA isolation and preparation for metagenomic and metatranscriptomic sequencing. L. Grüterich analyzed all data following bioinformatic processing. M. Wilson contributed equally to the manuscript by conducting lab work, contributing to data visualization, and sharing the writing of the initial manuscript with L. Grüterich.

Chapter 4: "Litter decomposition and prokaryotic decomposer communities along estuarine gradients"

L. Grüterich designed the microbial analysis and performed DNA isolation and preparation for metagenomic sequencing. L. Grüterich conducted 16S amplicon analyses by processing raw sequencing reads bioinformatically, and visualizing and interpreting the results. L. Grüterich wrote the initial methods and results sections of the microbial community analyses and contributed to the writing and editing other parts of the manuscript.

Minor changes were made to the manuscripts in order to integrate them stylistically into this thesis.

Hamburg, 20.09.2024

Clara Luise Grüterich (PhD candidate)

Prof. Dr. Wolfgang R. Streit (Supervisor)

Erstgutachter: Prof. Dr. Wolfgang R. Streit

Zweitgutachter: Prof. Dr. Hans-Peter Grossart

Tag der Disputation: 06.12.2024

Contents

Summary

Estuarine tidal wetlands have exceptional carbon sequestration rates that far exceed those of most other terrestrial and aquatic ecosystem types. They form interfaces between aquatic and terrestrial environments, leading to steep environmental gradients and coupling between these systems, making them ideal for studying the abiotic and biotic factors controlling microbial carbon dynamics. This dissertation consists of five chapters, three of which are manuscripts. At the time of publication of this dissertation, chapter 2 is published at Applied and Environmental Microbiology, chapter 3 is published at iScience and chapter 4 is in revision at Soil Biology and Biochemistry.

Chapter 1 provides an overview of the biogeochemistry and microbial ecology of estuarine wetlands, highlighting their role as dynamic ecosystems critical to carbon cycling. It provides insights into characteristic microbial groups and metabolic pathways, redox gradients and plant-microbe interactions, with a particular emphasis on dark CO_2 fixation pathways.

Chapter 2 focuses on the microbial dark CO_2 fixation processes in tidal wetlands along the Elbe estuary. The study shows that the microbiome of these wetlands possesses four major CO_2 fixation pathways: the Calvin cycle (operated by sulfur oxidizing chemoautotrophic microorganisms), the reverse tricarboxylic acid cycle (rTCA cycle), the Wood-Ljungdahl pathway (WLP) and the reverse glycine pathway. The presence and transcription of these pathways are strongly influenced by environmental factors such as nitrate and oxygen availability, and soil organic matter content. The biotechnological application of CO_2 fixation relies on the knowledge we can gain from these natural environments. Targeted screening of the environmental factors promoting CO_2-fixing microbes is a critical first step for lab-based downstream analyses and modifications in order to optimize microbial CO_2 uptake efficiency. Understanding the optimal environmental conditions for these metabolic pathways can also refine cultivation practices. For example, the results of this study show that high levels of organic matter are associated with increased Calvin cycle activity, that the rTCA cycle predominates in high nitrate niches, and that the WLP thrives under highly reduced conditions. This study further identifies specific bacterial phyla, namely Desulfobacterota, Methylomirabilota, Nitrospirota, Chloroflexota and Pseudomonadota, as major players of dark CO_2 fixation.

Chapter 3 investigates the interactions between plants and soil microbes, focusing on the transcriptomic responses of soil microbes to root exudates. Combining $^{13}CO_2$ pulse labeling and metatranscriptomic sequencing in a novel methodological approach, 399 microbial genes with differential expression in response to root exudate influence are identified. Metabolic

pathways related to infection, stress response and motility show the strongest upregulation in response to root exudate influence. The study shows shifts in the active microbial community, highlighting the impact of root exudates on microbial gene regulation and shifts in the active community in tidal wetlands. Although environmental gradients were investigated on a much smaller spatial scale compared to the landscape-scale estuarine gradients of chapter 2, the biochemical gradients forming around plant roots, resulted in microbial transcriptomic responses that were not necessarily weaker.

Chapter 4 focuses on the drivers of plant litter decomposition in estuarine tidal wetlands. The results show that increased salinity led to a higher stabilization of the litter, while flooding reduced its stabilization. The study further demonstrates that both estuarine abiotic gradients and the composition of litter influence the diversity and structure of microbial communities. The observed decrease in microbial diversity from soil via native litter to standardized tea litter indicates that different substrates support distinct microbial communities. The significant overlap between the microbial communities in soil and native litter suggests that soil microbes are well-adapted to the local vegetation.

Chapter 5 summarizes the findings of the previous chapters, emphasizing key concepts such as large-scale and small-scale environmental gradients, carbon cycling processes and microbial community composition, by relating and combining the results from the different studies. It also identifies possible directions for future research.

Zusammenfassung

Ästuarine Feuchtgebiete weisen außergewöhnliche Kohlenstoffspeicherraten auf, die weit über denen der meisten anderen terrestrischen und aquatischen Ökosystemtypen liegen. Sie bilden Schnittstellen zwischen aquatischer und terrestrischer Umwelt, was zu steilen Umweltgradienten und einer Kopplung zwischen diesen Systemen führt. Ästuarine Feuchtgebiete eignen sich daher ideal zur Untersuchung der mikrobiologischen Grundlagen des Kohlenstoffkreislaufs sowie von dessen abiotischen und biotischen Steuerungsfaktoren. Diese Dissertation besteht aus fünf Kapiteln, von denen drei Manuskripte sind. Zum Zeitpunkt der Veröffentlichung dieser Dissertation ist Kapitel 2 bei Applied and Environmental Microbiology und Kapitel 3 bei iScience publiziert. Kapitel 4 ist bei Soil Biology and Biochemistry unter Begutachtung.

Kapitel 1 gibt eine Einführung in die Biogeochemie und mikrobielle Ökologie ästuariner Feuchtgebiete als dynamische Ökosysteme mit einer Schlüsselrolle im Kohlenstoffkreislauf. Es bietet Einblicke in charakteristische mikrobielle Gruppen und Stoffwechselwege, Redox-Gradienten und Pflanze-Mikroben-Interkationen. Ein Schwerpunkt der Betrachtungen liegt dabei auf der lichtunabhängigen CO_2-Fixierung.

Kapitel 2 befasst sich mit den mikrobiellen Prozessen der lichtunabhängigen CO_2-Fixierung in tidebeeinflussten Feuchtgebieten entlang des Elbeästuars. Die Studie zeigt, dass das Mikrobiom dieser Feuchtgebiete über vier wichtige CO_2-Fixierungswege verfügt: den Calvin-Zyklus (betrieben von schwefeloxidierenden chemoautotrophen Mikroorganismen), den reduktiven Tricarbonsäurezyklus, den Wood-Ljungdahl-Weg und den reduktiven Glycin-Weg. Die Anwesenheit und Aktivität dieser Stoffwechselwege werden durch Umweltfaktoren wie Sauerstoff- und Nitratverfügbarkeit sowie den Gehalt an organischem Material im Boden beeinflusst. Für biotechnologische Anwendungen im Bereich der CO_2-Fixierung ist es vorteilhaft, wenn nicht sogar entscheidend, dieses Wissen über Umweltprozesse zu nutzen. Es ermöglicht ein gezieltes Screening von CO_2-fixierenden Mikroorganismen in der Natur, um sie im Labor weiter zu untersuchen oder zu modifizieren (z. B. zur Optimierung ihrer Effizienz bei der CO_2-Aufnahme). Das Verständnis der optimalen Umweltbedingungen für diese Stoffwechselwege kann dabei helfen, die Kultivierungsbedingungen gezielt zu verbessern. Die Ergebnisse der Studie zeigen beispielsweise, dass ein hoher Gehalt an organischem Material mit einer erhöhten Aktivität des Calvin-Zyklus einhergeht, dass der reduktive Tricarbonsäurezyklus in Nischen mit hohem Nitratgehalt vorkommt und, dass der Wood-Ljungdahl-Weg unter stark reduzierten Bedingungen dominiert. Die Studie identifiziert zudem

mehrere Bakteriengruppen als Hauptakteure der lichtunabhängigen CO_2-Fixierung identifiziert, nämlich Desulfobacterota, Methylomirabilota, Nitrospirota, Chloroflexota und Pseudomonadota.

In **Kapitel 3** werden die Wechselwirkungen zwischen Pflanzen und Bodenmikroben in tidebeeinflussten Feuchtgebieten untersucht, wobei der Schwerpunkt auf den transkriptomischen Reaktionen der Bodenmikroben auf Wurzelexsudate liegt. Unter Verwendung von $^{13}CO_2$-Pulsmarkierung und metatranskriptomischen Ansätzen wurden 399 mikrobielle Gene mit differenzieller Expression als Reaktion auf den Einfluss von Wurzelexsudaten identifiziert.

Stoffwechselwege, die mit Infektion, Stressreaktion und Motilität verbunden sind, zeigten die stärkste Hochregulierung als Reaktion auf Wurzelexsudate. Die Studie offenbart Verschiebungen in der aktiven mikrobiellen Gemeinschaft infolge von Wurzelexsudateintrag und unterstreicht dessen Einfluss auf die mikrobielle Genregulation in Feuchtgebieten. Obwohl die betrachteten Umweltgradienten auf einer wesentlich kleineren räumlichen Skala untersucht wurden als die in Kapitel 2 analysierten Gradienten entlang des gesamten Ästuars, waren die Effekte der biochemischen Gradienten um die Pflanzenwurzeln auf transkriptomische Reaktionen nicht weniger ausgeprägt.

Kapitel 4 befasst sich mit der biotischen und abiotischen Kontrolle der Pflanzenstreuzersetzung in ästuarinen Feuchtgebieten. Die Studie zeigt, dass ein erhöhter Salzgehalt zu einer stärkeren Stabilisierung der Streu führte, während Überschwemmungen ihre Stabilisierung verringerten. Die Studie zeigt außerdem, dass sowohl abiotische Umweltgradienten im Ästuar als auch die Zusammensetzung der Streu die Diversität und Zusammensetzung der mikrobiellen Gemeinschaften beeinflussen. Die beobachtete Abnahme der mikrobiellen Diversität von Boden über die native Streu bis hin zur standardisierten Teestreu zeigt, dass verschiedene Streusubstrate unterschiedliche mikrobielle Gemeinschaften hervorbringen. Die starke Überschneidung der mikrobiellen Gemeinschaften des Bodens und der nativen Streu deutet darauf hin, dass die Bodenmikroben stark an die lokale Vegetation angepasst sind.

Kapitel 5 fasst die Ergebnisse der vorangegangenen Kapitel zusammen und hebt Schlüsselkonzepte wie groß- und kleinskalige Umweltgradienten, Kohlenstoffkreislaufprozesse und die Zusammensetzung mikrobieller Gemeinschaften hervor, indem es die Ergebnisse der verschiedenen Studien in vergleicht und kombiniert. Schließlich werden weiterführende Forschungsperspektiven aufgezeigt.

Chapter 1

General Introduction

Tidal wetlands are dynamic, highly productive ecosystems located at the interface between terrestrial and marine environments (Bianchi, 2007). Tidal wetlands can be divided into tidal marshes and mangroves. Depending on their salinity, tidal marshes can be further subdivided into salt marshes, brackish marshes and freshwater marshes. These ecosystems play an important role in carbon and nutrient cycling and are not only hotspots for biodiversity and microbial turnover but also vital carbon sinks (Mcleod et al., 2011). They can help mitigate climate change by capturing CO_2 from the atmosphere and converting it into organic matter that gets further metabolized and ultimately preserved within the soil systems (Duarte et al., 2013).

Analyses of carbon budgets of marine vegetated benthic communities imply that they contribute significantly to carbon dynamics by exporting large amounts of organic carbon to adjacent ecosystems and accumulating vast quantities of it within their own soils and sediments (Brevik & Homburg, 2004; Chmura et al., 2003; Duarte & Cebrián, 1996; Jennerjahn & Ittekkot, 2002). Their high carbon burial rates can be maintained for thousands of years (Brevik & Homburg, 2004; Mateo et al., 2003). While carbon turnover within the biomass pool can occur quickly, with an average residence time of nine years in plant biomass across various biomes (Schlesinger, 1997), soils and sediments possess the potential to store carbon for hundreds to thousands of years (Duarte et al., 2005; Limpens et al., 2008). Salt marshes exhibit one of the highest average rates of long-term carbon sequestration in soils on an area basis, at 218 ± 24 g C m^{-2} yr^{-1} (about 48 times greater compared to terrestrial forest), which makes them one of the most effective carbon sinks of the biosphere (Figure 1; Duarte et al., 2005; Mcleod et al., 2011). Further, estuarine wetlands connect marine and terrestrial ecosystems, leading to

steep environmental gradients in oxygen levels, organic matter availability and salinity (Chapter 3, Table 2) among other environmental drivers.

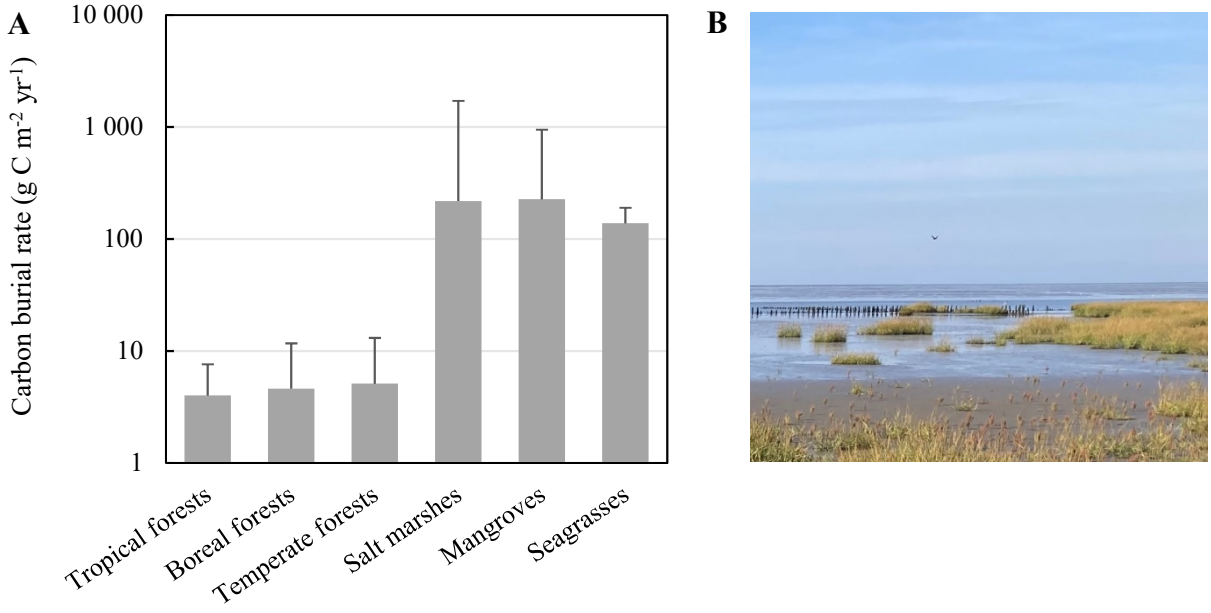

Figure 1. Panel **A** Data from (Mcleod et al., 2011) shows the mean long-term rates of C sequestration (g C m^{-2} yr^{-1}) in soils of upland forests and vegetated coastal ecosystems. Error bars indicate maximum rates of accumulation. Note the logarithmic scale of the y axis. Panel **B** shows a salt marsh pioneer zone of the Elbe estuary.

I conducted the work for my dissertation within the framework of the DFG Research Training Group 2530 (RTG2530) "Biota-mediated effects on carbon cycling in estuaries". The RTG2530 investigates the impact of biota on carbon cycling along the Elbe estuary in NW Germany through ecological, biogeochemical and molecular biological approaches and is structured into three research themes. Theme A deals with rhizosphere processes and effects of herbivory, theme B investigates the phycosphere processes and effects of trophic interactions and theme C looks at biota-mediated carbon fluxes across marsh-water boundaries (Figure 2).

Within the RTG2530, my project (A2) focused on the community composition and key metabolic pathways of microbes within the rhizosphere and along large-scale estuarine gradients. Closest collaboration was with projects A1 (Monica Wilson; Chapter 3 and 4), where interactions between plant roots and microbes were investigated, and C2 (Friederike Neiske; Chapter 4), where the focus lied on the interactions between plant litter and the associated microbial communities.

Sampling stations have been installed at three marsh sites along the estuary's salinity gradient, namely, a salt marsh, a brackish marsh and a freshwater marsh. At each of the sites, permanent

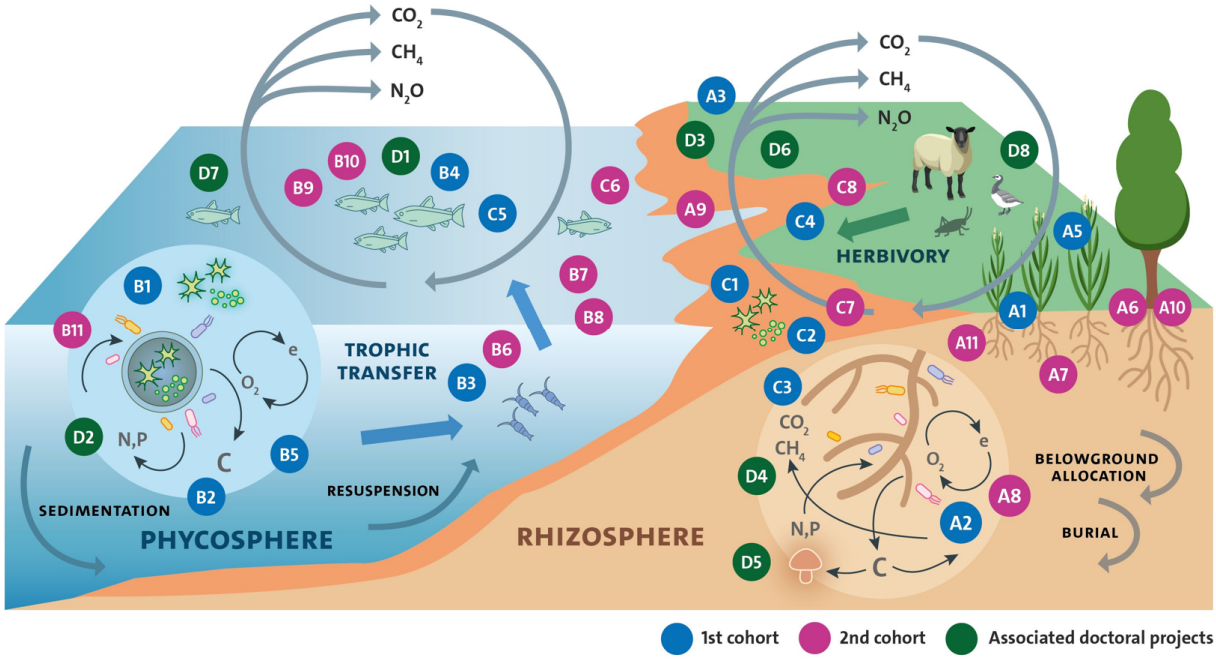

Figure 2. Conceptual overview of research themes and doctoral projects of the RTG2530. Depicted are all doctoral projects of the 1st (blue) and 2nd (pink) cohort and associated doctoral projects (green) within the three research themes A, B and C - Theme A: Rhizosphere processes and effects of herbivory, theme B: Phycosphere processes and effects of trophic interactions and theme C: Biota-mediated carbon fluxes across marsh-water boundaries. Image by courtesy of UHH/Alpen.

plots have been established in three zones along the surface elevation gradient, the high marsh, low marsh and pioneer zone (Figure 3). Salinity is a major environmental factor within estuaries, structuring animal, plant and microbial communities. Surface elevation in estuarine tidal wetlands determines the flooding frequency and thus, induces steep gradients in oxygen availability within the soil. My dissertation is focused on investigating the influence of these gradients on microbial functionality and community composition.

Sampling along the nine permanent plots including two different depths at each plot resulted in covering various environmental gradients. In addition, the plots exhibit site-dependent differences in the availability of possible electron acceptors and thus different redox conditions (see Chapter 2, Table S1). Oxygen availability is much lower in the deep soil layers than in the upper layers (more oxygen). Sulfate concentrations are particularly high in salt marshes, whereas brackish and freshwater marshes have similarly low sulfate concentrations. Soil redox gradients give an indication of the possible chemical reactions and dominant types of microbial metabolism that can take place in the soil environment (Megonigal et al. 2004).

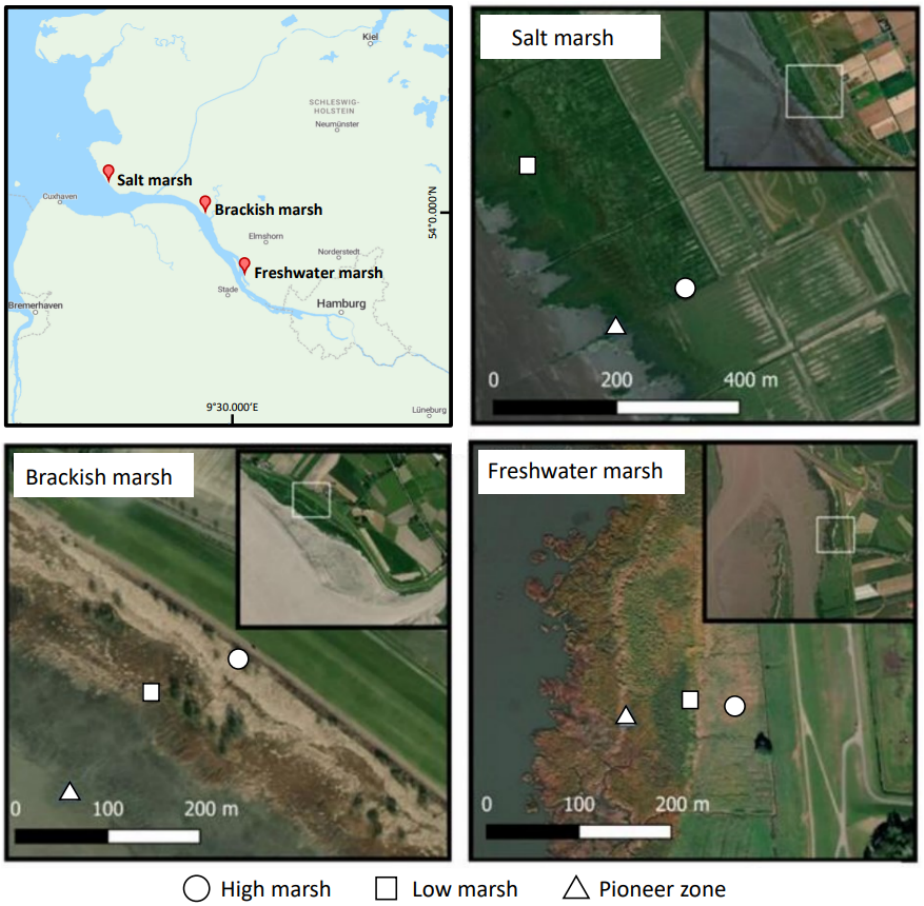

Figure 3. A total of nine permanent plots were established across three sites (Salt marsh, Brackish marsh, Freshwater marsh) along the Elbe estuary, NW Germany. Three zones were demarcated at each of three marsh sites - the pioneer zone, which is characterized by flooding twice a day, the low marsh, which is flooded twice a month and the high marsh, which is only flooded during storm tides (Source: Branoff, Grüterich et al. 2024).

Soil redox gradients

Oxygen diffusion in water is nearly 10,000 times slower than in air, which makes oxygen availability for aerobic microbial metabolism both spatially and temporally highly variable in tidal wetland soils (Megonigal et al., 2004). Decomposition of organic matter is often slower in the absence of oxygen and, depending on the chemical composition and free energy yield of the organic substrate, incomplete, so that organic matter accumulates in flooded, waterlogged soils and sediments. However, differences in decomposition rates in soils depend not only on the oxygen availability but also on other factors, including the availability of alternative terminal electron acceptors other than oxygen (e.g. sulfate) and the type and quality of the organic matter (Kristensen et al., 1995).

If oxygen is available at high concentrations, aerobic microorganisms dominate the soil environment. Tidal wetland soils, influenced by flooding, are often saturated with water or flooded in regular intervals, resulting in anoxic conditions just below the soil surface (Seybold

et al., 2002). In tidal wetlands, redox conditions vary with tidal inundation across elevation gradients (Luther et al., 1991) as the frequency of flooding differs from often flooded pioneer zones to rarely flooded high marshes. Potentially, the strongest impacts of altering soil water content and movement on decomposition arise from fluctuating redox gradients (Figure 4B; Spivak et al., 2019). These fluctuating redox conditions can also lead to differences in chemical properties and higher microbial activity compared to consistently anoxic conditions (Frindte et al., 2016) and influence the exchange of dissolved carbon and nitrogen between the water column and sediment by regulating organic matter degradation rates based on electron acceptor availability (Corzo et al., 2018).

As microorganisms derive energy by transferring electrons from an electron source (donor) to an electron sink (acceptor), they have to use alternative electron acceptors in the absence of oxygen. Commonly used terminal electron acceptors are nitrate (NO_3^-), manganic manganese (Mn^{4+}), ferric iron (Fe^{3+}), sulfate (SO_4^{2-}) and carbon dioxide (CO_2) (Figure 4A; Schlesinger, 1997). The sequence in which these terminal electron acceptors are utilized by microorganisms in soil or sediment environments is primarily determined by their availability and the redox potential (Eh) required for the reactions. At the surface layers of soil, where the Eh is higher due to greater oxygen availability, oxygen acts as the primary electron acceptor (Eh of around +810 mV). As conditions become increasingly anoxic with depth, less energetically favorable electron acceptors are used (Megonigal et al., 2004). Nitrate (NO_3^-), which requires an Eh of about +750 mV, is the next preferred acceptor after oxygen is depleted. Further down, where the Eh decreases to about +510 mV, manganic manganese (Mn^{4+}) is reduced to Mn^{2+}. At an Eh of around +200 mV, ferric iron (Fe^{3+}) is reduced to Fe^{2+}. In even deeper and more reduced conditions (Eh of around -220 mV), sulfate (SO_4^{2-}) reduction to hydrogen sulfide (H_2S) occurs. At the lowest energy yield and in very low or negative Eh environments (at about -240 mV), methanogenesis and acetogenesis takes place where CO_2 is reduced to CH_4 and acetate, respectively (Schlesinger, 1997). These processes reflect a sequential use of electron acceptors as determined by the free energy yield and availability, facilitating the degradation of organic matter from the soil surface to deeper layers.

Redox oscillations allow for greenhouse gas (GHG) recycling in soils. Oscillations in redox conditions can have multiple biotic and abiotic reasons, e.g. temporal dynamics like changes in tide and seasons but also root exudate input. Respiration processes along the redox ladder using oxygen or alternative terminal electron acceptors produce CO_2, which then can be released from the soil into the atmosphere. However, at the lowest redox potentials, methanogenesis and

acetogenesis in fact use the CO_2 produced by respiratory processes (Lyu et al., 2018). Methanotrophs further up on the redox ladder again use methane and oxidize it back to CO_2.

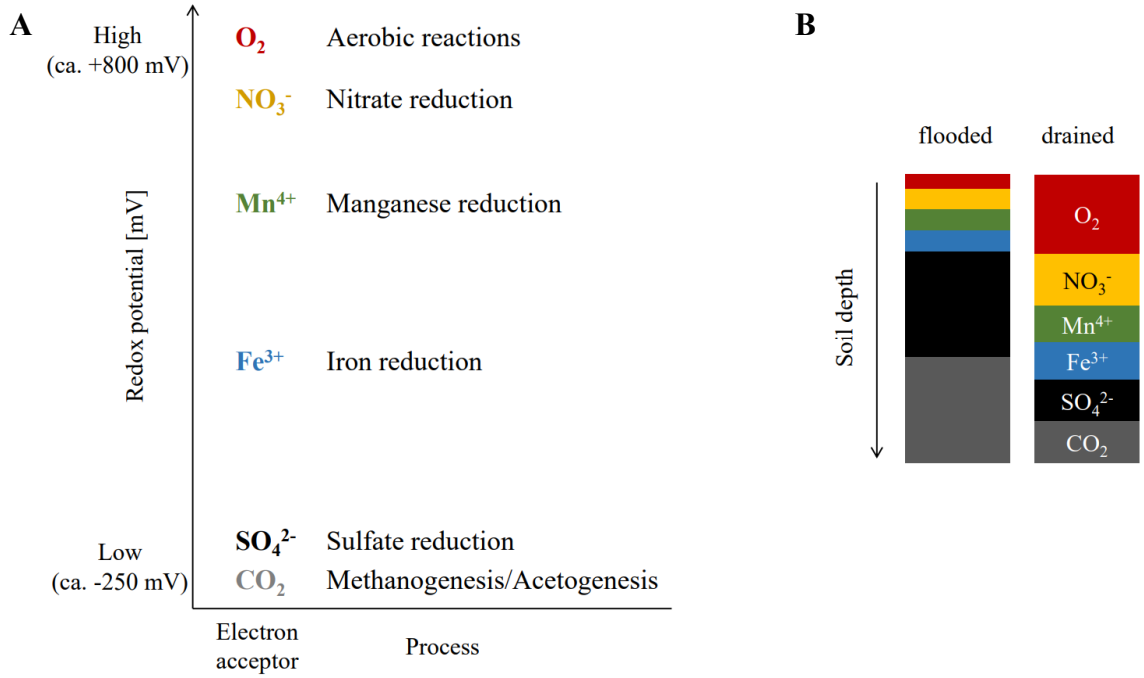

Figure 4. Panel **A** shows the redox ladder with the commonly used inorganic terminal electron acceptors nitrate (NO_3^-), manganic manganese (Mn^{4+}), ferric iron (Fe^{3+}), sulfate (SO_4^{2-}) and carbon dioxide (CO_2). The order in which the soil microorganisms use these terminal electron acceptors depends mainly on their availability and the redox potential required for their reactions. The concept of panel **B** illustrates that redox oscillations can reflect tides and drainage status within estuarine wetland soils (Source: Spivak et al., 2019).

While, conceptually, redox controls on soil and sediment GHG fluxes and recycling are long established, insights into the associated microbial metagenomic and metatranscriptomic patterns are still poorly understood. This knowledge might however be crucial for advancing GHG conversion and capture technologies.

Wetland rhizospheres as hotspots of redox oscillations

Wetland rhizospheres are dynamic environments in which rapid redox oscillations facilitate unique microbial interactions. Plant roots not only increase microbial activity in the soil by providing carbon substrates (electron donors) such as root exudates and other organic rhizodeposits, but also improve the accessibility of electron acceptors by supplying oxygen to an otherwise anoxic soil environment (Mueller et al., 2016). The movement of carbon substrates and oxygen from plant roots to soil microbial communities can strongly influence soil organic matter decomposition. In turn, plants benefit by receiving the nutrients necessary for their growth, which are released during the microbial degradation of soil organic matter and

subsequent nutrient transformation, resulting in a mutually beneficial relationship (Ren et al., 2022). The supply of electron acceptors and donors by roots can have important effects on microbial metabolism and community composition. For instance, sulfur-oxidizing bacteria in these zones, such as those of the genus *Ca*. *thiodiazotropha*, couple sulfur oxidation with nitrogen fixation and use the energy from sulfide conversion to support nitrogenase activity. This process is critical under low-oxygen conditions and helps wetland plants such as *Spartina alterniflora* to access nitrogen while mitigating sulfide toxicity (Rolando et al., 2024). Another example for root effects on microbial metabolism is, that vascular plants can increase the electron acceptor availability of wetland soils through oxygen release, thereby suppressing methane production by favoring non-methanogenic processes and simultaneously facilitating methanotrophy (Agethen et al., 2018; Mueller et al., 2020b).

While root-microbe interactions in terrestrial soils, particularly those focusing on crops, are becoming increasingly well understood, we know much less about their role in wetland soils, where the response of soil microbes is difficult to predict due to strong changes in redox gradients in response to root activity.

Dark CO_2 fixation

Soil microbes are generally considered heterotrophic organisms that produce GHGs such as CO_2 and methane, while CO_2 uptake is usually attributed to photosynthetic organisms such as algae and plants. However, CO_2 uptake can also occur independently of light (Miltner et al., 2005). Given the rising levels of atmospheric GHGs driving climate change, understanding the entire repertoire of microbial pathways involved in CO_2 fixation becomes increasingly important.

Rising levels of GHGs in the atmosphere cause global warming, posing major threats to human society. Thus, understanding biological processes that produce and fix GHGs can be essential to tackle the grand challenge of mitigating climate change (Claassens et al., 2016; Schuchmann & Müller, 2013). Current research is increasingly focusing on microbial pathways that fix GHGs, because these can mitigate rising GHG levels in the atmosphere. Photosynthesis, particularly the Calvin Benson Bassham cycle (Calvin cycle), is well-known and plays a crucial role in CO_2 fixation (Dusenge et al., 2019; Falkowski, 1994). However, non-photosynthetic GHG fixation, such as methanotrophy, also significantly impacts the climate system. Methanotrophs prevent up to 90% of methane from entering the atmosphere, depending on the ecosystem (Hanson & Hanson, 1996; Thauer, 2011; Zimmermann et al., 2019). Extensive

research has deepened our understanding of methanotrophy and its role in the global climate system (Chowdhury & Dick, 2013; Conrad, 2020; Reis et al., 2022; Thauer, 2011).

While methanogenesis, methanotrophy and acetogenesis are long studied (Drake, 1994; Hanson & Hanson, 1996; Zeikus, 1977), in recent years more and more pathways were identified that might also be important in soil GHG recycling (Mall et al., 2018; Sánchez-Andrea et al., 2020). Most studies on non-photosynthetic microbial CO_2 fixation (dark CO_2 fixation), which could be as crucial as methanotrophy for balancing the climate system, have been conducted in single-species cultures, leaving their global importance and ecological optima largely unexplored (e.g. Mall et al., 2018; Sakimoto et al., 2016). Nonetheless, light independent CO_2-fixing pathways have gained increasing attention by the research community in recent years (Mall et al., 2018; Steffens et al., 2021). There are seven known autotrophic CO_2 fixation pathways among the domains of life: the Calvin cycle, reductive tricarboxylic acid cycle (rTCA cycle), Wood-Ljungdahl pathway (WLP), 3-hydroxypropionate bicycle (3-HP bicycle), 3-hydroxypropionate/4-hydroxybutyrate cycle (3-HP/4-HB cycle), dicarboxylate/4-hydroxybutyrate cycle (DC/4-HB cycle) and reductive glycine pathway (rGlyP) (Table 1, Figure 5; Appel et al., 2013; Berg et al., 2010a; Fuchs, 2011; Sánchez-Andrea et al., 2020). **A central motivation of my dissertation is to understand the environmental factors that influence dark CO_2 fixation pathways, and assess them *in situ,* in order to help facilitate their future biotechnological application to mitigate climate change.**

The following list (Table 1) shows how the seven CO_2-fixing pathways differ in terms of ATP and reductant demand, the respective CO_2-fixing enzymes, the active CO_2 species, products arising from CO_2-fixing pathways and the key enzymes of each pathway.

- **Calvin Benson Bassham cycle (Calvin cycle)**

Light-driven photosynthesis and the associated Calvin cycle are well understood and play an obvious role in the climate system (Dusenge et al., 2019; Falkowski, 1994). The Calvin cycle functions in plants, algae, Cyanobacteriota and some members of the phyla Pseudomonadota, Bacillota, and the genera M*ycobacterium* and *Oscillochloris* (Berg, 2011). Key enzyme of the Calvin cycle is the ribulose-1,5-bisphosphate carboxylase/oxygenase (RuBisCO), which uses inorganic carbon in form of CO_2 as substrate. RuBisCO is known to be the most abundant protein on earth (Ellis, 1979; Hayer-Hartl & Hartl, 2020). The operation of the Calvin cycle is not very energy efficient as it requires nine ATP for the fixation of three CO_2 (Bährle et al., 2023). Its successful enforcement is probably due to the facts that, first, the Calvin cycle is mainly present in organisms that synthesize large quantities of sugars (e.g., plants). This sugar

can, in turn, play a role as an energy storage and thus compensate for the high energy requirements of the Calvin cycle. Second, its enzymes tolerate molecular oxygen well (Berg, 2011).

- **3-Hydroxypropionate bicycle (3-HP bicycle)**

The 3-HP bicycle functions in green non-sulfur phototrophs of the Chloroflexaceae family. It was discovered in *Chloroflexus aurantiacus* (Holo, 1989; Zarzycki et al., 2009). As the name indicates, the 3-HP bicycle consist of two cycles. In the first cycle, glyoxylate gets released as a first product, while using acetyl-CoA and bicarbonate (HCO_3^-) as carbon sources (Strauss & Fuchs, 1993). The second cycle assimilates glyoxylate by producing pyruvate and acetyl-CoA which further conversion to propionyl-CoA closes the cycle (Herter et al., 2002; Zarzycki et al., 2009). For the fixation of three CO_2 molecules, seven ATP are required. As the Calvin cycle it also functions under aerobic conditions (Zarzycki et al., 2009).

- **3-Hydroxypropionate/4-hydroxybutyrate cycle (3-HP/4-HB cycle)**

The 3-HP/4-HB cycle was discovered and described in Crenarchaeota (Berg et al., 2007). Succinyl-CoA is formed from two HCO_3^- and acetyl-CoA as carbon sources using six ATP (Berg et al., 2007). The cycle functions under aerobic conditions (Berg et al., 2010c). The 3-HP/4-HB cycle which uses CO_2 in the form of HCO_3^-, functions in mesophilic marine archaea represented in the worlds' oceans (Karner et al., 2001), where the main inorganic carbon species is HCO_3^- due to the slight alkalinity of the oceans' water. Furthermore, an advantage of the cycle is its thermotolerance making it function in hyperthermophilic crenarchaea that have growth temperatures of up to 113°C (Blöchl et al., 1997).

- **Reductive tricarboxylic acid cycle (rTCA cycle)**

As the name indicates, the rTCA cycle reverses the reactions of the oxidative citric acid cycle (TCA cycle) and was discovered in green sulfur bacteria (Evans et al., 1966; Fuchs et al., 1980; Ivanovsky et al., 1980) and further functions in various phyla such as Aquificota, Pseudomonadota and Nitrospirota. The cycle converts two CO_2 molecules into acetyl-CoA by utilizing two ATP to form pyruvate (Berg, 2011). To facilitate the reversal of the TCA cycle, the rTCA cycle requires three specific enzymes, as three steps of the TCA cycle are not reversible and have to be exchanged by the ATP-citrate lyase, the fumarate reductase and the ferredoxin-dependent 2-oxoglutarate synthase (Evans et al., 1966; Fuchs, 1989; Ivanovsky et al., 1980). It was recently reported that high levels of CO_2 drive the TCA cycle backwards

towards autotrophy (Steffens et al., 2021). This version of the rTCA cycle is called the reverse oxidative TCA cycle (roTCA cycle).

Table 1. Pathways for autotrophic CO_2 fixation (Sources: Berg et al., 2010a; Sánchez-Andrea et al. 2020)

Pathway	Amount of ATP for synthesis of one triose phosphate	Reductants for synthesis of one triose phosphate	CO_2-fixing enzymes	Active "CO_2" species	CO_2 fixation products which may be used for biosynthesis	Key enzymes
Calvin cycle	9	6 NAD(P)H	RuBisCO	CO_2	3-Phosphoglycerate	RuBisCO; phosphoribulokinase
rTCA cycle	5	3 NAD(P)H, 1 unknown donor[a], 2 ferredoxin	2-Oxoglutarate synthase Isocitrate dehydrogenase[b] Pyruvate synthase PEP carboxylase	CO_2 CO_2 CO_2 HCO_3^-	Acetyl-CoA, pyruvate, PEP, oxaloacetate, succinyl-CoA, 2-oxoglutarate	2-Oxoglutarate synthase, ATP-citrate lyase
WLP	4-5	3 NAD(P)H, 2-3 ferredoxin, 1 H_2 (in methanogens)	Acetyl-CoA Synthase/CO dehydrogenase Formate dehydrogenase Pyruvate synthase	CO_2 CO_2 CO_2	Acetyl-CoA, pyruvate	Acetyl-CoA synthase/CO Dehydrogenase, enzymes reducing CO_2 to methyltetrahydropterin
3-HP bicycle	10	7 NAD(P)H, but 1 FAD is reduced	Acetyl-CoA/propionyl-CoA carboxylase	HCO_3^-	Acetyl-CoA, Pyruvate, succinyl-CoA	Malonyl-CoA reductase, propionyl-CoA synthase, malyl-CoA lyase
3-HP/4-HB cycle	9	6 NAD(P)H	Acetyl-CoA/propionyl-CoA carboxylase	HCO_3^-	Acetyl-CoA, succinyl-CoA	Acetyl-CoA-propionyl-CoA carboxylase[c], enzymes reducing malonyl-CoA to propionyl-CoA, methylmalonyl-CoA mutase[c], 4-hydroxybutyryl-CoA dehydratase
DC/4-HB cycle[d]	8	2 NAD(P)H, 3 ferredoxin, 1 unknown donor	Pyruvate synthase PEP carboxylase	CO_2 HCO_3^-	Acetyl-CoA, pyruvate, PEP, oxaloacetate, succinyl-CoA	4-Hydroxybutyryl-CoA dehydratase
rGlyP	1-2	2 NAD(P)H, 1 thioredoxin, 2 ferredoxin	Formate dehydrogenase Glycine cleavage/synthase system	CO_2 CO_2	Acetyl-CoA, pyruvate	Glycine cleavage/synthase system

CoA, co-enzyme A; FAD, flavin adenine dinucleotide; PEP, phosphoenolpyruvate; RuBisCO, ribulose 1,5-bisphosphate carboxylase-oxygenase.

a) NADH in *Hydrogenobacter thermophilus* (Miura et al., 2008).

b) Biotin-dependent 2-oxoglutarate carboxylase in *Hydrogenobacter thermophilus* (Aoshima et al., 2004).

c) The presence of these enzymes is usual for Bacteria, but not Archaea, where this pathway was discovered.

d) As studied in *Ignicoccus hospitalis*

- **Dicarboxylate/4-hydroxybutyrate cycle (DC/4-HB cycle)**

As the 3-HP/4-HB cycle, the DC/4-HB cycle was described in Crenarchaeota (Huber et al., 2008) and is present in many autotrophic members of the orders Thermoproteales and Desulfurococcales (Berg et al., 2010b; Huber et al., 2008; Ramos-Vera et al., 2009). Compared to the 3-HP/4-HB cycle, the DC/4-HB cycle is strictly anaerobic because of the oxygen sensitivity of some enzymes and electron carriers as the pyruvate synthase and ferredoxin, although the two cycles share many enzymes. The DC/4-HB cycle uses CO_2, HCO_3^- and acetyl-CoA as carbon source to form succinyl-CoA, at the cost of five ATP (Erb, 2011; Huber et al., 2008).

- **Reductive glycine pathway (rGlyP)**

Recently a seventh CO_2 fixation pathway was confirmed in the sulfate-reducing bacterium *Desulfovibrio desulfuricans*. Only one ATP is needed to metabolize formate to acetyl-CoA in the end by fixing two CO_2 (Sánchez-Andrea et al., 2020). The rGlyP and the WLP are interconnected by sharing the first step, where one CO_2 gets reduced via the formate dehydrogenase (Song et al., 2020). This oxygen sensitive enzyme makes the rGlyP only functioning under anaerobic conditions. Also, the co-utilization of both WLP and rGlyP in acetogens has been confirmed by Song et al. (2020).

- **Wood–Ljungdahl pathway (WLP)**

The WLP is widespread among anaerobic microorganisms especially known to function in acetogenic bacteria. The genera *Acetobacterium* and *Clostridium* host the most well-known acetogenic bacteria (Drake et al., 2008), such as *Acetobacterium woodii* (Balch et al., 1977), *Moorella thermoacetica* (formerly *Clostridium thermoaceticum*) (Fontaine et al., 1942) and *Thermoanaerobacter kivui* (formerly *Acetogenium kivui*) (Leigh et al., 1981). The WLP consists of two converging branches, the methyl and carbonyl branches. In the methyl branch, a molecule of CO_2 is reduced to formate (Pierce et al., 2008; Wang et al., 2013). In the final step of the methyl branch, the methyl group from methyl-THF is transferred to a corrinoid-iron-sulfur protein (CoFeSP) (Hu et al., 1984). The bifunctional CO dehydrogenase/acetyl-CoA synthase (CODH/Acs) is the key enzyme of the WLP, catalyzing the reduction of a second molecule of CO_2 in a condensation reaction to enzyme-bound CO in the carbonyl branch (Pierce et al., 2008; Ragsdale, 2008). The methyl group bound to CoFeSP is transferred back to the same enzyme, uniting the two branches. CO is combined with methyl-CoFeSP and coenzyme A, and then converted to acetyl-CoA by CODH/Acs (Ragsdale et al., 1983; Ragsdale

& Wood, 1985). The WLP is highly energy efficient by requiring only one ATP and fixing two CO_2.

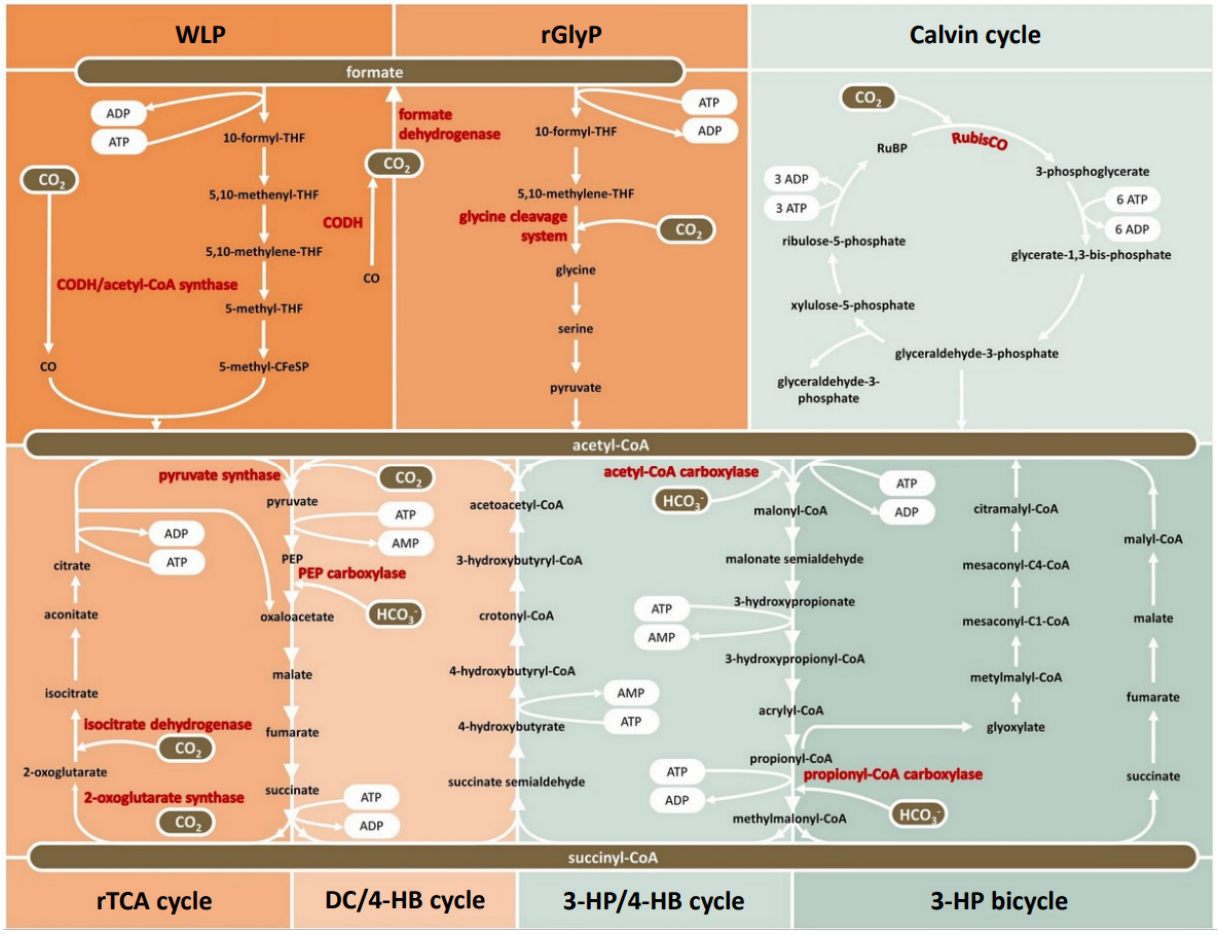

Figure 5. Currently known natural CO_2-fixing pathways. Depicted are the Wood-Ljungdahl pathway (WLP), Reductive glycine pathway (rGlyP), Calvin Benson Bassham cycle (Calvin cycle), Reductive tricarboxylic acid cycle (rTCA cycle), Dicarboxylate/4-hydroxybutyrate cycle (DC/4-HB cycle), 3-Hydroxypropionate/4-hydroxybutyrate cycle (3-HP/4-HB cycle) and 3-Hydroxypropionate bicycle (3-HP bicycle). Carbon-fixing enzymes are depicted in red font. Aerobic pathways are highlighted in green (Calvin cycle, 3-HP/4-HB cycle, 3-HP bicycle) and anaerobic pathways are highlighted in orange (WLP, rGlyP, rTCA cycle, DC/4-HB cycle) (Source: Bährle et al., 2023).

In the following chapters, I investigate the effects of large-scale spatial gradients i.e., the distance-to-sea gradient along the marshes of the Elbe estuary, the surface-elevation gradient and the soil-depth gradients that effect microbial community composition (Chapters 2 and 4), litter decomposition (Chapter 4) and the abundance of dark CO_2-fixing pathways (Chapter 2). I address the effects of a small-scale gradient that is defined as proximity to root exudates (Chapter 3), and asses the transcriptomic responses of the soil microbial community to root-sourced exudates entering a reduced soil environment.

Table 2. Overview of manuscripts represented in chapters 2, 3 and 4.

	Chapter 2	Chapter 3	Chapter 4
Study name	Assessing Environmental Gradients in Relation to Dark CO_2 Fixation in Estuarine Wetland Microbiomes	Transcriptomic Response of Wetland Microbes to Root Influence	Litter Decomposition and Prokaryotic Decomposer Communities along Estuarine Gradients
Knowledge gap	Limited knowledge about the presence of CO_2-fixing pathways *in situ* and environmental drivers	Responses of microbes to root exudates are not understood – especially studies in wetland ecosystems are lacking	Limited knowledge about drivers of litter decomposition in estuarine marshes and the role of microbial diversity in this process
Research questions	Which dark CO_2-fixing pathways are present in wetland soils, and what are their environmental drivers?	How do root exudates influence the transcriptomic response and the active community composition of microbes in wetland soils?	How do estuarine gradients affect litter decomposition and the litter associated microbial community?
Study area	Tidal marshes of the Elbe estuary, NW Germany	Wadden Sea salt marsh at Hamburger Hallig, NW Germany. Soils used for lab-based mesocosm experiment.	Tidal marshes of the Elbe estuary, NW Germany
Spatial scale addressed	Distance to sea, surface elevation, soil depth	Distance to root exudate source	Distance to sea, surface elevation, soil depth
Primary techniques	Metatranscriptomics, metagenomics (Shotgun and 16S amplicon)	$^{13}CO_2$ labeling, metagenomics (Shotgun), metatranscriptomics	Metagenomics (16S amplicon)

Chapter 2

Assessing Environmental Gradients in Relation to Dark CO_2 Fixation in Estuarine Wetland Microbiomes

Published at Applied and Environmental Microbiology (2024) – DOI: 10.1128/aem.02177-24

Luise Grüterich, Jason Nicholas Woodhouse, Peter Mueller, Amos Tiemann, Hans-Joachim Ruscheweyh, Shinichi Sunagawa, Hans-Peter Grossart and Wolfgang R. Streit

Abstract

The rising atmospheric concentration of CO_2 is a major concern to society due to its global warming potential. In soils, CO_2-fixing microorganisms are preventing some of the CO_2 from entering the atmosphere. Yet, the controls of dark CO_2 fixation are rarely studied *in situ*. Here, we examined the gene and transcript abundance of key genes involved in microbial CO_2 fixation along major environmental gradients within estuarine wetlands. A combined multi-omics approach incorporating metabarcoding, deep metagenomic, and metatranscriptomic analyses confirmed that wetland microbiota harbor four out of seven known CO_2 fixation pathways, namely, the Calvin cycle, reverse tricarboxylic acid cycle, Wood-Ljungdahl pathway, and reverse glycine pathway. These pathways are transcribed at high frequencies along several environmental gradients, albeit at different levels depending on the environmental niche. Notably, the transcription of the key genes for the reverse tricarboxylic acid cycle was associated with high nitrate concentration, while the transcription of key genes for the Wood-Ljungdahl pathway was favored by reducing, O_2-poor conditions. The transcript abundance of the Calvin cycle was favored by niches high in organic matter. Taxonomic assignment of transcripts implied that dark CO_2 fixation was mainly linked to a few bacterial phyla, namely, Desulfobacterota, Methylomirabilota, Nitrospirota, Chloroflexota, and Pseudomonadota.

Introduction

Rising atmospheric concentrations of the greenhouse gases (GHGs) CO_2 and methane are primary drivers of climate change and hence a major concern to society. Therefore, knowledge of fundamental processes linked to CO_2-producing and CO_2-fixing metabolisms is crucial (Claassens et al., 2016; Schuchmann & Müller, 2013). Within this framework, current research focuses on GHG-fixing microbial metabolic pathways that could be relevant to the climate system because of their ability to counteract the increasing atmospheric GHG concentrations.

Light-driven photosynthesis and the associated CO_2 fixation pathways (i.e., Calvin cycle) are well understood and play an obvious role in the climate system (Dusenge et al., 2019; Falkowski, 1994). Although the Calvin cycle contributes to light-dependent photosynthesis, it should be noted that it can operate independently of light in autotrophic microorganisms, such as sulfur-oxidizing bacteria and methylotrophs (Khadem et al., 2011; Rolando et al., 2024). In addition to light-dependent CO_2 fixation, also non-photosynthetic GHG fixation pathways can play a major role in the climate system. One prominent example of non-photosynthetic microbial GHG fixation is methanotrophy. Aerobic and anaerobic methane oxidizers are responsible for preventing up to 90% of methane produced in soils or aquatic systems from entering the atmosphere; the number varies depending on the ecosystem (Hanson & Hanson, 1996; Thauer, 2011; Zimmermann et al., 2019). Additionally, the conversion of methane to CO_2 by methanotrophs underscores the complexity of microbial interactions influencing soil-atmosphere GHG fluxes. Extensive research has refined our quantitative and mechanistic understanding of methanotrophy and its role in the global climate system (Chowdhury & Dick, 2013; Conrad, 2020; Thauer, 2011). By contrast, while pure culture studies have been conducted extensively, research on *in situ* studies of dark CO_2 fixation is limited. Most of these studies have focused on single-species pure cultures (e.g., Mall et al., 2018; Sakimoto et al., 2016), with only a few investigations exploring this process in natural environments, such as paddy soils, semiarid deserts, and grasslands (Huang et al., 2022; Liu et al., 2018; Xiao et al., 2014; Xiao et al., 2021). Thus, the environmental controls of dark CO_2 fixation and its potential effects on the global climate system remain largely unknown. Recently, however, this topic receives increasing attention from the scientific community (Mall et al., 2018; Steffens et al., 2021). Among the domains of life, at least seven autotrophic CO_2 fixation pathways can be distinguished: Calvin cycle, reductive tricarboxylic acid cycle (rTCA cycle), Wood-Ljungdahl pathway (WLP), 3-hydroxypropionate bicycle (3-HP bicycle), 3-hydroxypropionate/4-hydroxybutyrate cycle (3-HP/4-HB cycle), dicarboxylate/4-hydroxybutyrate cycle (DC/4-HB cycle) and reductive glycine pathway (rGlyP) (Table 1; Appel et al., 2013; Berg et al., 2010a;

Fuchs, 2011; Sánchez-Andrea et al., 2020). Importantly, a recent study reported that high levels of CO_2 drive the TCA cycle backwards toward autotrophy (Steffens et al., 2021). Due to the increase in CO_2 concentration in the atmosphere mainly caused by anthropogenic fossil fuel burning, it is now crucial to elucidate the environmental factors that determine occurrence and magnitude of the respective dark CO_2 fixation pathways *in situ*.

Table 1. List of CO_2-fixing pathways and affiliated key genes. The selection of key genes is based on Berg et al. (2010a) and was supplemented by the malate dehydrogenase for the DC/4-HB cycle and the key genes for the rGlyP (Sánchez-Andrea et al., 2020). Asterisks indicate the key genes selected for analyzing gene and transcript abundance (Figure 4) as well as for the correlation analysis of transcript abundance with environmental parameters (Table 3).

Pathway	Key enzyme	Key gene also present in another CO_2-fixing pathway	Key gene for abundance analysis	EC number
rTCA cycle	2-Oxoglutarate synthase	-		1.2.7.3
	ATP-citrate lyase *	-	*aclA*	2.3.3.8
WLP	Acetyl-CoA synthase *	-	*acsC/cdhE*	2.3.1.169/ 2.1.1.245
	CO dehydrogenase	-		1.2.7.4
Calvin cycle	RuBisCO *	-	*rbcL*	4.1.1.39
	Phosphoribulokinase	-		2.7.1.19
DC/4-HB cycle	4-Hydroxybutyryl-CoA dehydratase	3-HP/4-HB cycle		4.2.1.120
	malate dehydrogenase	rTCA cycle		1.1.1.37
3-HP bicycle	Malonyl-CoA reductase	3-HP/4-HB cycle		1.2.1.75
	propionyl-CoA synthase	3-HP/4-HB cycle		6.4.1.3
	malyl-CoA lyase	-		4.1.3.24
3-HP/4-HB cycle	Acetyl-CoA/propionyl-CoA carboxylase	3-HP bicycle		6.4.1.3
	methylmalonyl-CoA mutase	3-HP bicycle		5.4.99.2
	4-hydroxybutyryl-CoA dehydratase	DC/4-HB cycle		4.2.1.120
rGlyP	Glycine reductase *	-	*grdB*	1.21.4.2
	Methenyl-THF cyclohydrolase	-		3.5.4.9

The present study assessed the gene and transcript abundance of key genes of the different dark CO_2-fixing pathways along environmental gradients within an estuarine wetland landscape to provide insight into which CO_2-fixing pathways are most likely to be present in different environmental niches. With this, we aim to create a basis on which further in-depth research on

dark CO_2 fixation in the environment can be built. The estuarine wetland landscape is ideally suited to understand environmental constraints on CO_2-fixing pathways for at least two reasons. First, estuarine wetlands connect marine, limnic, and terrestrial environments, and are therefore characterized by steep environmental gradients in oxygen availability, organic matter availability and salinity. Second, estuarine wetland soils possess a tremendous carbon turnover rate and are among the most effective carbon sinks of the biosphere (Duarte et al., 2005; Mcleod et al., 2011). Our study was conducted along the salinity gradient of the Elbe estuary, NW Germany. The Elbe estuary with a coverage of 500 km^2 is one of the largest estuaries in Europe with various environmental gradients. For this study, we sampled along multiple small-scale and large-scale spatial gradients within the estuary, distance-to-sea, surface-elevation, and soil-depth, encompassing three sampling sites ranging from marine to freshwater marshes (Figure 1).

We assessed the following two hypotheses: (**I**) Dark CO_2 fixation occurs in anaerobic ecological niches with low reduction potential because many of the CO_2-fixing pathways have been described in anaerobic microorganisms (Fuchs, 2011). (**II**) Dark CO_2 fixation benefits from heterotrophic respiratory CO_2 production, which we expect to increase with increasing salinity in anaerobic environments, associated with the greater supply of alternative electron acceptors, i.e., sulfate, facilitating anaerobic heterotrophic respiration (Morrissey et al., 2014; Sutton-Grier et al., 2011). While some studies have examined the gene and transcript abundance of key genes for CO_2 fixation pathways in specific ecosystems or under specific environmental conditions, this study investigates transcript abundance across large- and small-scale environmental gradients, allowing for identification of niches of these pathways.

Material and Methods

Soil sample collection

Soil samples were collected from three wetland sites along the salinity gradient of the Elbe estuary (September 2021 (for metagenome and metatranscriptome samples) and September 2022 (for 16S samples)): a salt marsh (N53.927781° E8.914244°), a brackish marsh (N53.834175° E9.371009°) and a freshwater marsh (N53.665624° E9.553203°). Samples were collected with a peat sampler (Eijkelkamp, Giesbeek, Netherlands) to a depth of 50 cm below the soil surface in each of three elevation zones at each site, the high marsh, low marsh and pioneer zone. To ensure the integrity of the RNA, we immediately placed the samples on dry ice (-78.5 °C) upon sampling in the field. Subsequently, soil samples were stored at -80 °C until their use for DNA/RNA extraction and metabolite analysis.

DNA and RNA extraction from soil

DNA was extracted from aliquots of all collected soil samples, which were frozen at -80°C until analysis. Upon thawing on ice, 0.5 g of soil were used for DNA extraction using the NucleoSpin Soil Kit (Macherey-Nagel, Düren, Germany) following the manufacturer's protocol. Subsequently, the isolated DNA was analyzed at a wavelength of 280 nm using a Nanodrop spectrophotometer (NanoDrop 2000, Thermo Scientific, Waltham, USA). 2 g of soil were used for RNA extraction using the RNeasy PowerSoil Kit (Qiagen, Venlo, Netherlands) following the manufacturer's protocol. RNA concentrations were quantified using the Qubit 2.0 Fluorometer and the RNA High Sensitivity Assay Kit (RNA HS, Thermo Fisher, Berlin, Germany).

Determination of organic matter via Loss of Ignition method

The weight change related to high-temperature oxidation of organic matter was used to determine the organic matter content. About 30-40 g of soil was placed in porcelain crucibles and dried overnight at 60 °C in a drying oven. Before ignition the samples were further dried for 2 h at 105 °C in a drying oven to get rid of remaining water. The dry weight (DW) was measured. The soil samples were ignited for 2 h at 500 °C in a muffle furnace, cooled in a desiccator and weighed again. The organic matter content (%) was calculated as follows:
OM (%) = (DW after ignition : DW before ignition) * 100

Metabolite analyses via colorimetric assays

Acetate, pyruvate, and isocitrate concentration were determined by colorimetric assay kits that were used according to the respective manufacturer's protocol (Sigma; MAK086, MAK071, MAK061). 1 g of soil was mixed with 1 ml of VE H_2O, followed by ultrasonication and subsequent centrifugation at 11,000 x *g* for 1 min. The supernatant was used as sample for metabolite determination.

Anion analyses via ion chromatography

The concentrations of chloride (used as a proxy for salinity), nitrate, and sulfate (considered important alternative electron acceptors) in the soil porewater were approximated using the following method: Frozen soil samples were first thawed, then mixed with deionized water at a ratio of 1 part soil to 10 parts water. The mixture was then filtered through a 0.45 µm syringe filter, and the filtered solution was subsequently analyzed using ion chromatography (883 Basic IC plus, Metrohm, Herisau, Switzerland). Ion concentrations are reported per milliliter of water

present in the fresh soil samples after thawing. This calculation is based on the ratio of fresh weight to dry weight of the soil.

Soil reduction index analyses

Soil reduction, a proxy for oxygen availability, was measured using the indicator of reduction in soils (IRIS) technique (Rabenhorst, 2013; Rabenhorst & Burch, 2006); here modified based on Mueller et al. (2020b) and Mittmann-Goetsch et al. (2024). Briefly, PVC sticks (5 x 70 cm) coated with Fe-oxide paint were inserted into the soil to a depth of 60 cm for four weeks. Under reducing conditions, the paint dissolved due to the reduction of Fe(III) to Fe(II). A reduction index (0-1) was then calculated based on the area of paint removal. The sticks were incubated from February 2022 to March 2023, and a yearly average reduction index was used for the specific depth increments of our study. For detailed methods, see Neiske et al. 2024.

16S rRNA gene analyses

Metabarcoding sequencing of 16S rRNA variable regions V3-4 was performed at the Competence Centre for Genomic Analysis, Kiel, Germany using the Illumina Nextera XT Index Kit and primers 341F (5'-CCTACGGGNGGCWGCAG-3' and 785R (5'-GACTACHVGGGTATCTAATCC-3') and MiSeq Reagent Kit v3. Adaptor trimming of demultiplexed paired-end reads was performed using Cutadapt (v.4.4) (Martin, 2011). Read filtering and ASV inference was performed using the DADA2 pipeline (v.1.8), with the following specifications (maxEE=2, maxN=0, truncQ=2, truncLen=260,210). Taxonomic assignment of merged corrected reads was made using the SILVA (v.138.1) database. Downstream analyses were performed using the phyloseq (v.1.41.1) and ggplot2 (3.4.2) R packages.

Meta-omics sequencing and data processing

Size selection, library preparation and sequencing of metagenomes were performed at the Ramaciotti Centre for Genomics, Sydney, Australia, using the Ilumina DNA Prep kit and an Illumina NovaSeq 6000 S4 flow cell. Ribosomal RNA depletion, library preparation, and sequencing of metatranscriptomes were performed at the Competence Centre for Genomic Analysis, Kiel, Germany, using the Illumina Stranded Total RNA Prep with Ribo-Zero Plus Microbiome kit and Illumina NovaSeq 6000 S4 Reagent kit.

Our data analysis, which has been previously demonstrated (Paoli et al., 2022; Salazar et al., 2019), set a new benchmark for metagenomic and metatranscriptomic analyses. Metagenome-

assembled genomes (MAGs) represent partial population genomes rather than complete ones, leading to potential inaccuracies in gene and pathway representation. To address this, we constructed a pangenome for each population using multiple MAGs from various samples, allowing us to calculate gene abundances from dereplicated genes while preserving taxonomic information. This approach enables accurate inference of individual gene and pathway abundances without dependence on the completeness of any single MAG. Further, because complex metagenomes can be influenced by the heterogenous occurrence of eukaryotes, viruses and other genetic elements, rather than normalizing to the size of the library (i.e. FPKM, RPKM metrics), this approach normalizes the abundance of individual genes against prokaryotic single-copy marker genes allowing us to estimate the copies per prokaryotic cell. For specific details on the single-copy marker genes used in this study and their appropriateness see the following references (Milanese et al., 2019; Ruscheweyh et al., 2021; Salazar et al., 2019; Sunagawa et al., 2013).

Metagenomic (n=18) and metatranscriptomic (n=18) sequencing datasets were processed as previously described by Paoli et al. 2022. Briefly, BBMap (v.38.71) was used to quality control sequencing reads from all samples by removing adapters from the reads, removing reads that mapped to quality control sequences (PhiX genome) and discarding low-quality reads (trimq=14, maq=20, maxns=1 and minlength=45). Quality-controlled reads were merged using bbmerge.sh with a minimum overlap of 16 bases, resulting in merged, unmerged paired and single reads. The reads from metagenomic samples were assembled into scaffolded contigs (hereafter scaffolds) using the SPAdes assembler (v3.15.2) (Nurk et al., 2017) in metagenomic mode. Scaffolds were length-filtered (≥ 1000 bp) and quality-controlled reads from each metagenomic sample were mapped against the scaffolds of each sample. Mapping was performed using BWA (v0.7.17-r1188; -a) (Li & Durbin, 2009). Alignments were filtered to be at least 45 bp in length, with an identity of ≥ 97% and a coverage of ≥ 80% of the read sequence. The resulting BAM files were processed using the *jgi_summarize_bam_contig_depths* script of MetaBAT2 (v2.12.1) (Kang et al., 2019) to compute within- and between-sample coverages for each scaffold. The scaffolds were binned by running MetaBAT2 on all samples individually (--minContig 2000 and --maxEdges 500). Metagenomic bins were annotated with Anvio (v7.1.0) (Eren et al., 2015), quality-controlled using the CheckM (v1.0.13) (D. H. Parks et al., 2015) lineage workflow (completeness ≥ 50% and contamination < 10%) to generate 76,918 MAGs. Complete genes were predicted using Prokka (v1.14.6) (Seemann, 2014) and MAGs were taxonomically annotated using GTDB-TK (GTDB-TK v 1.7 and GTDB release R214).

Genes were subsequently clustered at 95% identity, keeping the longest sequence as representative using CD-HIT (v4.8.1) with the parameters -c 0.95 -M 0 -G 0 -aS 0.9 -g 1 -r 0 -d 0 -b 1000. Representative gene sequences were aligned against the KEGG database (release April.2022) using DIAMOND (v2.0.15) (Buchfink et al., 2021) and filtered to have a minimum query and subject coverage of 70% and requiring a bitScore of at least 50% of the maximum expected bitScore (reference against itself). Quality-controlled metagenomic and metatranscriptomic sequencing reads were aligned against the set of representative genes. Gene-length normalized read abundances (i.e., gene copies) were first summarized into KEGG orthologous groups (Kanehisa, 2002) and then normalized by the median of single-copy marker genes copies (Ruscheweyh et al., 2022) to calculate mean per-cell gene and transcript copy numbers of orthologous groups, respectively.

To analyze the abundance of CO_2-fixing pathways, we combined genomic context and taxonomic information. Our approach to assess the completeness of dark CO_2 fixation pathways began with identifying genomes containing key genes involved in dark CO_2 fixation (Tables S4-S7). We then validated the presence of these pathways by checking for additional critical genes and enzymes. To resolve conflicts between CO_2 fixation pathways where genes are shared, we compared pathway completeness among closely related genomes at the genus and species levels. Furthermore, a literature review was conducted to address missing genes in known dark CO_2-fixing taxa and to confirm the identified pathways. Only after ensuring that individual key gene orthologs were representative of organisms capable of dark CO_2 fixation did we include abundance estimations and subsequent analyses. Detailed criteria for selecting dark CO_2 fixation key enzymes and considerations at each stage are provided in Supplementary Text 1.

Statistical analyses

To test the correlations between the environmental parameter chloride, organic matter, acetate, pyruvate, isocitrate, nitrate, sulfate and reduction index against the key gene and transcript abundance of the CO_2-fixing pathways, we performed a Spearman's rank correlation.

Data availability

Raw reads of the metagenomic, metatranscriptomic and 16S rRNA analysis were deposited at the European nucleotide archive ENA under project accession number PRJEB54081 (Biosamples: SAMEA110291994 - SAMEA110292011 and SAMEA113954754 - SAMEA113954807). The gene catalog for the metagenomic and metatranscriptomic analyses

and ASV tables for the 16S rRNA analyses were deposited at the ZFDM repository of the University of Hamburg (https://doi.org/10.25592/uhhfdm.13933).

Results

In order to constrain the ecological niches of dark CO_2-fixing pathways *in situ*, the soil microbiome was assessed along different gradients within the marshes of the Elbe estuary: distance-to-sea, surface-elevation and soil-depth (Figure 1).

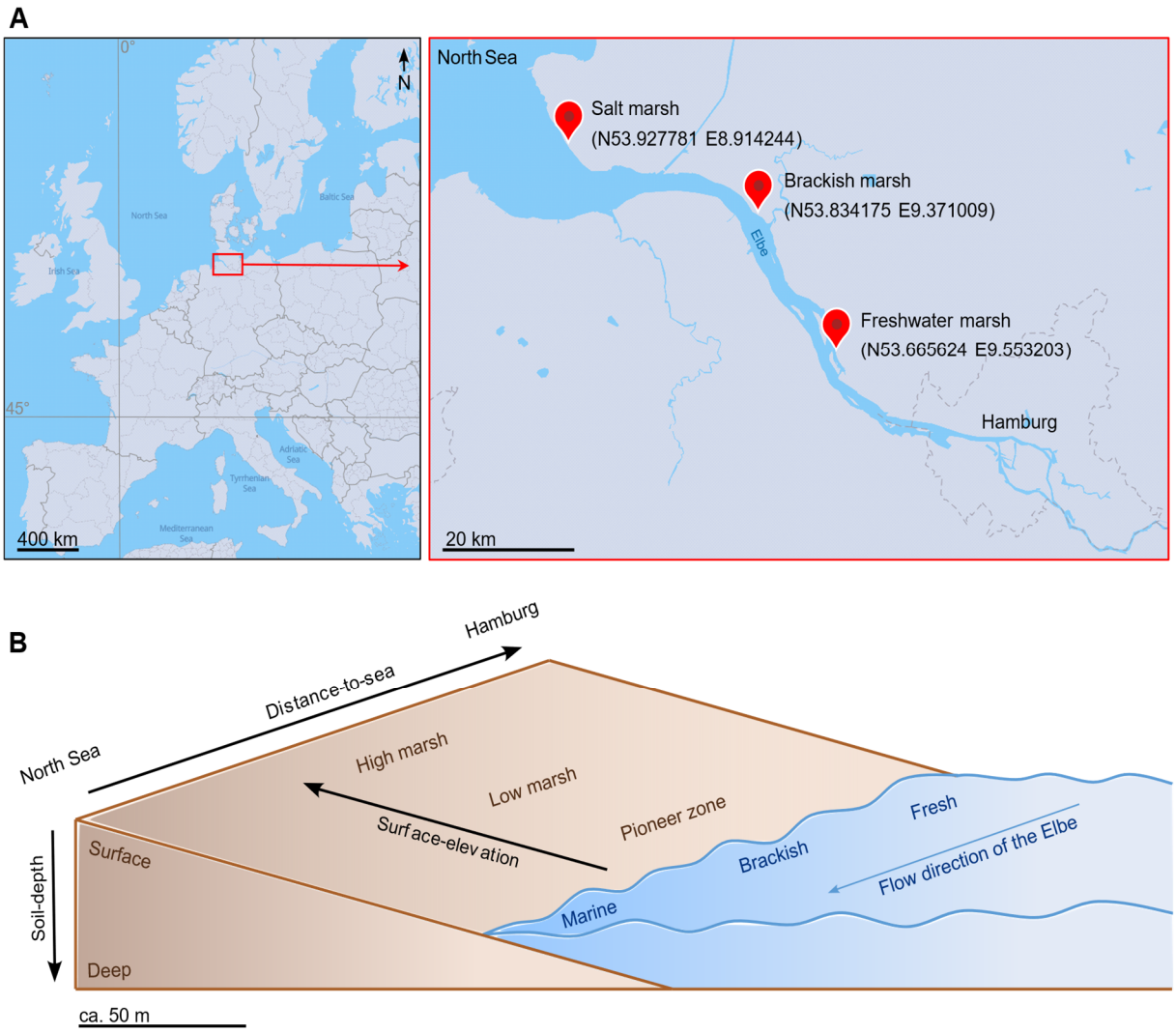

Figure 1. Location of the Elbe estuary and sampling sites along the distance-to-sea gradient of the Elbe estuary from the salt marsh to the brackish marsh to the freshwater marsh (**A**). **B** shows the environmental gradients given by the sampling locations along the river course from fresh to brackish to marine sites (distance-to-sea gradient), along the surface-elevation gradient from pioneer zones to low marshes to high marshes and the soil-depth gradient we sampled (surface layer (0-5 cm) versus deep layer (45-50 cm)). At each site, in each zone and depth, samples were taken with a peat sampler in September at low tide. Maps in **A** were created with MapTiler.

We measured several environmental parameters along these spatial gradients, namely, organic matter content, reduction index (as proxy for oxygen availability), chloride (as proxy for

salinity), nitrate, sulfate, acetate, pyruvate and isocitrate. We expected the availability of sulfate, as the dominant alternative electron acceptors for anaerobic heterotrophic respiration in marine and estuarine environments, to covary with the distance-to-sea gradient. We were able to confirm that, indeed, sulfate and chloride decreased significantly ($p < 0.05$) with increasing distance-to-sea. We further observed that oxygen availability and organic matter content decreased significantly ($p < 0.05$) with increasing soil-depth and that concentration of isocitrate increased significantly ($p < 0.05$) with higher distance-to-sea (Table 2, Table S1).

Table 2. Statistical analysis of environmental parameters correlating with the spatial gradients distance-to-sea, surface-elevation and soil-depth (Figure 1). Significant changes are indicated by bold numbers ($p < 0.05$). We performed a Spearman's rank correlation analysis with transcript abundances of the key genes and eight soil environmental parameters. Colors indicate increase (green) or decrease (red) of the measured environmental parameters with increasing distance-to-sea, surface-elevation or soil-depth. Given numbers and width of the red and green bars represent Spearman's ρ (metadata in Table S1).

	Chloride	Organic Matter	Acetate	Pyruvate	Isocitrate	Nitrate	Sulfate	Reduction
Distance-to-sea	**-0.77**	0.24	0.42	0.20	**0.61**	0.16	**-0.69**	0.22
Surface-elevation	-0.13	-0.31	-0.01	-0.28	0.05	0.27	-0.18	-0.11
Soil-depth	0.12	**-0.75**	-0.26	0.46	0.12	-0.24	0.08	**0.78**

We assessed the extent to which wetland microbiota harbor the potential for dark CO_2 fixation, and how gene and transcript abundance vary along environmental gradients in distance-to-sea, surface-elevation and soil-depth (Figure 1). In total, our sampling design includes 69 amplicon data sets (Figure 2) as well as 18 metagenome and the corresponding metatranscriptome data sets (Figure 4) with associated organic matter, reduction index, chloride, nitrate, sulfate, acetate, pyruvate and isocitrate data (Table 2, Table S1). All underlying samples were collected in September. Thus, all resulting data represent a snapshot at this time of year.

Community composition shifts of wetland microbiota

Phylogenetic analysis was performed to obtain further insight into the metabolic capabilities of wetland microbiota (Bowen et al., 2012; Tebbe et al., 2022). Samples were taken as soil cores at 18 locations, and DNA and RNA were extracted as specified in the Material and Methods. The 16S rRNA amplicon sequencing results of all 69 samples indicated that the top 4 most abundant orders were Campylobacterales with an average of 10.2%, Burkholderiales with an

average of 9.7%, Flavobacteriales with an average of 3.9% and Anaerolineales with an average of 3.3% (Figure 2). Campylobacterales, Burkholderiales and Anaerolineales harbor species capable of CO_2 fixation (Banda et al., 2020; Guo et al., 2015; Llorens-Marès et al., 2015). Comparing the abundance of the 25 most abundant orders, shifts in community composition occur along the different environmental gradients (Figure 2).

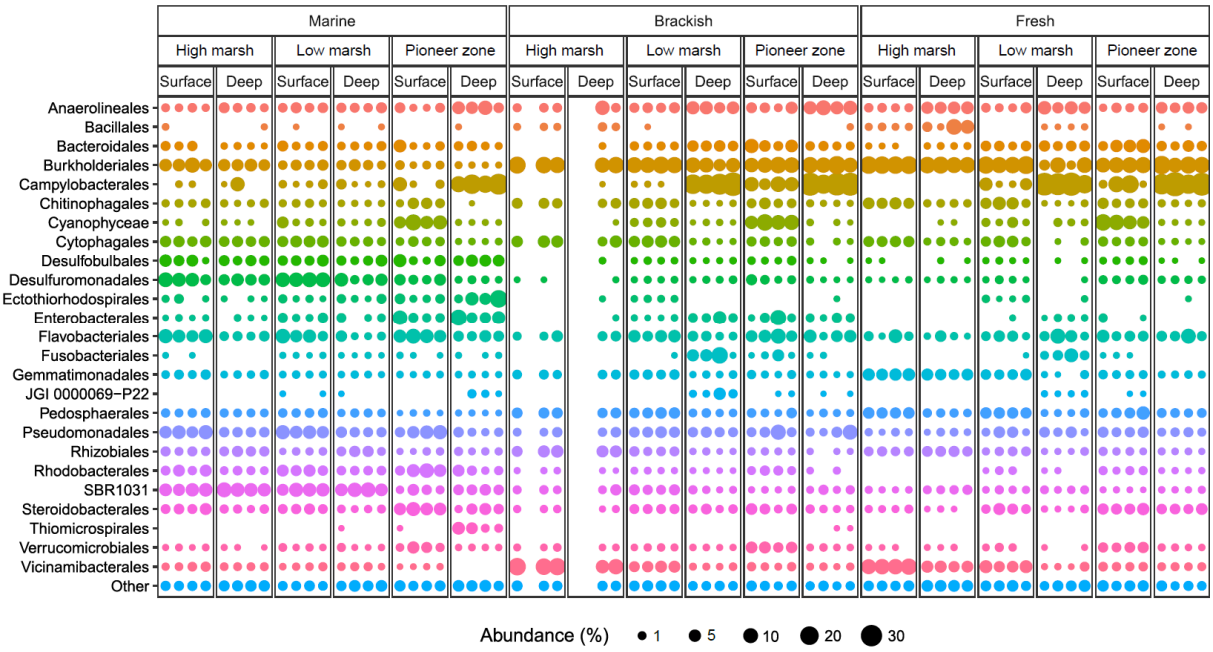

Figure 2. Taxonomic composition of bacterial communities at the order level for the 18 sampling locations with four biological replicates (four different cores with 2 m distance each) resulting in a total of 69 analyzed samples (three replicates could not be included due to insufficient sequence quality). Samples originate from the three sites: Salt marsh (marine), brackish marsh (brackish) and freshwater marsh (fresh). Each site was sampled at the three zones: High marsh, low marsh and pioneer zone. Each zone was sampled at the surface layer at 0 cm (surface) and the deep layer at 50 cm depth (deep). Depicted are the 25 orders with the highest average relative abundances. All other orders were combined into the "Other" group.

16S rRNA provides the advantage of observing multiple functional group shifts simultaneously. However, connecting phylogenetic groups to function is challenging due to microbial plasticity and functional redundancy. Limited knowledge exists about the impact of microbial composition on community-level physiological profiles (Yarwood, 2018).

Metagenomics show high potential for microbial CO_2 fixation in estuarine wetlands

The analyses presented above reveal a high phylogenetic diversity, which strongly suggests a corresponding high metabolic diversity within the marsh soil microbiota. While many of the identified orders harbor species capable of CO_2 fixation (Banda et al., 2020; Guo et al., 2015; Llorens-Marès et al., 2015), we wanted to assess the functional genetic potential for dark CO_2

fixation along environmental gradients (Figure 1B). We sequenced 18 metagenomes. For each sample a minimum of 54 million and an average of 99 million reads were obtained with an average N50 value of 1,173. A schematic overview of the bioinformatic workflow is provided below (Figure 3).

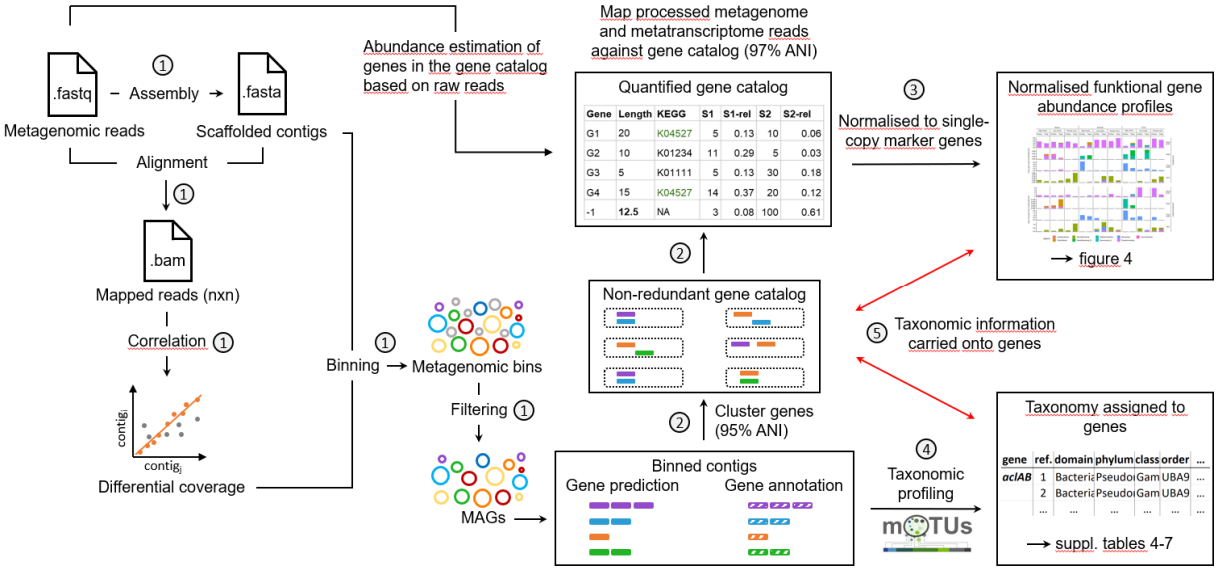

Figure 3. Schematic overview of sequence analyses using a gene catalog pipeline for metagenomic and metatranscriptomic reads. 1) Processed reads from each sample were assembled independently, and all samples were used to guide per sample binning. 2) Gene prediction and annotation were performed on all prokaryotic MAGs, and a non-redundant gene catalogue was built using a clustering threshold of 95% ANI. 3) Processed metagenome- and metatranscriptome reads were mapped against the gene catalogue and normalized based on gene length (within sample normalization) and single-copy marker gene abundance (between sample normalization). 4) MAGs were placed into species level mOTUs using single copy marker genes, and assigned taxonomy using GTDB-TK, used for accurate taxonomic profiling. 5) Information linking taxonomy from MAGs and gene/transcript abundance was maintained at all times to allow for taxonomic interrogation of functional gene abundance.

On the basis of the obtained metagenome data, we analyzed the relative abundance of key genes for the metabolic pathways involved in microbial CO_2 fixation. We aimed to develop a pipeline using multiple genes, genomic context and taxonomic information to assess the completeness of dark CO_2 fixation pathways. Detailed information on this pipeline are provided in the Material and Methods section and the supplement (Text S1, Figure 4, Table 1).

Based on this approach we were able to detect the presence of four out of seven CO_2-fixing pathways, although with varying copy numbers along the environmental gradients (Figure 1B). The copy number of the four key genes that belong to the four present CO_2-fixing pathways in our samples, ranged from a mean gene copy number/genome of 0 to 0.48.

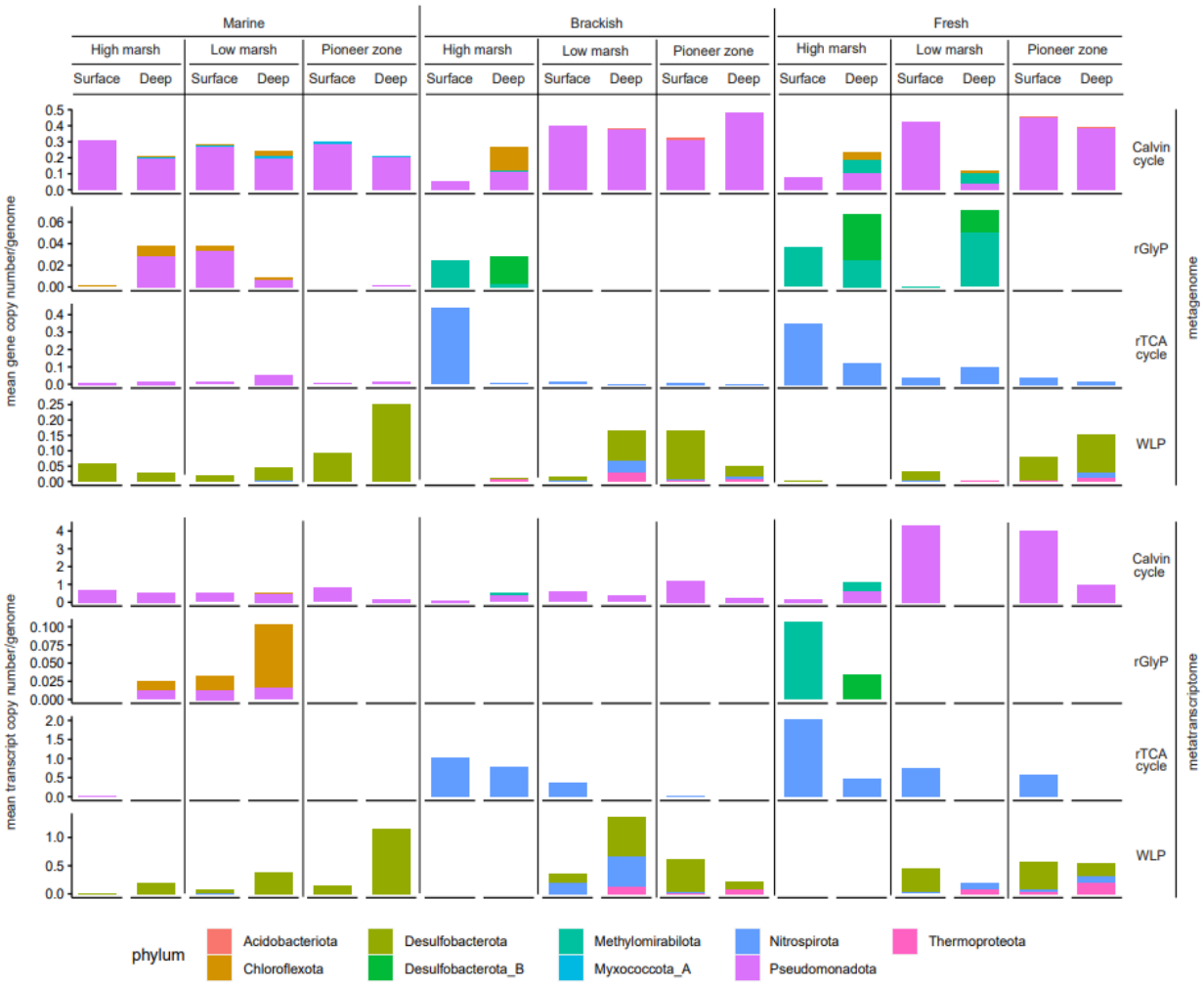

Figure 4. Metagenome and metatranscriptome analysis of CO_2-fixing pathways. Abundance of the key genes (copy number per genome) (metaG) ATP-citrate lyase (for rTCA), acetyl-CoA synthase (for WLP), RuBisCO (for Calvin cycle), glycine reductase (for rGlyP), and their respective transcripts (metaT) normalized to single copy marker gene. Colors represent the respective microbial groups of the MAGs to which the key genes were assigned to. The 18 depicted samples originate from the three sites: Salt marsh (Marine), brackish marsh (Brackish) and freshwater marsh (Fresh) reflecting the distance-to-sea gradient. Each from the three zones: High marsh, low marsh and pioneer zone reflecting the surface-elevation gradient. Each from the surface layer at 0-5 cm (Surface) and the deep layer at 45-50 cm depth (Deep) reflecting the soil-depth gradient.

The rGlyP had the lowest abundance of the four present CO_2-fixing pathways with a mean gene copy number of 0 to 0.07 per genome. The most frequently detected pathway was the Calvin cycle, which had copy numbers ranging from 0.05 to 0.48. (Figure 4).

The Calvin cycle was mainly assigned to MAGs belonging to the phylum Pseudomonadota. The taxonomy behind the rGlyP appeared to be more diverse and depending on the environmental niche. Chloroflexota and Methylomirabilota were the most prominent representatives of the rGlyP. The rTCA cycle was mainly assigned to the phylum of Nitrospirota. The WLP was predominantly assigned to Desulfobacterota.

Considering the number of shared genes/enzymes between the 3-HP bicycle, the 3-HP/4-HB cycle and the DC/4-HB cycle, their overlap with other carbon-fixing pathways and the potential redundancy of genes with other metabolic pathways, ultimately proving the functionality of these pathways from metagenome data is tenuous. Despite this we still sought to identify genomes, where these pathways are present and use this data to explore their ecological significance. Based on the complete absence of the relevant genes and transcripts from any genome we considered that the 3-HP bicycle, 3-HP/4-HB cycle and the DC/4-HB cycles were completely absent from genomes in our samples.

Metatranscriptomics reveal high transcript abundance of key genes related to microbial CO_2 fixation

Based on the observation that Calvin cycle, rGlyP, rTCA and WLP were present along the investigated environmental gradients (Figure 1B, 4), we asked to what extent these genes were transcribed. Therefore, we analyzed the transcription level of the key genes involved in these pathways (Table 1, Figure 4). RNA from a total of 18 soil samples was extracted as described in the Material and Methods section, used for mRNA sequencing, and mapped to the metagenome (Table 1, Figure 4). For each sample, a minimum of 50 million and an average of 80 million reads were obtained with an average N50 value of 750. We detected transcripts of all four CO_2 fixation-related key genes that were already detected in the metagenome analysis. The number of mapped transcripts varied strongly along the environmental gradients (Figure 1B, 4). Transcripts ranged from a mean transcript copy number/genome of 0 to 4.31 (Figure 4). Among all present CO_2-fixing pathways, the rGlyP key gene showed the lowest transcript abundance along all gradients (Figure 4B). For some pathways, the high transcript abundance was confined to specific environmental niches. Based on our MAG analysis, we were able to assign function to taxonomy (Figure 4, Tables S4-S7).

Transcripts for all key genes were predominantly associated with a limited number of microbial groups ranging from one to five different phyla for each pathway. The rTCA cycle was primarily driven by Nitrospirota. Main drivers behind the WLP were the phyla Desulfobacterota, Nitrospirota and Thermoproteota. The Calvin cycle was predominantly assigned to the phylum Pseudomonadota. Transcripts of the rGlyP at the marine site were mainly assigned to Chloroflexota and Pseudomonadota. The rGlyP transcripts at the freshwater site were assigned to Methylomirabilota and Desulfobacterota.

On the transcriptome level, we found three significant correlations ($p < 0.05$) with environmental soil parameters (Figure 4, Table 3). We observed a significant increase ($p < 0.05$)

in the transcript abundance of the WLP key gene with increasing reduction. We found, that with increasing transcript abundance of the rTCA cycle key gene, also the nitrate availability increased significantly ($p < 0.05$). Transcript abundance of the Calvin cycle key gene increased significantly ($p < 0.05$) with higher organic matter availability (Figure 4, Table 3).

Table 3. Statistical analysis of the transcript abundance for the key genes of the four present CO_2-fixing pathways correlating with environmental parameters. Significant correlations are indicated by bold numbers ($p < 0.05$). We performed a Spearman's rank correlation analysis with the transcript abundances of the key genes and eight soil environmental parameters. Colors indicate increase (green) or decrease (red) of the gene and transcript abundance with increase of the respective soil parameter. Given numbers and width of the red and green bars represent Spearman's ρ (metadata in Table S1).

	Chloride	Organic Matter	Acetate	Pyruvate	Isocitrate	Nitrate	Sulfate	Reduction
Calvin cycle	-0.23	**0.62**	0.22	0.06	0.22	-0.27	-0.13	-0.30
rGlyP	0.04	-0.24	-0.01	-0.07	-0.20	0.24	0.11	-0.24
rTCA cycle	-0.40	0.19	0.22	-0.28	-0.08	**0.67**	-0.30	-0.43
WLP	0.09	0.05	-0.16	0.35	0.05	-0.45	0.05	**0.48**

Discussion

Phylogenetic and metagenomic analyses identified both heterotrophic and chemo- or photoautotrophic microorganisms. The main orders observed were Campylobacterales, Burkholderiales, Flavobacteriales and Anaerolineales, of which Campylobacterales, Burkholderiales and Anaerolineales harbor species that are capable of CO_2 fixation (Banda et al., 2020; Guo et al., 2015; Llorens-Marès et al., 2015). Furthermore, it is known that the genetic potential for dark CO_2 fixation is spread over a broad taxonomic range (Šantrůčková et al., 2018). In general, for all sites, the diversity of 85 different phyla and 185 different classes indicated a highly diverse metabolic potential of the microbiota, considering there is a total of 89 bacterial phyla known in the Silva database (Yilmaz et al., 2013).

To analyze the genetic and transcriptomic potential of dark CO_2 fixation in Elbe estuary marsh soils, we examined the key genes crucial for the functioning of the respective microbial pathways. Key gene identification is a common concept explored in several previous studies using metagenomics, amplicon sequencing, or qPCR (Liu et al., 2022; Yang et al., 2021). However, our genome-guided approach questions the validity of using single marker genes to confirm occurrence, diversity, and abundance of these processes in complex soil environments.

Traditionally, the term 'marker gene' or 'key gene' likely derives from culture-based approaches where light-independent autotrophic growth indicates the necessity of a dark CO_2 fixation pathway. The identity of a specific dark CO_2 fixation pathway can be inferred from detecting particular key marker genes. However, the assumption that presence of these genes indicates light-independent autotrophic growth can be misleading. Although we identified genomes with many marker genes, we could confirm the entire pathway in only a limited number of genomes. The redundancy of these marker genes with other metabolic processes, along with incomplete CO_2 fixation pathways, necessitates additional scrutiny. This raises concerns about quantitative approaches like qPCR distinguishing between complete and incomplete pathways while still capturing a broad diversity that exists between genomes with complete pathways. Although tools like metaCyc are often used to estimate pathway completeness in incomplete MAGs and have been included in several studies, we did not use this approach in our analysis. These tools can overestimate pathway completeness as 60-70% of the genes may overlap with other CO_2 fixation pathways or metabolic processes. Detection thresholds of 75-80% can lead to scenarios where many pathway-specific genes may be absent while still indicating the genome's presence. We want to reiterate that these tools are valid for isolates with known physiological data or for initial screenings of many genomes. However, they may be inadequate for complex, often unknown soil metagenomes where key genes overlap across multiple metabolic pathways.

Metagenome and metatranscriptome sequence analyses indicate the functioning of the Calvin cycle, WLP, rGlyP and rTCA cycle in the marsh soils of the Elbe estuary, suggesting a relevant potential for microbial CO_2 fixation. Our sampling design covers steep environmental gradients, especially in relation to distance-to-sea and soil-depth. Distance-to-sea was significantly negatively correlated with porewater chloride (i.e., salinity), sulfate, and isocitrate concentrations. Soil-depth was significantly positively correlated with the reduction index, reflecting oxygen deficiency, and negatively with organic matter availability (Table 2, Table S1).

Our hypotheses that (I) increasing salinity and (II) decreasing oxygen availability increase dark CO_2 fixation could only partly be confirmed. No pathway shows a significant response to sulfate or chloride concentrations. The strongest albeit not significant response to sulfate and chloride shows the rTCA cycle which showed nearly no transcript abundance at the marine site (Table 3). In contrast, hypothesis (II) could be confirmed for the WLP that showed a high abundance in samples with a high reduction potential, i.e. low oxygen availability. The explanation for this lies in the fact that the WLP is a strictly anaerobic pathway (Figure 4, Table 3; Lücker et al., 2010; Sakoula et al., 2021).

Even if the rTCA cycle is restricted to anaerobic or microaerophilic organisms (Jiang et al., 2022), we show that it is not restricted to strictly anaerobic environments that we would expect in the deep soil layers. Our findings indicate a preference of the rTCA cycle to soil surface environments, which are rich in organic matter and have a higher oxygen availability than the deep soil environments (Figure 4, Table 3). Another characteristic of the organic-rich high marsh topsoils is the formation of anoxic microsites (Lehto et al., 2014). These areas, characterized by greater organic matter availability, support higher rates of heterotrophic microbial activity and thereby higher CO_2 concentrations in the soil. In previous studies, the resulting stimulation of CO_2 fixation was correlated with respiration (Berg et al., 2022; Miltner et al., 2005; Mueller et al., 2020a; Šantrůčková et al., 2018). The phylum behind the highest level of transcription of the rTCA was Nitrospirota, contributing nearly 100% of the ATP citrate lyase transcripts. *Nitrospira sp.* Palsa-1315 was the dominating genus behind the ATP citrate lyase transcripts (Figure 4, Table S4). It belongs to the clade B *Nitrospira* (Sakoula et al., 2021), and so far, no pure culture of clade B *Nitrospira* exists, therefore physiological responses to environmental controls need to be further established (Zhao et al., 2021). Our transcriptomic results reveal that the genus *Nitrospira sp*. Palsa-1315 only occurs in brackish to freshwater environments. Further, we observed a significant correlation between the transcript abundance of the reverse tricarboxylic acid (rTCA) cycle key gene (*aclA*) and measured nitrate levels, with nearly all transcripts assigned to the genus *Nitrospira*. This finding is consistent with the known metabolic function of *Nitrospira* species as nitrite oxidizers, which catalyze the conversion of nitrite to nitrate (Daims et al., 2015). The increased transcript levels of the rTCA cycle in *Nitrospira* suggest a heightened metabolic activity in response to elevated nitrite concentrations, thereby leading to increased nitrate production. This finding suggests that *Nitrospira* simultaneously oxidizes nitrite to nitrate and fixes CO_2 via the rTCA cycle in the marsh soils of the Elbe estuary. The energy derived from nitrite oxidation facilitates CO_2 fixation, supporting the autotrophic lifestyle of *Nitrospira*. This dual capability underscores the importance of *Nitrospira* in both the nitrogen and carbon cycles (Lücker et al., 2010; Mundinger et al., 2019).

The gene abundance and transcription for the key enzyme of the Calvin cycle, i.e. RuBisCO, is not strictly dependent on the availability of light although its highest transcript abundance was recorded in two surface layer samples. For other wetland ecosystems, Burkholderiales was found to be one of the dominant photosynthetic orders (Guo et al., 2015). However, in our study, we did not detect any photosynthetic genes (*puf* operon) in the genomes of organisms with the *rbcL* gene. This suggests that the Calvin cycle is not driven by photosynthesis. Rather,

we detected sulfur oxidizing genes in the form of either the thiosulfate dehydrogenase (*tsd*) or the sulfur oxidizing protein (*soxZ*) in the genomes of nearly all *rbcL* positive genomes (Figure 4, Text S1). This indicates that the Calvin cycle is used for chemoautotrophic growth (Storelli et al., 2013). Sulfide oxidation relies on the availability of oxygen but at the same time reducing conditions that enable sulfate reduction to provide sulfide (Starkey, 1966). We assume this coupled process of sulfide oxidation and sulfate reduction might be facilitated in organic matter-rich topsoils with anaerobic microsites. Yet, it is surprising that the Calvin cycle transcript abundance exhibited by Pseudomonadota is particularly high at the freshwater sites where sulfate availability is lower than in the salt marsh, but comparable to the brackish marsh (Table S1). Potentially, greater sulfur cycling despite lower sulfur input in the freshwater marsh is linked to differences in plant community composition among the three marsh sites (Branoff et al., 2024). Marsh rhizospheres are characterized by strong redox-oscillations that accelerate coupled sulfate reduction/sulfide oxidation (Grüterich et al., 2024b; Rolando et al., 2024).

We observed that transcript abundance for the WLP is linked to the deep soil layers (Figure 4, Table 3). The data therefore suggest that low oxygen availability is the driving environmental factor favoring WLP activity because deep soil layers are primarily characterized by low-O_2 concentrations. Recent transcriptome studies in brackish water microbial mats showed that Desulfobacterota are capable of expressing the WLP and subsequent acetate and pyruvate metabolism (Vigneron et al., 2021). This notion is supported by our taxonomic assignment, which indicates that Desulfobacterota play an important role in the transcription of WLP key genes (Figure 4, Table S5).

Conclusion and perspective

Our study demonstrates that wetland microbiota are drivers for dark CO_2 fixation. Wetlands cover only 1% of the Earth's surface, but store about 20% of the total ecosystem organic carbon stock (Temmink et al., 2022). Their disproportionate role in the global organic carbon budget arises from an imbalance between plant primary production, which adds organic carbon to the soil, and microbial decomposition, which breaks it down (Temmink et al., 2022). In wetlands, microbial decomposition is typically slow due to in general oxygen-poor conditions in the soils. However, the CO_2 produced through microbial decomposition accumulates, reaching high concentrations under the waterlogged conditions of wetland soils (Beer & Blodau, 2007; Megonigal et al., 2004). Therefore, dark CO_2 fixation seem to be of high relevance in wetland soils with potentially important consequences for the climate system. Therefore, our study

assessed how the expression of dark CO_2 fixation in wetland ecosystems varies along environmental gradients within one of the major European estuaries.

Our major findings are a) Only five microbial phyla (Pseudomonadota, Chloroflexota, Methylomirabilota, Nitrospirota and Desulfobacterota) are associated with the majority of dark CO_2 fixation assigned transcripts. b) Both community composition and the gene and transcript abundance of CO_2 fixation related genes show a high variability in relation to environmental gradients within the estuarine wetland landscape. c) Transcript abundance for the WLP seems to be driven by oxygen. d) Transcript abundance for the rTCA cycle positively correlates with nitrate, indicating a coupled nitrite oxidation and CO_2 fixation in *Nitrospira* species. e) Transcript abundance for the Calvin cycle significantly correlates with organic matter availability. f) Variations in the expression of specific functional genes across environmental gradients are more prominent than phylogenetic variations of microbial groups related to dark CO_2 fixation. These findings suggest that functional diversity plays a crucial role by allowing microorganisms to adapt to their specific environment. This, in turn, leads to niche formation as microorganisms specifically use the pathways that make the most efficient use of their ecological potential.

Concerning our metatranscriptomic analyses it is important to note that although transcriptomes are a good tool to demonstrate the actual transcription of a gene, it must be considered that this is always only a snapshot at the time of sampling. Therefore, in further studies, a temporal component, either short-term to cover the tidal cycle or long-term to cover seasonal effects, should be considered in addition to spatial scales. Our study aimed at understanding the drivers of dark CO_2 fixation pathways along environmental gradients, and, for the majority of pathways, we succeeded at identifying important environmental controls. However, our study cannot determine the relative importance of dark CO_2 fixation pathways in terms of counterbalancing ecosystem GHG production. There is an increasing number of studies indicating negative CO_2 fluxes in the dark for many ecosystem types such as saline/alkaline soils, dry inland waters and dry river sediments (Koschorreck et al., 2022; Ma et al., 2013; Marcé et al., 2019). Future molecular research will need to incorporate various biogeochemical tools to understand the relative importance of microbial dark CO_2 fixation in the climate system.

Acknowledgements

This study was funded by the Deutsche Forschungsgemeinschaft (DFG, German Research Foundation) within the Research Training Group 2530 (RTG2530): “Biota-mediated effects on Carbon cycling in Estuaries” (project number 407270017; contribution to Universität Hamburg

and Leibniz-Institut für Gewässerökologie und Binnenfischerei im Forschungsverbund Berlin e.V. (IGB)).
This work was supported by the DFG Research Infrastructure NGS_CC (project 407495230) as part of the Next Generation Sequencing Competence Network (project 423957469) and core funding from ETH Zürich to the Microbiome Research Laboratory headed by S.S. Metatranscriptome and 16S rRNA sequencing were carried out at the Competence Centre for Genomic Analysis (Kiel).
Peter Mueller was supported by the Deutsche Forschungsgemeinschaft (DFG; German Research Foundation) in the framework of the Emmy Noether Program (502681570).

Author contributions

L.G. and W.R.S. designed the study and wrote the manuscript. H.J.R. led the metagenomic and metatranscriptomic data processing. P.M. contributed to the development of the conceptual framework and developed the statistical approach. H.-P.G., P.M and J.N.W. edited the manuscript. S.S. contributed computational resources. L.G. and A.T. performed laboratory work and analyzed the data. J.N.W. contributed to the analysis of data. W.R.S. and H.-P.G. supervised the work of L.G. within the RTG2530. All authors reviewed the manuscript.

Chapter 3

Transcriptomic Response of Wetland Microbes to Root Influence

Published at iScience (2024) – DOI: 10.1016/j.isci.2024.110890

Luise Grüterich*, Monica Wilson*, Kai Jensen, Wolfgang R. Streit, Peter Mueller

*these authors contributed equally to the manuscript.

Abstract

Wetlands are hotspots for carbon and nutrient cycling. The important role of plant-microbe interactions in driving wetland biogeochemistry is widely acknowledged, prompting research into their molecular biological basis for a deeper understanding of these processes. We analyzed transcriptomic responses of soil microbes to root exudates in coastal wetland soils using $^{13}CO_2$ pulse labeling. Metatranscriptomics revealed 388 upregulated and 11 downregulated genes in response to root exudates. The Wood-Ljungdahl pathway and dissimilatory sulfate reduction/oxidation were the most active microbial pathways independent of root influence, whereas pathways with the strongest upregulation in response to root influence were related to infection, stress response, and motility. We demonstrate shifts within the active community toward higher relative abundances of Betaproteobacteria, Campylobacterota, Kiritimatiellota, Lentisphaerota, and Verrucomicrobiota in response to exudates. Overall, this study improves our mechanistic understanding of wetland plant-soil microbe interactions by revealing the phylogenetic and transcriptional response of soil microorganisms to root influence and exudate input.

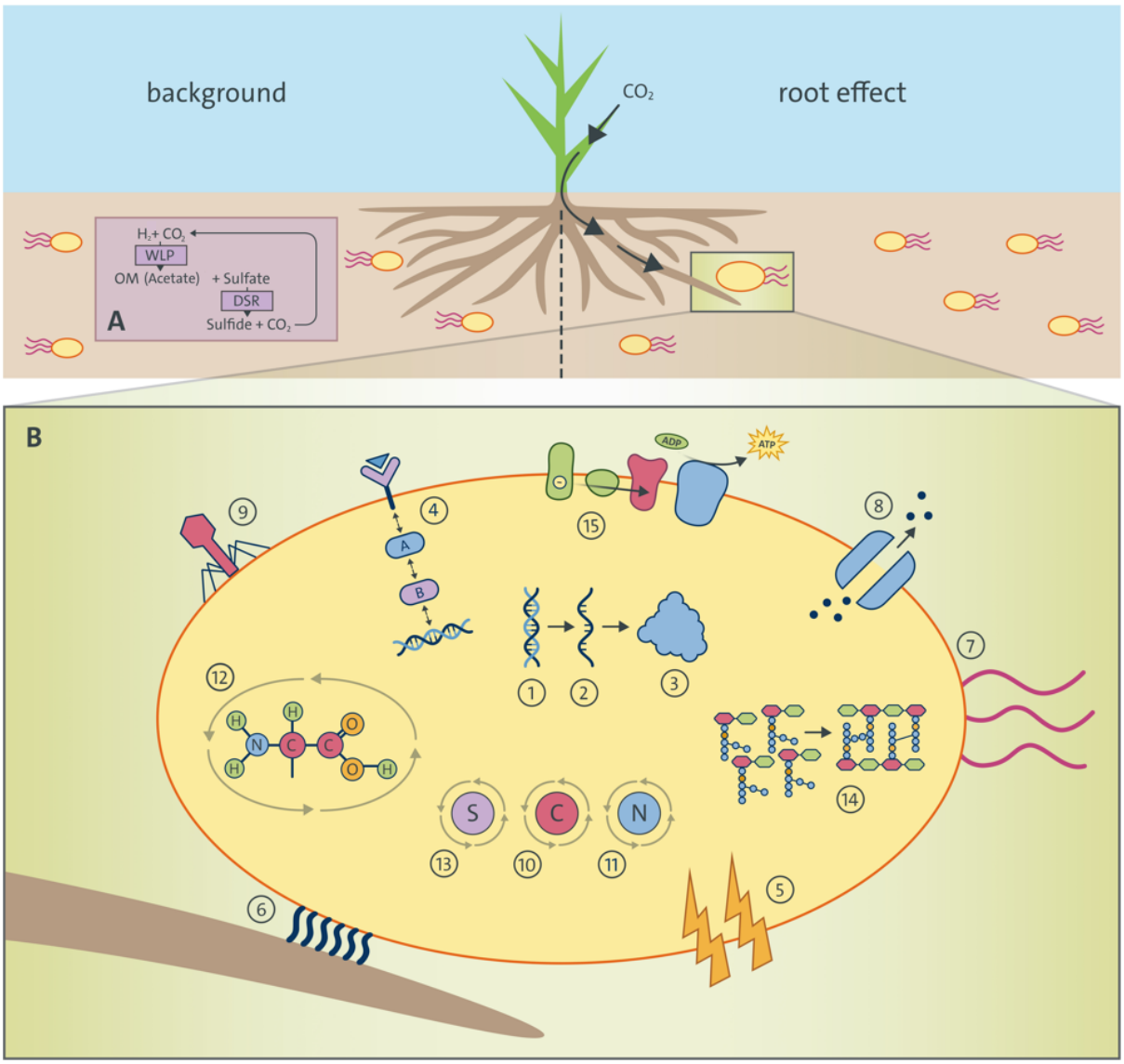

Figure 1. Conceptual representation of upregulated microbial processes in response to plant influence (B) and independent of plant influence **(A).** Yellow objects represent the soil microbes. Independent of plant influence, key genes of the Wood-Ljungdahl pathway and dissimilatory sulfate reduction exhibit the highest transcript abundances (A). Frame B shows a zoom into one of the microbes influenced by exudate input. In response to exudate input, 338 genes show significant upregulation (adjusted $p < 0.05$) and can be categorized into the following metabolic pathways. 1) Transcription, 2) Translation, 3) Proteostasis, 4) Signal transduction and exchange, 5) Stress response, 6) Adhesion, 7) Motility, 8) Transport, 9) Infection, 10) Carbon metabolism, 11) Nitrogen metabolism, 12) Amino acid metabolism, 13) Sulfur metabolism, 14) Cell wall synthesis and 15) Electron transport. Image by courtesy of UHH/Alpen.

Introduction

The rhizosphere is defined as the volume of soil influenced by root activity (Hiltner, 1904). Roots influence the physical and chemical properties of the soil matrix, the availability of soil resources (e.g., water and dissolved nutrients), and the activity of soil biota within the rhizosphere. The extent of root influence is a heterogeneous continuum that is characterized by strong biological, physical and chemical gradients (Koop-Jakobsen et al., 2021; Koop-Jakobsen

et al., 2018). These gradients are produced by a complex array of factors, including biota-mediated processes such as rhizodeposition, root and microbial respiration, plant nutrient uptake, microbial signaling, and microbial degradation (Kuzyakov & Razavi, 2019; Ren et al., 2022). Strong biotic interactions between plant roots and soil biota to access limited soil resources make the rhizosphere a hotspot for biological activity and element exchange (Kuzyakov & Blagodatskaya, 2015; Neumann & Römheld, 2012).

Rhizodeposition is a key process shaping plant-soil microbe interactions in the rhizosphere (Dijkstra et al., 2021). While rhizodeposits encompass all root-derived organic inputs that enter the soil matrix regardless of origin and release mechanism (Oburger & Jones, 2018), primary and secondary metabolites released from intact, living roots, i.e. root exudates (Neumann, 2007), are particularly strong drivers of the microbial community (Eisenhauer et al., 2017; el Zahar Haichar et al., 2014; Nguyen, 2009). Root exudates include low-molecular-weight compounds (e.g. sugars, amino acids, and organic acids) (Canarini et al., 2019) and secondary metabolites (e.g. phenolics, flavonoids and terpenoids) (Gargallo-Garriga et al., 2018) as well as high-molecular-weight compounds (e.g. polymer-rich mucilage and proteins). Long-term tracer studies using isotopically labeled CO_2, e.g., continuous labeling, have been conducted to quantify net rhizodeposition (Jones et al., 2004; Kuzyakov & Domanski, 2000; Pausch & Kuzyakov, 2018). However, pulse labeling, applied over short periods, is best suited to trace the fraction of new assimilates (Oburger & Jones, 2018; Studer et al., 2014), dominated by low-molecular-weight compounds via root exudation into the rhizosphere (Meharg, 1994; Stevenel et al., 2019).

There are a number of favorable and adverse effects of root exudates on soil microbial communities (Bais et al., 2006). These biotic interactions are enabled through complex chemical signaling both to and from the roots (Hirsch et al., 2003; Rasmann & Turlings, 2016; Wang et al., 2021). Root exudates provide carbon- and energy-rich metabolic substrates for microorganisms in an otherwise carbon-limited environment. The input of carbon and increased soil respiration can shift the microbial community composition toward rapidly growing bacteria, *r*-strategists (Sun et al., 2021). Numerous studies have demonstrated that the plant-controlled recruitment of rhizosphere microorganisms such as plant growth-promoting bacteria (Samaras et al., 2022) and symbiotic mycorrhizal fungi (Jones et al., 2004) is regulated by root exudates (Herz et al., 2018; Schmid et al., 2019). Additionally, the exudation of secondary metabolites, antimicrobial compounds or chemo-attractants can be seen as a plant-defense mechanism to suppress pathogenic microbial groups (Bais et al., 2004; Bezerra et al., 2021).

Finally, plant-derived B-vitamins and other metabolites can affect the growth of soil microbes (Rovira & Harris, 1961; Streit et al., 1996).

The majority of rhizosphere studies on plant-soil microbe interactions has been conducted in upland terrestrial soil systems, with a particular focus on crops in agricultural soils. Studies on the rhizospheres of legumes (Hartmann et al., 2008; Phillips & Streit, 1996), wheat (Ji et al., 2023), barley (Kuzyakov & Domanski, 2000; Timmusk et al., 2011) and maize (Rudolph-Mohr et al., 2017; Rüger et al., 2021) have revealed many aspects of rhizosphere biology, such as the quantitative estimation of rhizodeposition (Kuzyakov & Schneckenberger, 2004; Pausch & Kuzyakov, 2018; Qiao et al., 2017), microbial substrate utilization (Oburger & Jones, 2009), nutrient competition between plants and soil biota (Dijkstra et al., 2013), and the regulation of rhizosphere processes under elevated temperature (Zhang et al., 2020). Yet, while there is a growing body of research refining our understanding of plant-soil microbe interactions in upland terrestrial soils, there remains a significant gap in our knowledge regarding the transferability of these findings to plant-soil microbe interactions in rhizospheres characterized by contrasting abiotic and biotic environmental conditions, such as those found in wetlands and marine sediments (Ren et al., 2022; Rolando et al., 2022). (Meta-)transcriptomic approaches are increasingly being used to elucidate key genes expressed in wetland plant-microbe interactions (Cai et al., 2022; Rolando et al., 2024; Su et al., 2019), however, transcriptomic analysis of prokaryotes in wetland rhizospheres remains challenging (Carvalhais et al., 2013) with markedly few studies available (e.g., Lu & Conrad, 2005; Rolando et al., 2024).

Frequent flooding and waterlogging in wetland soils strongly reduces the availability of oxygen, thereby limiting terminal electron acceptors and leading to lower rates of major microbial metabolic pathways as well as a shift toward anaerobic metabolism compared to well-aerated upland soils (Megonigal et al., 2004). The impact of oxygen limitation on metabolic diversity has been predominantly studied in hydric soils, given that anaerobic sites in upland systems are mainly restricted to the interior of aggregates (Keiluweit et al., 2017). However, in wetlands, microbial communities are constrained by both carbon substrates (i.e., electron donors) and the availability of oxygen or alternative terminal electron acceptors (Sutton-Grier et al., 2011). Thus, root exudates may cause fundamentally different plant-microbe interactions in wetland compared to upland soils (Yamauchi et al., 2013).

The present study aims to improve our mechanistic understanding of wetland plant-soil microbe interactions by studying the phylogenetic and transcriptional response of soil microorganisms to root influence and exudate input. Using $^{13}CO_2$ pulse labeling and carbon tracing, we analyzed the microbial response to root influence in the anoxic rhizosphere of the common coastal

wetland grass *Spartina anglica*. In particular, we aimed to determine the influence of root exudation on microbial gene expression, identify which metabolic pathways are affected, understand which microbial taxonomic groups are primarily involved, and compare these responses to the bulk soil microbial community.

Material and Methods

To evaluate the influence of root activity and, particularly, exudate input on soil microbial gene expression, we conducted a $^{13}CO_2$ pulse labeling experiment and traced the flux of recently formed photo-assimilates into the rhizosphere. We used the ^{13}C signal of soil samples as a proxy for the presence of root exudates (Figure S2) and distinguished soil and rhizosphere micro-environments that received root exudates (n = 3) from those that did not (n = 3) using isotope-ratio mass spectrometry. We conducted metatranscriptome sequencing of the soil microbial RNA (of bacteria and archaea) and employed both functional annotation and a differential expression analysis for N = 6 metatranscriptomes.

Plant cultivation

Spartina anglica (also known as *Sporobolus anglicus*) is a common salt marsh plant along the European Atlantic coast (Granse et al., 2022). It is the direct allopolyploid descendent of the hybrid *Spartina x townsendii*, which formed in Southern England by hybridization between native *S. maritima* and the introduced *S. alterniflora* (originating from North America) at the end of the 19th century. All individuals of *Spartina anglica* and soil were sampled in June of 2021 from the pioneer zone of a Wadden Sea salt marsh situated at the Hamburger Hallig (54°36’06.2”N, 103 8°49’00.1”E) and cultivated thereafter in a greenhouse on a mixture of native pioneer zone soil, sand and fertilizer until the start of experimentation at the Institute of Plant Science and Microbiology (Universität Hamburg, Hamburg, Germany). Plants were given several weeks to adapt to greenhouse conditions upon sampling from the field. Two weeks prior to pulse labeling, three individuals of similar size and vitality (new shoot growth was observed) were rinsed and transferred into non-transparent plant pots without fertilizer and filled only with freshly homogenized and sieved native soil (pioneer zone; Hamburger Hallig). All pots, including unplanted control pots, were kept under waterlogged conditions prior to and during pulse labeling.

$^{13}CO_2$ pulse labeling

We used a plexiglass cylinder (thickness: 3 mm, diameter: 200/194 mm, height: 45 cm) with a removable lid to construct a labeling chamber. The chamber was equipped with a fan for air

mixing and a sensor measuring atmospheric CO_2, temperature and humidity (K33 LP T/RH Sensor; Senseair). The sensor was connected to an Arduino computer outside the chamber, which recorded the data on a SD card. Only the aboveground plant biomass was placed inside the chamber for $^{13}CO_2$ labeling and was sealed around the shoot base using clamps and plastic film (Figure S1). $^{13}CO_2$ was produced inside the chamber by adding 8 mL of 10% HCl to 0.1 g $NaH^{13}CO_3$ (Sigma-Aldrich, St. Louis, USA). We used a 300-W LED light (Roleadro) as a light source for plant photosynthesis (Figure S1). Plants were labeled daily over eight consecutive days. Label duration was 2-3 h and dependent on the time it took for the plants to draw chamber CO_2 concentrations (>1500 ppm) well below atmospheric concentrations (250-350 ppm).

Soil sample collection and ^{13}C enrichment analysis

After eight days of daily pulse-labeling, intact soil sods (2 liter) extracted from three planted pots and one unplanted control pot were vertically separated into two halves exposing the soils and rhizospheres for sampling. 10 soil subsamples (approximately 1.5 cm^3) were collected from each soil sod at random positions along a transect from the bulk soil toward the root mass using a spatula (N = 40). Subsequently, all 40 soil samples were frozen in 2-ml cryotubes using liquid nitrogen and stored at -80°C until further processing.

Soil samples were dried at 60°C to constant weight and ground using a ball mill (Retsch, Haan, Germany). Carbonates were removed through direct acidification of the soil samples using 10% HCl. Sample were weighed into tin capsules and analyzed for their isotopic ^{13}C signatures using an element analyzer (EURO-EA 3000, Euro Vector, Pavia, Italy) coupled to an isotope-ratio mass spectrometer (Nu Horizon, Nu Instruments, Wrexham, United Kingdom). Among these 40 samples, bulk and rhizosphere soil samples were not pre-determined by their proximity to the root but were operationally defined by their ^{13}C signature. Soil samples with isotopically enriched ^{13}C signatures were defined as impacted by root exudates, i.e. rhizosphere soil, whereas soil samples that showed no indication of ^{13}C enrichment in relation to control soils were defined as not affected by exudates, i.e. bulk soil. All soil samples were ranked by their ^{13}C enrichment in relation to control soils, and samples with the greatest ^{13}C enrichment (n = 3) were compared to samples that showed no ^{13}C divergence from the control (n = 3).

RNA and DNA extraction from soil

2 g of soil were used for RNA extraction using the RNeasy PowerSoil Kit (Qiagen, Venlo, Netherlands) following the manufacturer's protocol. RNA concentrations were quantified using the Qubit 2.0 Fluorometer and the RNA High Sensitivity Assay Kit (RNA HS, Thermo Fisher,

Berlin, Germany). To efficiently assign the RNA sequences to the respective genes, we also sequenced the DNA of two soil samples (one from the rhizosphere and one from the unplanted soil). DNA was extracted from soil samples, and frozen at -80°C until analysis. 0.5 g of soil were used for DNA extraction using the NucleoSpin Soil Kit (Macherey-Nagel, Düren, Germany) following the manufacturer's protocol. Subsequently, the isolated DNA was analyzed at a wavelength of 280 nm using a Nanodrop spectrophotometer (NanoDrop 2000, Thermo Scientific, Waltham, USA).

Metatranscriptome and metagenome analysis

First, the two metagenomes were combined and co-assembled. We used the ATLAS pipeline v2.12.0 (Kieser et al., 2020) that includes an extended workflow for quality control, contig assembly, gene prediction and functional annotation, binning of contigs into MAGs and taxonomic annotation of the MAGs. Among the included tools are several gold-standard tools, e.g. metaSPAdes v3.15.3 for read assembly (Nurk et al., 2017), eggNOG mapper v2.1 and eggNOG database v5.0 for functional gene annotation (Cantalapiedra et al., 2021), maxBin2 v2.2, metabat2 v2.15 and DAS_Tool v1.1.4 for binning and refinement of MAGs (Kang et al., 2019; Sieber et al., 2018; Wu et al., 2016), checkM v1.1.10 for MAG quality assesment (Donovan H Parks et al., 2015) and GTDBtk tool v2.1.1 with GTDB database release207 for taxonomic annotation of the MAGs (Chaumeil et al., 2020). Default parameters were used, except for RAM (up to 1.5 TB) and CPU/threads (up to 80 threads). The co-assembled metagenome had a total of 38 million reads assembled into 87362 contigs with an N50 value of 14,475. 13 MAGs with contamination <10% and with completeness between 70 and 99.8% were extracted. Second, the metagenome data for individual samples were quality controlled using the ATLAS pipeline and the high-quality reads were mapped to the MAGs from the co-assembly using minimap2 v2.14 (Li, 2021) to assess the abundance of the MAGs within the single samples (Table S1). Third, metatranscriptomes were quality controlled using the ATLAS pipeline and high-quality reads were mapped to the genes detected on the assembled contigs from the metagenome co-assembly using minimap2 v2.14 (Li, 2021). Differential genes expression analysis was performed using R 4.0 and DESeq2 package v1.34 (Love et al., 2014). Transcript counts were normalized using the RPM (read per million mapped reads) normalization method to correct for different sequencing depth between the sample. One sample (S3_10_low) has low total reads (Table S1B), but this should be accounted for by DESeq normalization and reflected by a poorer p-value.

Future studies could increase sequencing depth to 40 million reads for better data accuracy. To reduce the large proportion of eukaryotic reads, removing polyA-tailed RNA during library preparation may enrich prokaryotic RNA.

Statistical analyses and data visualization

All transcriptomes were filtered for only prokaryotic reads, to exclude reads that were assigned to the plant. We did this by employing the ATLAS pipeline, which includes the metaSPAdes tool optimized specifically for prokaryotic reads filtering. Despite the more complex gene structures of eukaryotes, such as exons and introns, making gene prediction more challenging, parts of eukaryotic genes could still be predicted and annotated by eggNOG. Subsequently, in the second step, we removed all gene queries annotated to eukaryota. This constituted 0.38% of all gene queries with at least one transcript assigned. Further, 3.77% of all gene queries could not be taxonomically assigned (Figure S3). Since these genes also could not be functionally assigned, they were excluded from the key gene analysis (Figure 3) and the differential expression analyses where we investigated the impact of root exudates on soil microbes (Figure 5). With this we ensured to only analyze the response of bacteria and archaea to root influence. The selection of genes for the key gene analysis (Figure 3) was modified after (Yang et al., 2021). The key gene analysis is based on all transcripts independent of differential expression. The given transcript abundances depict the average of six metatranscriptomes.

For identification of differentially expressed genes, we applied an adjusted p-value < 0.05 and a $\log_2$ fold change > 2, < -2. To investigate which metabolic pathways are upregulated and which are downregulated in response to plant exudate influence, pathway annotation was performed on genes with a significant change in gene expression ($p < 0.05$) based on the „Kyoto Encyclopedia of Genes and Genomes“ (KEGG) database and complemented by in depth literature search in order to cover most of the genes, that could not be assigned through the KEGG database. The distribution of all differentially expressed genes assigned to a given pathway subcategory was visualized in a box and whisker plot in the style of Tukey. All data points that extend beyond 1.5 * IQR of the upper hinge (upper whisker) or below 1.5 * IQR of the lower hinge (lower whisker) are defined as outliers.

Data availability

Raw reads of the metagenomic and metatranscriptomic analysis were deposited at the European nucleotide archive ENA under the project accession number PRJEB73855 (Biosamples:

SAMEA115420425 - SAMEA115420432). The gene catalog is provided as supplementary table 2.

Results

Microbial gene expression

$^{13}CO_2$ pulse labeling and carbon tracing were employed to study the microbial response to root exudation by the common coastal wetland grass *Spartina anglica* under wetland-typical waterlogged conditions. A total of six metatranscriptomes of the bulk and rhizosphere microbiota (Tables S2 and S3) were studied. For each group (i.e., bulk vs. rhizosphere), three independent biological replicates were analyzed. For all six metatranscriptomes, an average of 16 million reads was obtained. In total, 85,886 genes showed a minimum of 1 transcript.

After setting the p-value and log_2-fold change significance thresholds (see methods section metagenome and metatranscriptome analysis), we observed that 388 of the resulting differentially expressed genes were significantly (adjusted $p < 0.05$) upregulated and 11 were significantly (adjusted $p < 0.05$) downregulated (Figure 2A) in response to root exudate influence. A principal component analyses (PCA) using normalized counts showed a clear distinction between the three replicates with high root exudate influence and the three replicates with no root exudate influence. The first principal component (PC1) explained 63% of the variance between the two depicted groups (Figure 2B).

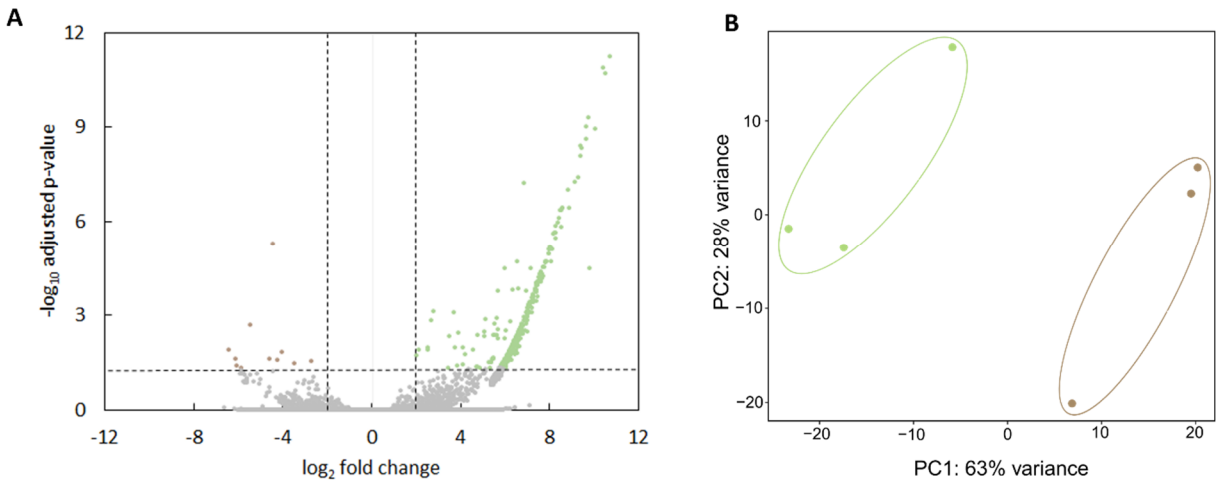

Figure 2. Volcano plot depicts all 85,886 genes with a minimum of 1 transcript assigned. An adjusted p-value < 0.05 and a log_2 fold change > 2, < -2 were used as cutoff (dashed lines). Colored dots indicate genes with significant upregulation (green) or downregulation (brown) in response to root exudate influence. Grey dots indicate genes without significant differential expression (**A**). PCA using normalized counts shows a separation between the three replicates with high root exudate influence (green) and no root exudate influence (brown) (**B**).

Gene expression of the background microbial community

We conducted a key gene analysis on microbial processes independent of root exudate influence to establish the background environmental context of the bulk soil microbial community. This analysis examined the transcript abundances of indicator genes involved in carbon, nitrogen and sulfur cycles (Figure 3A) (gene selection based on Yang et al., 2021).

A

	genes	average transcript abundance
Denitrification	*nosZ*	9
	norB	3
	nirk	0
	nirS	4
	napA	22
	narG	6
Dissimilatory nitrate reduction	*nirB*	8
	nrfA	10
Methanogenesis	*mcrA*	0
Methylotrophy	*mdo*	0
Nitrification	*amoA*	0
	hao	0
Nitrogen fixation	*nifD*	1
	nifH	3
	nifk	2
Sulfur metabolism	*aprA*	4093
	dsrA	967
	dsrB	1235
Thiosulfate oxidation	*soxA*	4
	soxB	57
	soxY	34
Wood-Ljungdahl pathway	*CODH/ACS*	1170
rTCA cycle	*aclAB*	0
RuBisCO	*cbbL*	62
	rbcS	5
DC/4-HB cycle	*abfD*	0
3-HP bicycle	*accD*	22
	PCCB	5
3-HP/4-HB cycle	*K15019*	0
Fructose degradation	*xylA*	26
Glycolysis	*pfkA*	58
	pyk	105
Pentose phosphate pathway	*gnd*	33

B

Wood-Ljungdahl pathway	genes	average transcript abundance
formate dehydrogenase	*fdhA*	223
formyl-THF synthetase	*fhs*	3063
formyl-THF cyclohydrolase	*folE*	45
methylene-THF dehydrogenase	*folD*	263
methylene-THF reductase	*metF*	144
methyltransferase	*aceE*	141
CO dehydrogenase/acetyl-CoA synthase	*CODH/ACS*	1170
phosphotransacetylase	*pta*	38
acetate kinase	*ackA*	19

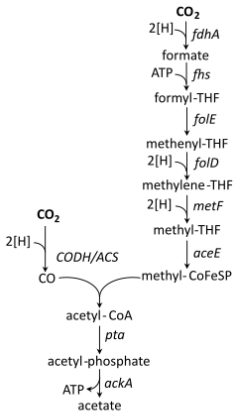

C

Sulfur metabolism

	genes	average transcript abundance
Assimilatory sulfate reduction	*sat*	812
	cysNC	59
	cysH	7
	cysIJ	11
Dissimilatory sulfate reduction/oxidation	*sat*	812
	aprA	4093
	aprB	1066
	dsrA	967
	dsrB	1235
SOX system	*soxA*	4
	soxB	57
	soxC	5
	soxD	1
	soxX	17
	soxY	34
	soxZ	3

Figure 3. Average transcript abundance based on n=6 metatranscriptomes of selected key genes of the carbon, nitrogen and sulfur cycles (**A**), entirety of genes involved in the WLP (**B**) and entirety of genes involved in sulfur metabolism (**C**).

Key genes of the Wood-Ljungdahl pathway (WLP) (*CODH/ACS*) and dissimilatory sulfate reduction/oxidation (DSR) (*sat*, *aprA*, *aprB*, *dsrB*) exhibited the highest transcript numbers across all investigated pathways independently of differential expression with transcript abundances of 4093 (*aprA*), 967 (*dsrA*), 1235 (*dsrB*) and 1170 (*CODH/ACS*) (Figure 3A). We dissected both WLP and sulfur metabolism into their constituent genes and examined their respective transcript abundances (Figure 3B, C). We observed that within these pathways some genes are higher transcribed than others. For the WLP the last two genes (*pta, ackA*), that are responsible for the conversion of acetyl-CoA to acetate, showed nearly no transcripts.

Regarding sulfur metabolism, only the full gene repertoire for DSR showed notable transcript numbers.

To obtain further insight into which microbial groups drove sulfate metabolism and WLP, we performed phylogenetic analysis. The top three microbial groups behind sulfate metabolism were Thermodesulfobacteriota with 34.7%, Gammaproteobacteria with 24% and Deltaproteobacteria with 10.7%. The main microbial groups involved in the WLP were Thermodesulfobacteriota with 66.7% and Deltaproteobacteria with 25%. Community composition analysis for the sulfate metabolism was based on all 75 gene entries assigned to sulfur metabolism key genes. Community composition analysis for the WLP was based on all 12 gene entries assigned to the WLP key genes (Figure 4).

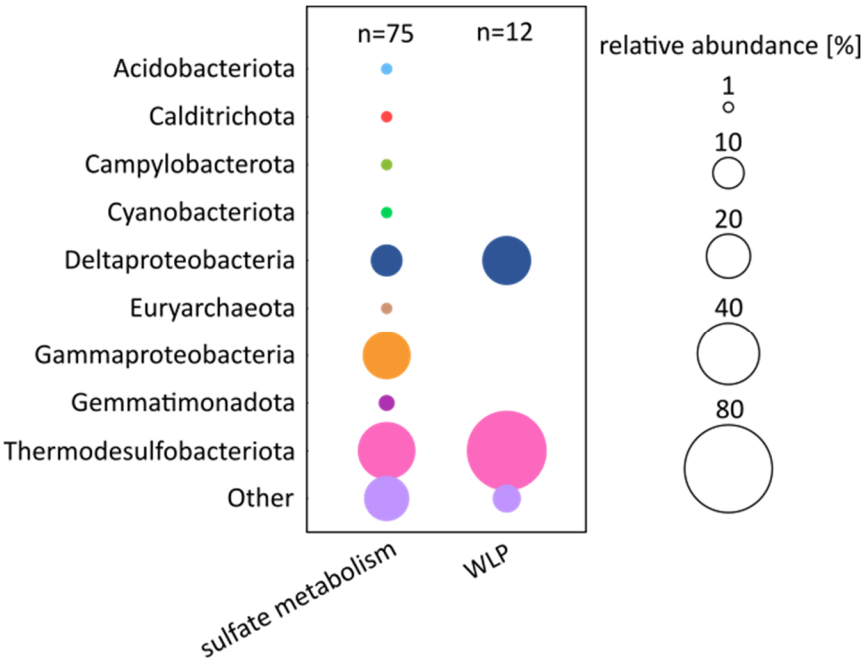

Figure 4. Microbial community composition based on transcripts of key genes assigned to sulfur metabolism (first bar; n=75) and based on transcripts of key genes assigned to the WLP (second bar; n=12).

Transcriptomic changes in response to root exudates

For 338 differentially expressed genes ($p < 0.05$), pathway annotation was possible. Notably, 327 of these genes were upregulated and only 11 were downregulated. These genes were sorted for functional categories into four pathway supercategories and 15 subcategories (listed in Table 1). 'Infection', 'Stress response', and 'Motility' showed with 7.3, 7.0, and 6.8 the highest log_2-fold change median values indicating the strongest effect of root exudate influence on these pathway categories (Figure 5). Within the 'Stress response' and 'Transport' categories, genes associated with oxidative stress and iron transport showed strong upregulation. Rubrerythrin

(log_2-fold change = 8.54) and thioredoxin (log_2-fold change = 6.63) were linked to oxidative stress, while the FecR protein (log_2-fold change = 6.24) and TonB-dependent receptor (log_2-fold change = 5.84) were linked to iron transport (Table S2, Queries: Gene184520, Gene169819, Gene12770, Gene015030).

Table 1. List of functional categories for KEGG pathway enrichment analysis of 338 annotated gene queries with a significant change in expression (adjusted $p < 0.05$). Median log_2-fold change values are shown.

Pathway supercategory	Pathway subcategory	Log_2-fold change	Queries (n)
Gene expression and regulation	Transcription	6.4	15
	Translation	6.1	51
	Proteostasis	6.3	24
Cellular processes in response to environmental stimuli	Signal transduction and exchange	6.0	7
	Stress response	7.0	11
	Adhesion	6.5	16
	Motility	6.8	31
	Transport	6.2	37
	Infection	7.3	10
Carbon, nitrogen and sulfur metabolism	Carbon metabolism	6.3	53
	Nitrogen metabolism	6.1	15
	Amino acid metabolism	6.1	25
	Sulfur metabolism	6.7	7
Cellular structure and energy supply	Cell wall synthesis	5.9	5
	Electron transport	6.5	31

Microbial community shifts

A phylogenetic analysis was conducted to assess the shifts in the community caused by the presence and absence of root exudates, respectively. Initially, we assigned phylogenetic classifications to all transcripts present in the soil. The most abundant microbial groups, namely Gammaproteobacteria and Thermodesulfobacteriota collectively accounted for 51.4% of all transcripts.

In relation to the 388 transcripts that exhibited significant upregulation due to the influence of root exudates ($p < 0.05$), notable changes were observed in the proportions of certain taxa. Specifically, the proportion of Betaproteobacteria increased from 1% to 15.3%, Campylobacterota increased from 0.6% to 1.8%, Kiritimatiellota from 0.8% to 13%, Lentisphaerota from 0.3% to 6.5% and Verrucomicrobiota from 0.4% to 3.4%. 65.9% of all

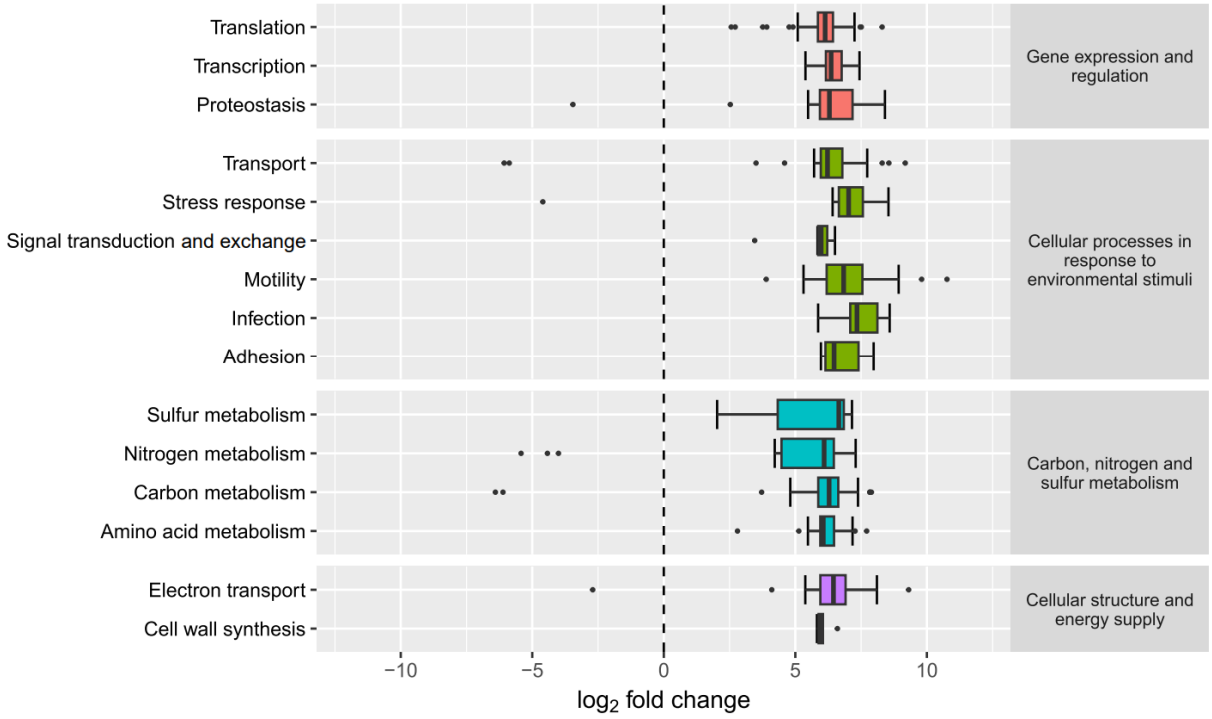

Figure 5. Boxplot of KEGG pathway enrichment analysis for 338 annotated gene queries with a significant change in expression (adjusted $p < 0.05$) grouped by functional categories (Table 1). Positive $\log_2$ fold changes reflect upregulation and negative $\log_2$-fold changes reflect downregulation of genes due to high root exudate influence. Outliers are displayed as individual points.

Table 2. List of functional categories for KEGG pathway enrichment analysis of 338 annotated gene queries with a significant negative change in expression, i.e. downregulation (adjusted $p < 0.05$). Median $\log_2$-fold change values are shown. The downregulated genes shown in this table correspond to 11 gene queries.

Down regulated genes (Description)	**Subcategory**	**$\log_2$-fold change**
Glutamate dehydrogenase	Nitrogen metabolism	- 5.4
Glutamate dehydrogenase (*gdhA*)	Nitrogen metabolism	- 4.4
Glutamate dehydrogenase (*gluD*)	Nitrogen metabolism	- 4.0
Phycobilisome protein (*apcA*)	Carbon metabolism	- 6.4
Protein involved in exopolysaccharide biosynthesis	Carbon metabolism	- 6.1
PFAM ABC transporter	Transport	- 6.1
Predicted permease	Transport	- 5.9
COG1842 Phage shock protein A (IM30) (*pspA*)	Stress response	- 4.6
Peptidase S1C (*degP-2*)	Proteostasis	- 3.4
NADH ubiquinone oxidoreductase (*nuoF2*)	Electron transport	- 2.7
NA	NA	- 4.2

transcripts were assigned to Betaproteobacteria, Gammaproteobacteria and Kiritimatiellota (Figure 6).

Of the upregulated genes assigned to Betaproteobacteria, the majority were categorized into the pathway groups of translation, motility, and transport. For Kiritimatiellota, these were carbon metabolism, translation, and transport. For Lentisphaerota, the upregulated pathway groups were carbon metabolism and translation and for Verrucomicrobiota, they were motility and transport.

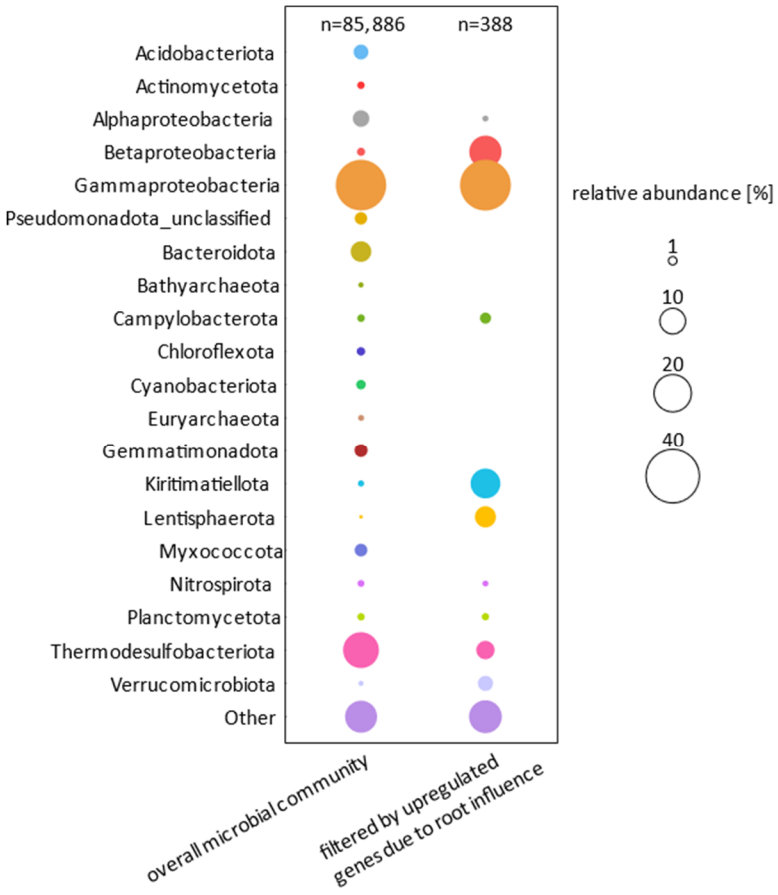

Figure 6. Microbial community composition based on all transcribed genes (first column; n=91.563) and based on transcribed genes upregulated due to root influence (second column; n= 388; p adj. < 0.05).

Discussion

This study offers insight into the wetland microbial response to root exudation via metatranscriptomic analysis. We identified both upregulated and downregulated microbial metabolic pathways in response to exudate input (Figure 1, Table S1, 2), shedding light on the complex plant-microbe interplay in wetland soils. We assigned the microbial taxonomic groups which reacted to root exudates and compared them to those groups driving bulk soil microbial processes (Figure S4, 6). Notably, the upregulated fraction of genes was around 30-fold higher than the downregulated fraction.

Metabolic background of soil microbes independent of differential expression

We acquired metatranscriptomic data on microbial processes independent of root exudate influence (Figure 1A) to establish the background environmental context of the bulk soil microbial community subjected to root influence (Figure 1A and 1B).

The WLP and DSR were the primary metabolic pathways in the plant-independent soil microbial community of the bulk soil (Figure 3). It has been demonstrated in upland beech and pine forest soils that the WLP was one of the least dominant autotrophic pathways predicted (Akinyede et al., 2022). Furthermore, in (semi-)arid soils, it has been shown that the WLP had the lowest relative abundance of key genes compared to the other CO_2-fixing pathways (Yang et al., 2024). This study demonstrates that anaerobic wetland soils, in contrast, create conditions that favor the WLP. The prominence of WLP and DSR transcripts indicate the active utilization of these pathways under anoxic conditions, with a preference for low ATP consumption (Geng et al., 2022; Momper et al., 2017). While the dominance of sulfate reduction as an anaerobic microbial pathway in marine and coastal ecosystems is long established (Capone & Kiene, 1988; Jørgensen et al., 2019; Lin et al., 2018), recent metatranscriptomic work from our group and others also demonstrate a high prevalence of dark CO_2 fixation via WLP in the anoxic soils of these ecosystems (Grüterich et al., 2024a; Yang et al., 2021). WLP and DSR are interconnected or mutually beneficial pathways, because the end-product of the WLP, acetate, can flow into the DSR as carbon and energy source (Capone & Kiene, 1988). Conversely, the DSR end-product, CO_2, can serve as carbon source in the WLP (Figure 1A). It is therefore possible that a single bacterial species or organism is making use of both processes (Dörries et al., 2016). Indeed, our data show that Thermodesulfobacteriota and Deltaproteobacteria are associated with transcripts related to both DSR and WLP (Figure 4) and reveal several species transcribing for both WLP and DSR key genes at high frequencies.

The high transcription of *fhs* and *CODH/ACS* indicates high abundances of acetogenic bacteria that typically utilize the acetyl-CoA pathway to produce acetate as an end-product (Ragsdale & Pierce, 2008). However, low transcriptional levels of genes responsible for converting acetyl-CoA to acetate (*pta* and *ackA*, Figure 3B) may indicate anabolic incorporation of acetyl-CoA as the primary metabolic process, possibly reflecting a strategy to conserve energy. Acetyl-CoA is essential in various metabolic pathways, including CO_2 fixation pathways (Bährle et al., 2023), potentially making it more energy-efficient to channel it directly into other metabolic processes rather than converting it to acetate.

Anoxic, sulfate-rich wetland soils promote Deltaproteobacteria, Gammaproteobacteria and Thermodesulfobacteriota to be the drivers behind the main active microbial pathways, namely

DRS and WLP (Figure 4). Gammaproteobacteria are known to be abundant in anoxic environments (Crump et al., 2007; Li et al., 2018) and increase towards marine conditions (Tebbe et al., 2022). The abundance of methanogenic microbial groups and transcripts encoding for methanogenesis was negligible in our study (Figure 3A). This high prevalence and activity of sulfate-reducing bacteria in comparison to methanogens is often explained by the higher free energy yield of sulfate reduction in relation to methanogenesis (Megonigal et al., 2004), which allows sulfate reducers to outcompete methanogens for energy or carbon substrates, such as H_2 and acetate in sulfate-rich environments typically observed in coastal and marine ecosystems (Lovley et al., 1982; Oremland & Polcin, 1982; Poffenbarger, 2010).

Root activity-driven change in expression of soil microbial genes

The three replicates with root exudate influence and the three replicates without root exudate influence show a clear distinction in the expression of soil microbial genes (Figure 2B). The majority of differentially expressed genes is upregulated in response to root exudate influence (Figure 2A). This observation implies a strong stimulatory effect of the various plant exudates on the microorganisms and their metabolism that can be attributed to few pathway categories (Figure 5, Table 1). The metabolic categories with the strongest microbial response to root exudates were assigned to infection (log_2-fold change = 7.34), stress response (log_2-fold change = 7.03) and motility (log_2-fold change = 6.84) (Figure 5, Table 1). Notably, infection-related genes also include those involved in establishing plant-beneficial symbiotic interactions. Thereby, microorganisms (pathogens and non-pathogens) are able to sense the root presence using root exudates and prepare to infect the plant (Büttner, 2016; Kloock et al., 2020).

Regarding stress response, genes can be part of defense mechanisms that microbes activate to protect themselves from toxic environmental influences. This could, for example, be a response to the release of secondary plant compounds, oxygen, or reactive oxygen species upon pathogen recognition or response to abiotic stress (Chiang & Schellhorn, 2012; Huang et al., 2019). Concerning motility, microbes direct their movement along chemical gradients in their environment and thus locate optimal conditions for growth and survival (Tan et al., 2013). Microbial motility is also crucial for surface colonization and attachment to the root. The occurrence of transcripts relating to the cellular response to environmental stimuli, e.g., motility, aligns with finding from Wu et al., 2023, who also found motility, and additionally, polymer utilization to be enriched in the rhizosphere of maize, although, in contrast to our transcriptomic approach, the findings are based on metagenomics. Here, we demonstrated that also wetland plants influence the mobility of rhizosphere microbial communities.

Amino acid biosynthesis comes at a high cost for microorganisms and the corresponding biosynthesis pathways are tightly regulated. By utilizing amino acids via root exudates, soil microbes can save energy by abstaining from producing them internally. 3 of the 11 genes that were downregulated under the influence of plant exudates were assigned to the glutamate dehydrogenase (Table 2). The glutamate dehydrogenase catalyzes the conversion of glutamate to α-ketoglutarate and ammonium. This reaction is important for further downstream synthesis of other amino acids. In the presence of high levels of exudate-derived compounds, microbes may favor the use of these compounds over endogenous glutamate metabolism. By downregulating glutamate dehydrogenase, they can reduce competition for substrates and channel available resources toward other metabolic pathways that benefit from the exudates (Verhagen et al., 1995).

The metabolic categories translation, transport, and carbon metabolism have the highest query numbers (Figure 5, Table 1). Upregulation of translation genes typically indicate increased protein synthesis or enhanced efficiency in the translation process in response to environmental changes (Tollerson & Ibba, 2020). Upregulated carbon metabolism genes indicate increased expression of proteins involved in utilizing carbon compounds, particularly in soils influenced by root exudates. Transport genes are upregulated to facilitate the movement of compounds between plant and microbial cells or the transport of enzymes for molecule degradation outside of the cell. Further, anaerobic wetland microbiota are known to rely on alternative terminal electron acceptors (Sutton-Grier et al., 2011). Input of molecular oxygen via radial oxygen loss from roots into reduced soils can provide terminal electron acceptors for the oxidation of reduced Fe(II) (Megonigal et al., 2004). Additionally, it has been demonstrated by Yang et al. (Yang et al., 2014), that wetland plants tend to have high Fe concentrations on root surfaces and in their rhizosphere. Our data suggest that, for example, Fe(III) deposition resulting from the oxidation of Fe(II) at the oxic-anoxic interface may serve as terminal electron acceptor by Fe-reducers. Root exudates can acidify the surrounding soil and increase the mobility of iron (Chen et al., 2017), which is supported by our observation of strong upregulation of genes directly related to iron transport in samples associated with high exudate influence (Table S2, Queries: Gene184520, Gene169819, Gene12770, Gene015030).

Higher relative abundance of transcripts assigned to certain microbial groups in response to root exudates compared to the abundance of these groups in the bulk soil reflect more favorable conditions for these taxa in the short-term and potentially increased competitive advantage in the long-term. The microbial community that reacts to root exudates by upregulation of genes differs from the community based on all transcripts (Figure 6). Specifically, the relative

abundance of Betaproteobacteria, Campylobacterota, Kiritimatiellota, Lentisphaerota, and Verrucomicrobiota increased based on assignment to upregulated genes due to root exudate influence (Figure 6). These results echo a similar metagenomic and metatranscriptomic rhizosphere study investigating rhizosphere effects of *Avena fatua* in a loamy upland soil (Nuccio et al., 2020), in which Betaproteobacteria and Verrucomicrobiota also significantly increased in the rhizosphere relative to the bulk soil based on 16S cDNA.

Method considerations and limitations

Our experimental approach aimed to capture microbial responses to exudates beyond their role as a carbon source, thus differing from RNA-SIP (RNA-stable isotope probing) approaches, which rely on the uptake and metabolic utilization of exudates. Microbes can respond to exudates by different mechanisms without necessarily metabolizing them. For example, microbes may sense exudates and invest in flagella to move closer to or away from them. Also, exudates can act as repellents, toxins or inhibitors and influence microbial activity without directly serving as a carbon source. A drawback of our approach is, however, that it cannot clearly distinguish the effects of organic exudate release from those of other root processes, such as proton and oxygen release, as it uses a ^{13}C label to specifically track the exudate input to the soil. It is important to recognize that none of the currently available approaches alone are sufficient to fully capture the microbial response to exudates while excluding the influence of other root-related factors. To address this limitation, future research investigating microbial transcriptomic responses to root influence should assess options for combined approaches integrating multiple methods.

This study is further limited by its small sample size (n = 3 for each of 'background' and 'root affected' samples) and its focus on a single, albeit dominant and globally distributed plant species of coastal wetlands (Borges et al., 2021). These constraints may limit the generalizability of our findings. Therefore, future research should investigate larger sample sizes and wider geographic coverage to confirm these results at a larger scale.

Acknowledgements

This study was funded by the Deutsche Forschungsgemeinschaft (DFG, German Research Foundation) within the Research Training Group 2530 "Biota-mediated effects on Carbon cycling in Estuaries" at Universität Hamburg (project number 407270017) and the DFG Emmy Noether project "Rhizosphere-mediation of biosphere-climate feedbacks" (project number 502681570) at Universität Münster. We thank Simon Thomsen and Clarisse Gösele for

designing and testing the labeling chamber used in our experiments. We furthermore thank GreenGate Genomics for bioinformatic services.

Author contributions

Conceptualization, P.M., L.G.; Methodology, P.M., L.G. and M.W.; Investigation, L.G. and M.W.; Formal analysis, L.G. and M.W, Writing – Original Draft, L.G. and M.W.; Writing – Review & Editing, L.G., M.W., P.M. K.J., W.S.; Resources, P.M., K.J., W.S.; Supervision, P.M., K.J., W.S.

Chapter 4

Litter Decomposition and Prokaryotic Decomposer Communities along Estuarine Gradients

In revision at Soil Biology and Biochemistry

Friederike Neiske, Luise Grüterich, Annette Eschenbach, Monica Wilson, Wolfgang R. Streit, Kai Jensen, Joscha N. Becker

Abstract

Climate change driven sea-level rise and saltwater intrusion will impact carbon (C) cycling in estuarine marshes. To understand impacts of tidal inundation and changing salinity on microbial organic matter turnover, we investigated litter decomposition and the prokaryotic community in three marsh salinity and three flooding frequency zones of the Elbe estuary. Standardized litter (Tea Bag Index) was used to assess direct effects of the estuarine gradients on seasonal litter decomposition. Indirect effects of the estuarine gradients through mediating plant species composition and litter quality was studied using litter bags filled with native plant litter. 16S rRNA gene amplicon sequencing was used to identify the prokaryotic communities colonizing tea litter, native litter and soil along the estuarine gradients. Tea litter decomposition rates decreased with increasing salinity and flooding, with 2x faster rates in brackish and freshwater high marshes compared to the salt marsh pioneer zone. Native litter decomposition was significantly influenced by local vegetation properties, particularly higher lignin contents at the freshwater compared to salt marsh, as well as pioneer zones compared to high marshes contributed to a decreased litter decomposition. Greater diversity within the soil prokaryotic community increased tea litter mass loss, indicating indirect controls of salinity via changes in prokaryotic community composition and diversity. Our results indicate that litter decomposition and prokaryotic communities are strongly influenced by estuarine gradients, and these processes are dependent upon local site conditions and litter quality. The complex interplay of these factors, will strongly affect C cycling in estuarine marsh soils under climate change.

Introduction

The breakdown of organic matter (OM), such as plant litter, is a fundamental ecosystem process, controlling the recycling of nutrients and carbon (C) (Swift et al., 1979) Plant litter decomposition is driven by the complex interplay of substrate quality, decomposer community and environmental conditions including climate or local soil characteristics (e.g. oxygen availability, salinity) (Aerts, 1997; Makkonen et al., 2012). Therefore, litter turnover can vary strongly along environmental gradients (Becker & Kuzyakov, 2018; Stagg et al., 2018).

Estuarine marshes, located at the interface of aquatic and terrestrial as well as freshwater and marine ecosystems, are shaped by dynamic interactions between abiotic factors, such as tidal inundation and salinity and biotic components, including vegetation and soil microorganisms (e.g. prokaryotic communities) (Engels & Jensen, 2009; Grüterich et al., 2024a). Contradictory results have been reported regarding the effects of flooding and salinity on OM decomposition in tidal marshes (Craft, 2007; Hemminga et al., 1991; Morrissey et al., 2014; Stagg et al., 2018). In frequently flooded soils of tidal marshes, decomposition can be slowed down due to oxygen limitation (Macreadie et al., 2019; Yarwood, 2018). Variations in flooding regime and salinity have been shown to alter the composition and diversity of prokaryotic communities in marsh soils (Schreckinger et al., 2021; Trevathan-Tackett et al., 2021; Yarwood, 2018), as well as the predominant metabolic pathway (Grüterich et al., 2024a; Yarwood, 2018). Although microbial diversity in soil has been linked to OM decomposition, the strength and direction remain debated (Nielsen et al., 2011). Salinity can also enhance OM decomposition by stimulating extracellular enzyme activities (Morrissey et al., 2014; Yang et al., 2022). Furthermore, direct effects of salinity and flooding on litter decomposition are accompanied by indirect ecosystem responses, such as modifications of vegetation composition and subsequent changes in litter quality (Stagg et al., 2018). The chemical and physical properties of plant materials, including nitrogen (N) content, lignin and cellulose concentrations, and C:N and lignin:N ratios, are recognized as key determinants of litter decomposition in different ecosystems (Djukic et al., 2018; Valiela et al., 1985; Zhang et al., 2008). Moreover, litter quality can impact the microbial community by promoting specific taxa that are adapted to decomposing local vegetation (Bezemer et al., 2010; Wang et al., 2007).

Climate is one of the most important regulators of litter decomposition (Aerts, 1997), which has been also observed for tidal wetlands (Mueller et al., 2018; Trevathan-Tackett et al., 2021). In terrestrial ecosystems, litter decomposition varies seasonally, typically increasing with higher temperatures but strongly depending on soil water content (Becker & Kuzyakov, 2018; Daebeler et al., 2022; Petraglia et al., 2019). In estuarine marshes, the relationship can be more

complex through the interaction of tidal inundation and salinity. Even though tidal marshes generally maintain high soil water contents, levels can drop in summer in infrequently flooded locations; this reduction, combined with elevated salinity, can adversely impact litter decomposition (Hemminga et al., 1991). Given the sensitivity of litter decomposition to environmental changes, climate change can significantly impact OM decomposition dynamics in estuarine marshes, but predicting the direction of these effects remains challenging. For instance, experimental warming has been shown to increase both the rate and amount of tea litter decomposition; while the effect of warming on decomposition rate appeared unaffected by flooding, the warming-effect on tea stabilization differed along a flooding gradient (Tang et al., 2023). Thus, it is essential to consider the complex interactions among flooding, salinity, climate and litter quality in understanding litter decomposition dynamics in estuarine marshes. Moreover, sea-level rise due to climate change may alter local soil conditions by increasing salinity and modifying flooding dynamics, potentially shifting vegetation zones along estuaries and thereby affecting litter quality and decomposition (Craft et al., 2009; Li et al., 2022).

With respect to changing environmental conditions induced by climate change and the high C sequestration potential of tidal wetlands, understanding the controls of C cycling in these ecosystems is crucial. However, disentangling the importance of external abiotic conditions, such as salinity or flooding, from internal factors, such as litter quality, for litter decomposition and the prokaryotic decomposer community remains challenging. The Tea Bag Index (TBI), introduced by Keuskamp et al. (2013), can provide valuable insights into the role of environmental drivers for litter decomposition, excluding the interfering effect of litter quality across ecosystem gradients. The effectiveness of the TBI to compare litter break-down across ecosystems and along environmental gradients has been demonstrated in several studies (Becker & Kuzyakov, 2018; Mueller et al., 2018; Trevathan-Tackett et al., 2021). However, prior studies indicate that highest decomposition rates of plant material in tidal wetlands occur in proximity to its natural distribution (Franzitta et al., 2015; Lopes et al., 2011). Therefore, incorporating native litter into decomposition studies is essential to avoid misleading interpretations due to the home-field advantage.

The aim of this study was to identify the role of estuarine environmental conditions on litter decomposition, using the Elbe estuary as a model system. Our specific research objectives were to investigate (i) the effect of estuarine gradients (i.e. salinity and flooding frequency) on decomposition of standardized and native litter, ii) seasonal patterns of litter decomposition, and (iii) prokaryotic community composition and diversity in soil, as well as standardized and native litter.

Material and Methods

Study area

We conducted our study in the marshes of the Elbe estuary (Northern Germany) (Figure 1). The regional climate is oceanic with a mean annual temperature of 9.3 °C and mean annual rainfall of 812.8 mm (1991 - 2020, federal state of Schleswig-Holstein) (DWD, 2024). The Elbe estuary extends from the estuaries' mouth at Cuxhaven until a weir at Geesthacht, which restricts the tidal influence further upstream. The semi-diurnal tidal regime of the estuary is meso- to macrotidal (Boehlich & Strotmann, 2008).

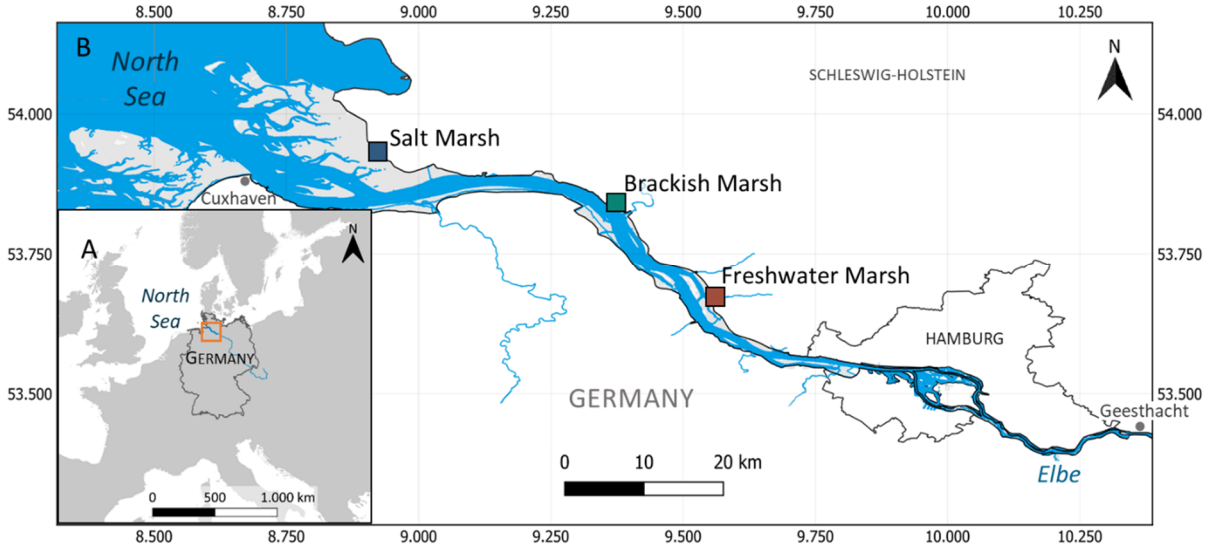

Figure 1. (A) Location of the Elbe estuary in central Europe (orange rectangle) and (B) location of the marsh sites along the Elbe estuary (salt marsh: 53°55'40.0"N 8°54'51.3"E/river-km: 710; brackish marsh: 53°50'03.0"N 9°22'15.6"E/river-km: 680; freshwater marsh: 53°39'56.3"N 9°33'11.5"E/river-km: 658) (Data sources: (WSV, 2011; EEA, 2017; WSV, 2017).

Three sites were selected along the salinity gradient of the Elbe estuary (Boehlich & Strotmann, 2008; Branoff et al., 2024). The salt marsh at Kaiser-Wilhelm-Koog is situated in the Schleswig-Holstein Wadden Sea National Park at the estuarine mouth. For the brackish marsh, a site close to Hollerwettern and for the freshwater marsh, a site in the nature conservation area "Haseldorfer Binnenelbe" were chosen. Within each of these three marsh sites, we selected three locations along the flooding gradient: Pioneer zones (PZ) are located closest to the main channel and are flooded during high tide (twice per day), low marshes (LM) are inundated during spring tide (occurring twice per month at new and full moon), while high marshes (HM) are occasionally flooded during storm tides (few times per year). All sites are located on the seaward side of a dike and exhibit near-natural conditions. The selection of the marsh locations was based on dominant plant species that are typical for the respective salinity and flooding

regime (Engels & Jensen, 2009) (Table S2). At each selected marsh location (n = 9), research stations were established consisting of five adjacent replicate plots (2 x 2 m).

Litter decomposition

Tea bag index

The standardized Tea Bag Index (TBI) was applied following the protocol of Keuskamp et al. (2013). Five pairs of weighed green and rooibos tea bags were deployed at 8 cm depth in each of the five replicate plots of the nine research locations. After approximately 90 days, tea bags were exchanged with new tea bags. Tea bags were incubated during four periods over the course of one year to assess seasonal variation in litter decomposition (spring: March – June 2022, summer: June - September 2022, fall: September – December 2022, winter: December 2022 – March 2023). After retrieval, tea bags were dried at 60 °C until constant weight. The dried tea bags were opened, roots or other non-tea material was removed and the content of the tea bags was weighed. To account for sediment contamination, tea bags were additionally combusted at 550 °C and weight loss was corrected in comparison to initial ash contents.

Native litter decomposition

In addition to the TBI, self-made litter bags were used to include litter-quality effects in the assessment of litter decomposition. A representative mixture of native plants was collected in late fall 2021 from each of the nine marsh locations. The litter was cleaned and dried at 60 °C. Polyamide mesh bags with a mesh size of 1000 µm were filled with 5 g of the respective litter. Four litter bags were inserted into the soil to a depth of 0 - 15 cm in each of the five replicate plots of the corresponding marsh location in March 2022. One litter bag was retrieved from each replicate plot after 1, 3, 6 and 12 months. After retrieval, the litter bag content was washed over a sieve (1 mm) to remove sediments, and separated from roots and other external debris. The remaining litter was dried at 60 °C until constant weight and the mass remaining relative to the initial mass was calculated.

Analyses of prokaryotic community structures

An additional set of tea and litter bags was incubated in the field for the characterization of the prokaryotic community composition in spring 2023 (March - June). One litter bag (0 - 15 cm depth) and two (HM and LM) to three (PZ) pairs of green and rooibos tea bags (8 cm depth) were deployed in three replicate plots of each marsh location. Tea and litter bags were retrieved after three months, along with one soil sample from each replicate plot (taken in close proximity

to the tea and litter bags). Tea bags, litter bags and soil samples were cooled in the field and immediately frozen (- 20 °C) in the laboratory until further analyses. We also included tea and native litter materials that were not incubated in the field in our analysis as controls, allowing us to ascertain the community composition prior to incubation. DNA was extracted from 0.5 g of tea litter, native litter or soil using the NucleoSpin Soil Kit (Macherey-Nagel, Düren, Germany) according to the manufacturer's instructions and following standard DNA protocols for extraction of eDNAs (Refs). Concentration and quality of the isolated DNA was then analyzed using a Nanodrop spectrophotometer at a wavelength of 280 nm (NanoDrop 2000, Thermo Scientific, Waltham, USA). Metabarcoding sequencing of the 16S rRNA gene variable regions V3-4 was carried out at the Competence Centre for Genomic Analysis in Kiel, Germany. For this, the Illumina Nextera XT Index Kit, primers 341F (5'-CCTACGGGNGGCWGCAG-3') and 785R (5'-GACTACHVGGGTATCTAATCC-3') and the MiSeq Reagent Kit v3, were used. For adaptor trimming of demultiplexed paired-end reads, BBDuk (v.38.8) was employed. The DADA2 pipeline (v.1.8) (Callahan et al., 2016) was used to filter reads and infer ASVs, with the following specific parameters (maxEE=2, maxN=0, truncQ=2, truncLen=270,230). Taxonomic assignment of the merged corrected reads was conducted using the SILVA database (v.138.1) (Quast et al., 2013). Raw reads of the 16S rRNA analysis were deposited at the European nucleotide archive ENA under project accession number PRJEB79857.

Environmental parameters

Field site monitoring and characterization

At each research location, sensors for continuous measurement of soil volumetric water content (VWC) were installed (SMT100, Truebner GmbH, Neustadt, Germany). For physico-chemical soil characterization, soil samples (0 - 10 cm) were collected in February and March 2022 from each research location. Air-dried soil samples were sieved to 2 mm. Samples were dried at 105 °C and ground for measuring inorganic and organic C contents (soli TOC® cube, Elementar Analysensysteme GmbH, Langenselbold, Germany) and total C and N contents (vario Max cube, Elementar Analysensysteme GmbH, Langenselbold, Germany). Soil texture was assessed by the sieving and sedimentation method based on the Köhn-pipette fractionation for mineral soils (Müller et al., 2009). A vibratory sieve shaker (Retsch GmbH, Haan, Germany) and a Sedimat 4–12 (Umwelt-Geräte-Technik GmbH, Muencheberg, Germany) were used to analyze coarse (2.0 - 0.063 mm) and fine fractions (< 0.063 mm), respectively. Soil pH was measured with a pH meter (MP230 GLP, Mettler-Toledo GmbH, Gießen, Germany) in a

suspension with 0.01 M $CaCl_2$ solution (pH_{CaCl2}) while the EC was determined in a soil-water-suspension with a conductivity meter (WTW Cond 330i with TetraCon 325, Xylem Analytics Germany Sales GmbH & Co. KG, Weilheim, Germany).

We analyzed reducing soil conditions by the "Indicator of Reduction in Soil" (IRIS) method (Castenson & Rabenhorst, 2006; Rabenhorst, 2008) based on the approach described by Mueller et al. (2020a) and Mittmann-Goetsch et al. (2024). White PVC sticks (5 x 70 cm) covered with orange $FeCl_3$-paint were inserted into the soil of each replicate plot to a depth of 0 - 60 cm. Sticks were retrieved after four weeks and a reduction index (RI) (0 - 1) was calculated based on the area of removed orange $FeCl_3$-paint. Field incubation of IRIS sticks was conducted over the course of one year (12 x 4 weeks from May 2022 until April 2023). We calculated annual and seasonal RI values for depth increments 0 - 10 cm and 0 - 20 cm corresponding to the incubation of tea and litter bags.

Vegetation characteristics

Identification and coverage estimation of plant species were conducted in late July 2022 in two subplots (60 x 60 cm) of each replicate plot (n = 10) at the nine research locations. Three litter subsamples of each marsh location (collected for litter bags in fall 2021) were ground and dried for the analysis of total C and total N contents (vario Max cube, Elementar Analysensysteme GmbH, Langenselbold, Germany). Contents of cellulose and lignin (Naumann et al., 1976) were measured at the "Professor Hellriegel Insitut e.V." at Anhalt University of Applied Sciences.

Data analyses

Decomposition rate and stabilization of tea litter

Median start and end weights of retrieved tea bags from one replicate plot (2 – 5 recovered tea bags per type and replicate plot) were calculated and used to derive the decomposition rate (k_{TBI}) and stabilization factor (S_{TBI}) following Keuskamp et al. (2013). For k_{TBI} the following equation was used:

$$(1)\ W(t) = ae^{-kt} + (1 - a)$$

in which, *W(t)* is the remaining mass (median end weight) of rooibos tea after incubation time *t*, *a* is the labile fraction of rooibos tea, while *1 - a* reflects the recalcitrant fraction, *k* is the decomposition rate constants of the labile fraction.

Environmental factors can impede decomposition and lead to the incomplete decomposition of litter. The deviation of the potentially decomposable (hydrolyzable) fraction from the actual decomposed fraction is expressed in stabilization factor *S*:

$$(2)\ S = 1 - \frac{a_g}{H_g}$$

where a_g represents the decomposable fraction and H_g the hydrolyzable fraction of green tea. We calculated k_{TBI} and S_{TBI} for each season and as annual mean (mean over four seasons).

Decomposition of native litter

The relative remaining dry mass of native litter over time in litter bags was used to determine the decomposition rate k_{LB}. We fitted a single negative exponential model on the relative remaining mass over five time steps (0, 1, 3, 6, 12 months) for each replicate plot separately using the R package "litterfitter" (Cornwell and Weedon, 2014). The model type was selected based on the lowest values for the corrected Akaike's information criterion (AICc) (Figure S2). In case the remaining biomass increased to a later time step, we set the weight to the weight of the previous time step (Stagg et al., 2018).

Analyses of prokaryotic community structure and diversity

To test for differences in prokaryotic community composition among the different substrate types (tea, native litter and soil) and along the estuarine gradients, we applied a nonmetric multidimensional scaling (NMDS) based on Bray-Curtis distances at the genus level. Alpha diversity (indices richness, evenness, Shannon Diversity Index and Inverse Simpson Index) were calculated at the phylum-level. Multiple indices were used to derive a broader perspective on diversity estimates (Daebeler et al., 2022; Pioli et al., 2020). Both analyses were conducted using the vegan package in R (Oksanen et al., 2013).

Statistical analyses

Differences in litter decomposition (k_{TBI}, S_{TBI}, k_{LB} and relative mass remaining of LB) and alpha diversity indices of the prokaryotic communities (richness, evenness, Shannon Diversity Index and Inverse Simpson Index) along the estuarine gradients were assessed by analysis of variance (ANOVA) or linear mixed effect model (LME). The LME were applied including sampling location as random factor and either (I) season or (II) salinity, flooding and season as main factors. Assumptions of normality and variance homogeneity were checked by visual inspection of model residuals. Dixon's Q test was applied to check groups for potential outliers.

Relationships between variables were assessed by linear regression and Pearson correlation, as well as Spearman rank correlation to account for potential non-linearity. Simple linear and log-linear fits were selected according to reduction in Akaike Information Criterion (AIC) values. Statistical differences were accepted as significant at p-level < 0.05 and p-levels between 0.10 and 0.05 were considered significant by tendency. Statistical analyses were conducted in R 4.2.0, using "multcomp" (Hothorn et al., 2016) and "multcompView" (Graves et al., 2015) packages, as well as "ggplot2" (Wickham et al., 2016) for data visualization.

Results

Tea bag index

Effect of estuarine gradients on tea litter decomposition

The salinity and flooding gradient, as well as their interaction, had significant effects on annual k_{TBI} and S_{TBI} of tea litter (Figure 2).

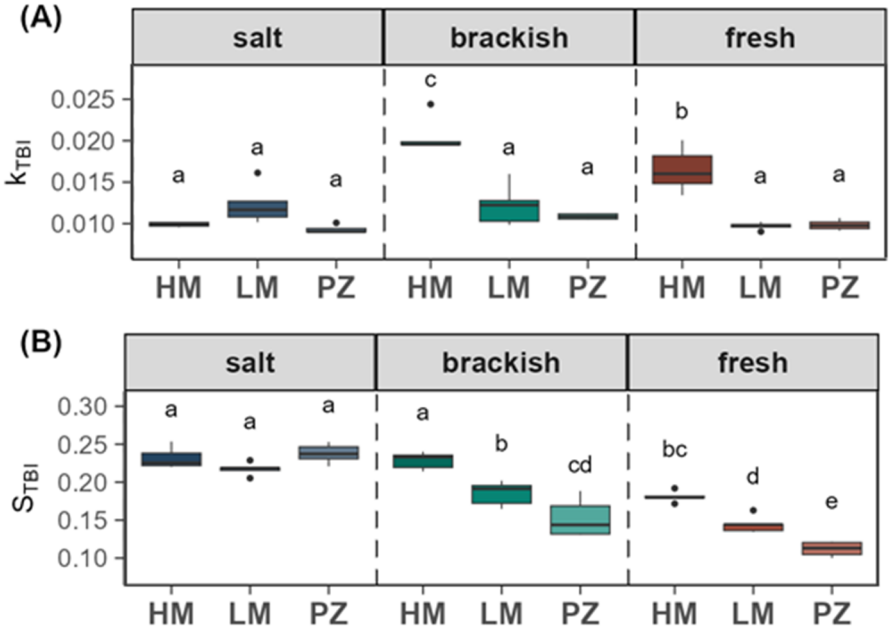

Figure 2. Annual means of (A) decomposition rate k_{TBI} and (B) stabilization factor S_{TBI} of tea litter along the salinity (salt marsh, brackish marsh, freshwater marsh) and flooding gradient (HM = high marsh, LM = low marsh, PZ = pioneer zone) of the Elbe estuary (n = 5). Lowercase letters indicate significant differences ($p < 0.05$) derived from ANOVA with TukeyHSD post-hoc comparison.

Highest annual k_{TBI} were found in high marshes of the brackish (0.021) and freshwater marsh (0.017), from where it decreased with increasing salinity and flooding towards salt marsh pioneer zones (0.009). In low marshes and pioneer zones, annual k_{TBI} did not change along the salinity gradient. Annual S_{TBI} increased with increasing salinity in all flooding zones by 20% - 50% and decreased with increasing flooding at the brackish and freshwater marsh by 35%.

Effect of seasons

Tea litter decomposition indices followed a strong seasonality (Figure 3 and S3). Average decomposition rate k_{TBI} was 100% higher in summer compared to winter (summer > spring = fall > winter) (Figure 3A). Stabilization factor S_{TBI} was almost 50% higher in winter compared to summer (S_{TBI}: winter > spring > fall > summer) (Figure 3B). Spring and fall are on the level of the annual average.

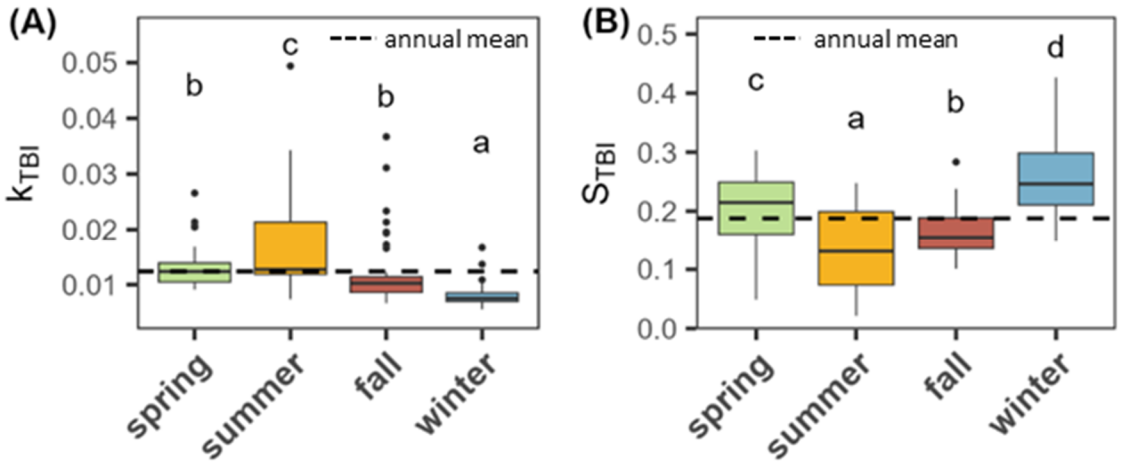

Figure 3. Effect of season on (A) decomposition rate k_{TBI} and (B) stabilization factor S_{TBI} of tea litter (n = 45). Lowercase letters indicate significant differences ($p < 0.05$) derived from linear mixed effect model.

The seasonal variation of tea litter decomposition was affected by the estuarine gradients (Figure S3). Seasonal variation of k_{TBI} decreased with increasing salinity and flooding, while S_{TBI} showed a higher seasonality in pioneer zones. For k_{TBI}, the strongest seasonal effect was observed in the brackish and freshwater high marshes which also showed highest k_{TBI} during summer (0.024 and 0.033). Stabilization factor S_{TBI} was low in summer and high in winter especially in locations with higher flooding frequency (low marshes and pioneer zones). With decreasing flooding, less seasonal variation was observed. Strongest effects of the salinity gradient on k_{TBI} were observed for high marshes and in summer. The strongest effect of the flooding gradient on k_{TBI} and S_{TBI} occurred in summer.

Native litter decomposition

Effect of estuarine gradients on native litter decomposition

Decomposition rate of native litter k_{LB} was lowest at the low marsh and pioneer zone of the freshwater marsh (both 0.002), while highest k_{LB} values occurred at the low marsh (0.011) and pioneer zone (0.008) of the salt marsh and the brackish high marsh (0.009) (Figure 4A).

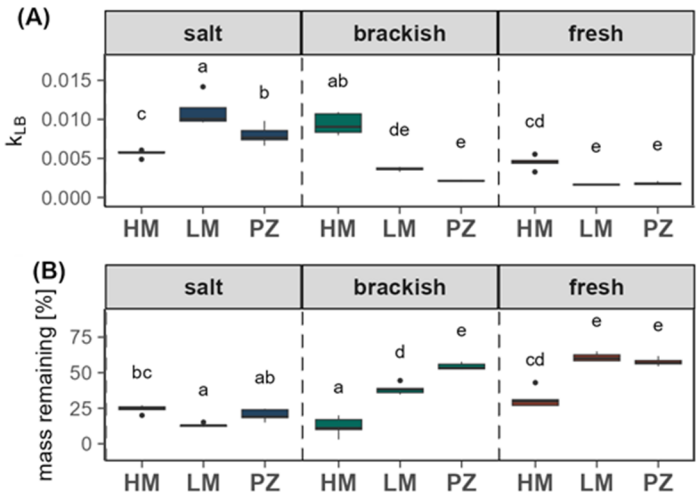

Figure 4. Annual (A) decomposition rate k_{LB} and (B) relative mass remaining of native litter after one year along the salinity (salt marsh, brackish marsh, freshwater marsh) and flooding gradient (HM = high marsh, LM = low marsh, PZ = pioneer zone) of the Elbe estuary. Lowercase letters indicate significant differences ($p < 0.05$) derived from ANOVA with TukeyHSD post-hoc comparison.

Decomposition rate k_{LB} increased with increasing salinity at pioneer zones and low marshes or was highest at the brackish marsh (high marshes). Increasing flooding decreased k_{LB} at the brackish marsh and freshwater marsh and increased k_{LB} at the salt marsh. Relative remaining mass of native litter after one year showed the reverse trend along the estuarine gradients (Figure 4B).

Structure and diversity of prokaryotic communities

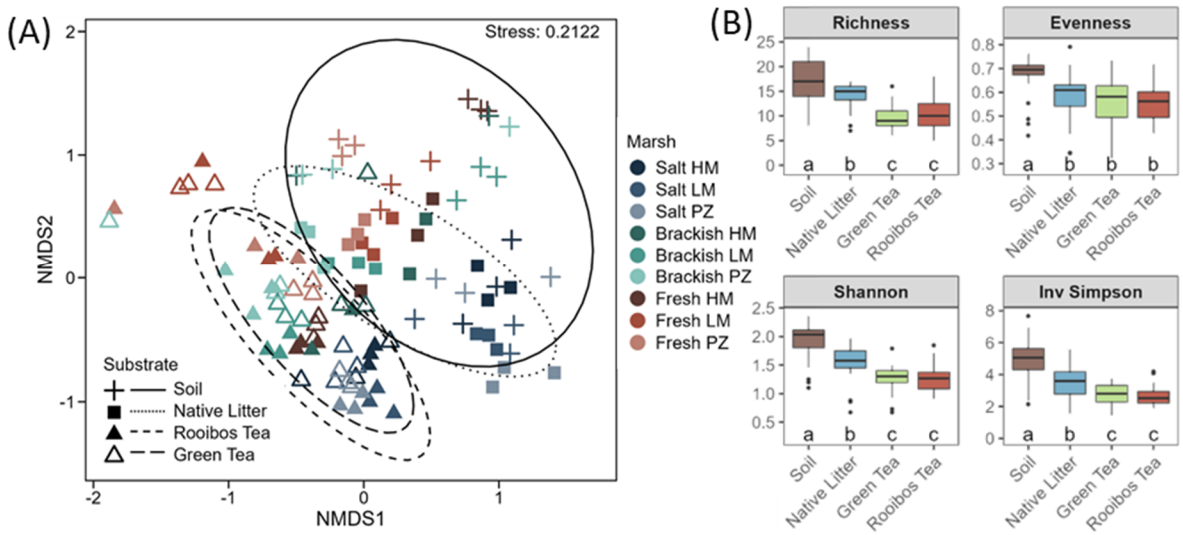

Figure 5. (A) NMDS based on Bray-Curtis dissimilarity of the prokaryotic community associated with tea, native litter and soil at genus level along the salinity (salt marsh, brackish marsh, freshwater marsh) and flooding gradient (HM = high marsh, LM = low marsh, PZ = pioneer zone) of the Elbe estuary. Ellipses indicate 90% confidence area per substrate type. (B) Alpha diversity (richness, evenness, Shannon Diversity Index and Inverse Simpson Index) of the prokaryotic community at phylum level in the different substrate types (soil, native litter, green tea, rooibos tea).

Prokaryotic community structure and diversity

The estuarine gradients and the substrate type (soil, native litter, green tea and rooibos tea) had a strong effect on the structure and alpha diversity (richness, evenness, Shannon Diversity Index and Inverse Simpson Index) of the prokaryotic community (Figure 5A, B). We observed a partial overlap of communities associated with soil and native litter and a strong overlap between the communities associated with green tea and rooibos tea, whereas communities associated with tea showed distinct differences compared to communities associated with soil and native litter (Figure 5A). Highest alpha diversity of the prokaryotic community was observed in soil, followed by native litter, while communities associated with green and rooibos tea showed similar alpha diversity. The assemblage of communities associated with tea and native litter differed from their non-incubated controls (Figure S6). Across all substrate types, the communities at the salt marsh showed a different assemblage and lower alpha diversity than the brackish and freshwater marsh communities.

Prokaryotic taxa

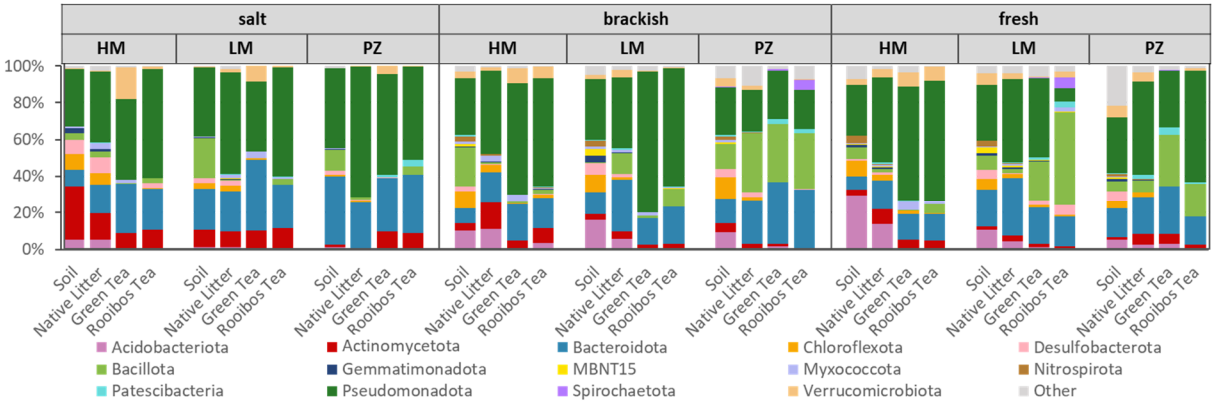

Figure 6. Prokaryotic community composition in soil, native litter, green tea and rooibos tea (relative abundance of phyla) along the salinity (salt marsh, brackish marsh, freshwater marsh) and flooding gradient (HM = high marsh, LM = low marsh, PZ = pioneer zone) of the Elbe estuary. Each bar reflects the average of three biological replicates.

The most abundant phyla (> 1%) were Pseudomonadota (43.8%), Bacteroidota (21.2%), Bacillota (10.1%), Actinomycetota (6.1%), Acidobacteriota (4.1%), Verrucomicrobiota (2.7%), Chloroflexota (2.6%), Desulfobacterota (1.9%), Campylobacterota (1.3%) and Myxococcota (1.1%), which made up 95% of the total prokaryotic community (Figure 6). The estuarine gradients and substrate type affected the relative occurrence of certain prokaryotic phyla. Pseudomonadota, Bacteroidota, Bacillota and Patescibacteria were more dominant in tea and native litter than in soil in several marshes. Lower abundance in tea compared to soil was

observed for Acidobacteriota and Chloroflexota. Increasing salinity led to a reduced abundance of Bacillota, Acidobacteriota, Nitrospirota and Spirochaetota while the abundance of Bacteroidota, Actinomycetota and Patescibacteria was higher. The occurrence of Actinomycetota and Acidobacteriota increased with frequent flooding while Bacillota and Bacteroidota decreased in their abundance.

Relationships between litter decomposition and environmental variables

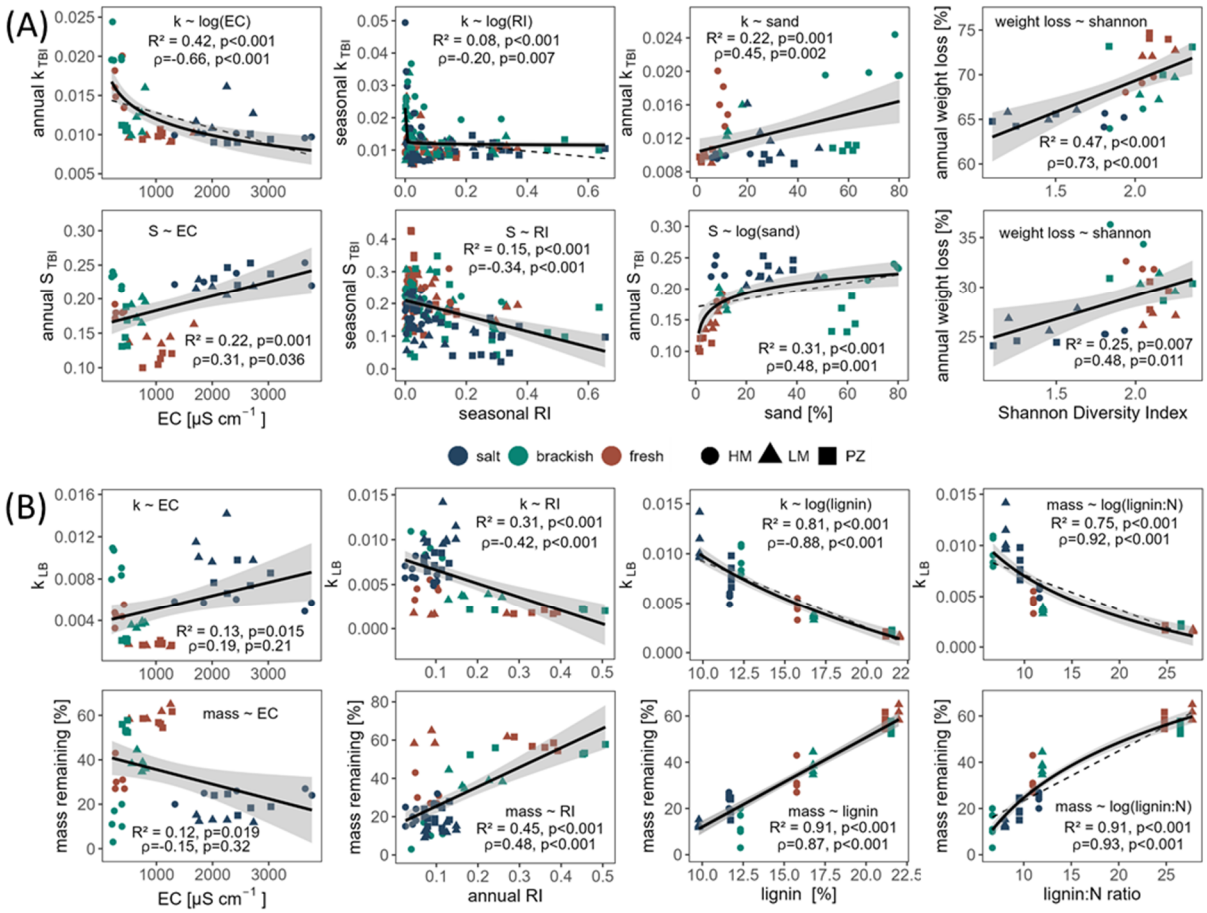

Figure 7. Relationship between decomposition indices of (A) tea litter (decomposition rate k_{TBI}, stabilization factor S_{TBI}, relative weight loss of green tea (upper panel) and rooibos tea (lower panel)) and (B) native litter (decomposition rate K_{LB}, relative mass remaining after one year) and selected site characteristics (soil EC, soil reduction index (RI), soil sand content, Shannon Diversity Index of the prokaryotic soil community, litter lignin content, litter lignin:N ratio) with Spearman rank correlation coefficients (ρ). Black solid lines indicate linear or logarithmic regression lines with 95% confidence bands and respective coefficients of determination (R^2). Additional dashed lines indicate significant simple linear relationship in case logarithmic regression was used.

Annual tea litter k_{TBI} correlated negatively with the EC and clay content of the soil, while it was positively affected by the sand content (Figure 7A and S4). Annual S_{TBI} increased with increasing EC and sand content while it decreased with increasing clay content. Seasonal k_{TBI} and S_{TBI} were negatively affected by the seasonal RI of the soil. Relative weight loss of green

and rooibos tea was positively linked to the richness and diversity (Shannon Diversity Index, Inverse Simpson Index) of the prokaryotic soil community. We found a positive correlation between native litter k_{LB} and the sand content, as well as EC of the soil, while k_{LB} was negatively correlated with clay content and annual RI of the soil (Figure 7B and S4). The relative native litter mass remaining after one year showed the opposite trend regarding sand content, clay content, EC and annual RI. Decomposition of native litter (k_{LB}, relative mass remaining after one year) was strongly affected by litter quality indices of the aboveground vegetation (contents of lignin, cellulose, N, C and ratios of C:N, lignin:N) (Figure 7B and S4). In this context, litter quality varied along the estuarine gradients (Figure S5).

Discussion

Effect of estuarine gradients on litter decomposition

Effect of estuarine gradients on tea litter decomposition

We observed two different trends in tea litter decomposition rates along the salinity gradient: First, increasing salinity slowed down tea litter decomposition rates in high marshes; second, salinity did not affect decomposition rates in low marshes and pioneer zones. Therefore, fastest tea litter decomposition occurred in high marshes of the brackish and freshwater marsh. Tea litter stabilization benefitted from increasing salinity in all flooding zones leading to highest tea litter stabilization in the salt marsh and brackish high marsh. We observed decreasing tea litter decomposition rates and increasing tea litter stabilization with increasing EC of the soil. In accordance with our findings, previous studies reported direct negative effects of salinity on OM decomposition or found higher OM decomposition rates in freshwater compared to marine environments (Bierschenk et al., 2012; Hemminga et al., 1991; Mendelssohn et al., 1999; Qu et al., 2019; Quintino et al., 2009). These trends might be related to reduced microbial activities, microbial biomass and enzyme activities with increasing salinity (Roache et al., 2006; Yan et al., 2015). However, the literature on OM decomposition in relation to salinity in tidal wetlands presents inconsistent results, with studies reporting higher OM decomposition rates in marshes with elevated salinities compared to freshwater marshes (Craft, 2007; Stagg et al., 2018). Moreover, research indicates that extracellular enzyme activities and bacterial abundance can increase with rising salinity from freshwater to oligohaline tidal wetlands (Morrissey et al., 2014). These inconsistent trends suggest that the effect of salinity on OM decomposition is not straightforward but rather influenced by several interacting factors, such as litter quality,

exposure time, OM decay stage, salinity levels and nutrient availability (Franzitta et al., 2015; Lopes et al., 2011; Mendelssohn et al., 1999; Quintino et al., 2009).

In our study, tea litter decomposition rates decreased with increasing flooding from high marshes to pioneer zones at the brackish and freshwater marshes. Reduced oxygen availability induced by increasing flooding might have slowed down microbial litter decomposition (Day & Megonigal, 1993). This is supported by a negative correlation between seasonal tea litter decomposition rates and reducing soil conditions (measured as Reduction Index RI; Figure 7A). However, a high soil water content can have a dual role for OM decomposition as it can also increase mass low due to strong leaching of OM which plays a particularly large role in intertidal ecosystems (Aerts, 1997; Marley et al., 2019; Trevathan-Tackett et al., 2021). This might be the reason why the reduced tea litter decomposition rates were not accompanied by higher litter stabilization. In contrast, tea litter stabilization was also largely negatively affected by increasing flooding leading to a positive correlation between k_{TBI} and S_{TBI} at the brackish and freshwater marsh. Similar trends were previously reported in tidal wetlands (Mueller et al., 2018). The different qualities of green and rooibos tea might lead to the varying patterns of tea decomposition along the flooding gradient. Green tea is more nutrient-rich and contains a higher fraction of soluble compounds compared to rooibos tea which has less nutrients, fewer soluble compounds, and is rich in lignin (Keuskamp et al., 2013). Consequently, rooibos tea may be less susceptible to leaching than green tea and less appealing to microbial decomposers, as its breakdown is energetically less favorable under oxygen-limited conditions. It was demonstrated that the decomposition of rooibos tea is more strongly influenced by soil conditions than that of green tea, likely due to differences in litter quality (Fanin et al., 2020). This finding aligns with previous studies demonstrating that the effects of oxygen availability on OM decomposition depend on OM quality. Labile materials generally decompose at similar rates in both oxic and anoxic environments while the breakdown of lignin occurs more slowly and incompletely in the absence of oxygen (Basile-Doelsch et al., 2020; Benner et al., 1984; Hulthe et al., 1998; Kristensen et al., 1995). As a result, the mass loss of rooibos tea decreased with increasing flooding frequency, leading to a lower decomposition rate k, whereas the mass loss of green tea increased with increasing flooding, resulting in a lower stabilization factor S. An underlying assumption of the TBI is that stabilization factor S is the same for green and rooibos tea. Certain environmental conditions (strong leaching in our case) can lead to a deviation from this assumption resulting in a decoupling and seemingly positive correlation between k and S (Mori et al., 2022; Sarneel et al., 2024). This observation underlines the importance to consider litter quality in decomposition studies.

Tea vs. native litter decomposition along estuarine gradients

Native litter decomposition was also affected by the estuarine gradients but showed partly different responses than tea litter. For example, while decomposition rates of tea litter were not affected by the salinity gradient, decomposition rates of native litter increased with increasing salinity in low marshes and pioneer zones. Increasing flooding at the salt marsh did not affect tea litter decomposition rates but increased native litter decomposition rates. These findings suggest that litter quality might have caused differences in native and tea litter decomposition. It is important to note that decomposition indices of both methods cannot be compared directly due to differences in the methodological approach (e.g. mesh size, volume of litter material, incubation period and time). Nevertheless, it can be used to derive some general trends. Several studies have shown the direct link between litter quality and litter decomposition (Carrasco-Barea et al., 2022; Stagg et al., 2018). Thereby, high initial N contents of litter are known to favor microbial decomposition and leaching (Valiela et al., 1985) while higher cellulose and lignin contents, as well as higher ratios of C:N and lignin:N are indicators of recalcitrant litter with low degradability (Aerts, 1997; Wider & Lang, 1982). In our study, decomposition of native litter was strongly affected by litter quality parameters, as the decomposition rate of native litter decreased with indices of recalcitrant litter and increased with labile litter components. The lignin content was the strongest overall predictor for native litter decomposition, followed by the lignin:N ratio which was also highlighted in other studies (Stagg et al., 2018). Moreover, rates of native litter decomposition followed the trend of increasingly labile aboveground litter with increasing salinity and less flooding (Figure S5). This supports previous findings that estuarine gradients indirectly control litter decomposition by shaping the local plant community (Schulte Ostermann et al., 2024). Our findings therefore support existing literature on the importance of litter quality in driving litter decomposition (Zhang et al., 2008).

However, external conditions induced by estuarine gradients for litter decomposition cannot be completely neglected. Decomposition rates of both tea and native litter decreased with increasing flooding at the brackish and freshwater marsh and were negatively influenced by reducing soil conditions. Therefore, the effect of flooding on native litter decomposition at this location might be the combined result of litter quality and environmental conditions induced by the flooding gradient. The estuarine gradients can directly affect litter decomposition by increasing salinity and flooding, or indirectly through controlling other site conditions. For example, we found that tea and native litter decomposition rates were negatively affected by the clay content, while it was positively affected by the sand content of the soil. The soil texture

of estuarine marshes can be the result of the sedimentation dynamics along the estuarine gradients as freshwater marshes often receive finer textured sediments compared to their marine counterparts (Butzeck et al., 2015). A higher sand content in soil might increase drainage and the aeration of the soil which might have enhanced litter decomposition (Carrasco-Barea et al., 2022). But higher contents of sand were not always related to higher decomposition rates (and vice versa for the clay content) which indicates that the effect of soil texture also depends on the interplay with other factors.

Based on these observations, climate change is likely to influence litter decomposition through various pathways. If inland migration of marshes is restricted, the area of freshwater marshes may decline due to increased salinity associated with sea-level rise (Craft et al., 2009). This shift may lead to increased labile plant material, potentially enhancing decomposition rates. Our study also demonstrated that flooding, which may be also enhanced with sea-level rise, can impede or increase litter decomposition depending on litter quality. Therefore, the overall impact of climate change on litter decomposition will be influenced by the complex interplay of multiple factors within tidal ecosystems.

Effect of season

Climate has been identified as a major driver of OM decomposition (Aerts, 1997). We therefore expected strong seasonal variations in litter decomposition. Indeed, we observed high tea litter decomposition rates and low tea litter stabilization in summer, while winter showed the opposite trend. Seasonal maxima of k_{TBI}-values in our study occurred during summer and reached or exceeded upper values reported by Keuskamp et al. (2013) and Mueller et al. (2018) (Figure S1). Annual and seasonal values of stabilization factor S_{TBI} were in the lower to mid-range of S-values found by Keuskamp et al. (2013) and Mueller et al. (2018). This seasonal pattern is typical for temperate regions (Daebeler et al., 2022; Sarneel et al., 2024). Decomposition of OM increases with temperature, which has also been demonstrated for tidal wetlands (Mueller et al., 2018; Trevathan-Tackett et al., 2021). In addition to temperature, litter decomposition is affected by soil moisture which also varies seasonally (Petraglia et al., 2019). In winter, higher soil water content induced by a lower evaporation and increased storm floods might also limit decomposition. In summer, low water availability can hamper decomposition in rarely flooded locations of marshes, particularly when co-occurring with high salinities (Hemminga et al., 1991). This might have been the case in the high salt marsh, being the only location with lowest tea litter decomposition rates during summer. In contrast, tea litter decomposition rates at the brackish and freshwater high marshes exceeded k-values found by Keuskamp et al. (2013) and

Mueller et al. (2018) during summer. This indicates that brackish and freshwater high marshes provided optimal conditions for tea litter decomposition in summer.

The strength of seasonal variation in tea litter decomposition decreased with increasing flooding as high marshes showed a stronger seasonal variation than pioneer zones. The high and relatively constant soil water content in pioneer zones throughout the year might diminish seasonal variations in litter decomposition. The soil water content at the freshwater high marsh (10 cm depth) showed a significant stronger seasonal fluctuation than the pioneer zone (Table S4). Variations in soil water content might also explain the varying effects of estuarine gradients on tea litter decomposition throughout the year. A high and more similar soil water content in all flooding zones during winter might reduce the flooding effect. The overall high water content and cold temperature might reduce microbial decomposition and leaching, leading to the low decomposition rates and high stabilization in winter. In warmer seasons, the soil water content showed a stronger differentiation along the flooding gradient and therefore tidal inundation might have had a stronger impact on decomposition.

Projected climate warming has the potential to enhance litter decomposition in the Elbe estuary. Although rising sea levels may lead to increased soil moisture and promote anoxic conditions, this does not necessarily result in reduced OM decomposition rates as tea litter decomposition rates were highest during the summer months, also in wet pioneer zones. Experiments have demonstrated that warming can increase tea litter decomposition rates in salt marshes, regardless of flooding frequency. However, the response of tea litter stabilization to warming were found to be inhibited by increasing reducing soil conditions (Tang et al., 2023).

Prokaryotic communities and litter decomposition

Effect of substrate on prokaryotic community structure

The substrate type (soil, native litter and tea litter) had a strong effect on the composition and diversity of the prokaryotic communities. This was mainly observed by a different composition of the prokaryotic communities associated with green and rooibos tea, while the native litter and soil communities showed a strong overlap with each other. Similar to other studies (Daebeler et al., 2022; Pioli et al., 2020; Trevathan-Tackett et al., 2021), the soil-associated community had the highest diversity and evenness compared to the communities associated with native litter and tea. Together with a different assemblage of the non-incubated tea and native litter controls, these findings indicate the selective colonization of tea and native litter with prokaryotic taxa originating from the soil pool (Figure S7) (Pioli et al., 2020). The taxa that benefited from or were better adapted to the specific substrate became dominant, whereby

a certain degree of diversity and evenness was lost compared to the surrounding soil. The strong overlap of native litter and soil-associated communities reflected the adaptation of the soil prokaryotic community to the local litter. In contrast, the foreign tea litter provided new substrate and created a specific ecological niche that not all microbial groups can equally exploit and therefore different prokaryotic taxa were selected. Further, green tea and rooibos tea contain compounds with antimicrobial properties, which might lead to the observed decrease in the diversity of the prokaryotic community colonizing the tea compared to communities associated with native litter and soil (Friedman, 2007; Simpson et al., 2013). Plants influence the soil microbial communities not only through the supply of litter material but also by releasing root exudates into the rhizosphere. Root exudation creates redox oscillations by either inducing reducing conditions through OM input or promote oxidation in an otherwise anoxic environments by releasing O_2 to which the microbial community reacts (Grüterich et al., 2024b; Rolando et al., 2024). The introduction of non-native litter (green tea or rooibos tea) leads to shifts in the prokaryotic community composition as different taxa respond to the altered availability of resources and environmental conditions, which were well adapted to both the native litter and root exudates before.

Estuarine gradients and prokaryotic community structure

Besides substrate type, the prokaryotic communities were influenced by the estuarine gradients. The composition of the prokaryotic community at the salt marsh showed a clear distinction from the brackish and freshwater marsh and was characterized by a lower diversity. Salinity is known to strongly affect prokaryotic communities by reducing biomass and diversity as not all taxa can cope with the osmotic stress induced by increased salinity (Chen et al., 2022; Lozupone & Knight, 2007). The lower diversity of the salt marsh community is supported by a negative correlation between soil EC and alpha diversity indices of the soil community. Flooding also negatively affected the diversity of the prokaryotic communities in soil and native litter at the salt marsh (Figure S8). This might also be related to the enhanced input of saltwater with increasing inundation frequency as we did not observe this negative effect at the brackish and freshwater marsh. At the brackish and freshwater marsh, we observed a slight increase (not significant) with increasing flooding in alpha diversity indices of the communities associated with native litter and soil which might be the result of increased input of different prokaryotic taxa with regular inundation. As this is only a slight tendency, this requires further investigation. The observed patterns in alpha diversity of the prokaryotic soil community along the estuarine

gradient are less pronounced in communities associated with native litter and tea. Particularly the tea-associated communities often deviate from patterns in the soil community. This observation underlines the importance of the substrate type and litter quality for the prokaryotic community.

Relative abundance of prokaryotic taxa

16S rRNA offers the benefit of allowing simultaneous observation of shifts in multiple functional groups. Nonetheless, linking phylogenetic groups to specific functions can be difficult due to microbial plasticity and functional redundancy. There is still limited understanding of how microbial composition affects community-level physiological profiles (Yarwood, 2018). Nonetheless, some phylogenetic groups are recognized for specific functions. While these characteristics may not be universally applicable to every member of this group, they provide insight into the general capabilities associated with many members within that group.

The prokaryotic taxa found in tea, native litter and soil are typical for marine and estuarine sediments (Baker et al., 2015; Chen et al., 2022; Zhang et al., 2021). The substrate type and the estuarine gradients had strong effects on the relative abundance of dominant prokaryotic taxa. The clearest distinction in dominant taxa was observed between communities associated with soil and tea, while communities associated native litter often had an intermediate position. This observation suggests the adaptation of the local prokaryotic community to the local litter. Similar to a previous study (Daebeler et al., 2022), green and rooibos tea showed similar patterns regarding dominant prokaryotic taxa (Figure 5A and 6).

On phylum level, Bacillota, Pseudomonadota and Bacteroidota showed an increased abundance in tea and native litter compared to soil, indicating that these phyla take over an important role in the breakdown of litter and proliferate rapidly on the rich substrates provided by the tea and native litter. Bacteroidota are known for their ability to break down complex organic compounds, which could explain their prevalence in both substrates (Bauer et al., 2006). Significant increase of Bacillota in tea litter, especially in the freshwater low marsh and in pioneer zones, suggests that Bacillota are particularly efficient at degrading the tea litter and that the conditions in these zones favor their growth. Bacillota are often involved in the decomposition of organic material (Jiang et al., 2019; Wegner & Liesack, 2016). Several orders of these phyla, such as Pseudomonadales (Pseudomonadota), Rhizobiales (Pseudomonadota) Flavobacteriales (Bacteroidota), Sphingobacteriales (Bacteroidota), together with

Micrococcales (Actinomycetota) also showed a larger abundance in litter compared to soil which was also observed in other studies with tea bags (Daebeler et al., 2022) or straw (Yan et al., 2024). The phyla Acidobacteriota and Chloroflexota had a lower abundance in tea compared to soil. The decline in Acidobacteriota abundance when colonizing tea litter suggests that this prokaryotic group may not thrive under the conditions or resource availability provided by the tea litter. Acidobacteriota are often found in nutrient-poor soils and can effectively use scarce resources which provide an advantage compared to other taxa (Ward et al., 2009) and might explain their higher abundance in soil. With regard to tea, Acidobacteriota may struggle to adapt to the chemical composition or physical properties of the tea substrate. The minimal occurrence of Chloroflexota in tea indicates that this group of bacteria may be reduced by the secondary metabolites present in the tea (Friedman, 2007; Simpson et al., 2013), as it is a common phylum in soils and usually known for its diverse role in C metabolism (Hug et al., 2013).

Litter decomposition and prokaryotic community diversity

Previous studies have highlighted the role of microbial diversity for litter decomposition (Hättenschwiler et al., 2005; Liu et al., 2023; Maron et al., 2018). In this study, the decomposition of tea litter (weight loss of both tea types and k_{TBI}) was positively affected by the diversity of the prokaryotic soil community, while the stabilization factor S_{TBI} was negatively affected. This observation indicates that a diverse pool of prokaryotes in soil is important for the successful colonization of the foreign tea litter by taxa capable of utilizing this substrate. We found highest green tea mass loss with increasing flooding at the brackish and freshwater marshes, which coincided with a slight (but not significant) increase in soil prokaryotic richness and diversity with increasing flooding. A higher diversity with increasing flooding might be beneficial to increase the functional diversity of the community while environmental conditions become more adverse (e.g. oxygen limitation) (Maron et al., 2018). The green tea might be usable by a wider set of microorganisms and therefore benefits directly from a diverse soil pool. In contrast, the diversity of the prokaryotic community associated with the tea litter was less important for tea decomposition and native litter mass loss was negatively correlated with increasing soil diversity. These observations suggest that diversity is not necessarily predictive for the effectiveness of the prokaryotic community to decompose the specific litter under the local conditions. In general, a high microbial diversity promotes ecosystem functioning, but at the same time, the species identity and community composition are essential for adaptation to specific environments (Peter et al., 2011).

Conclusion

In this study, we provided insights into litter decomposition and associated prokaryotic communities in marsh soils of the Elbe estuary. Significant spatio-temporal variations in litter decomposition were observed, driven by the dynamic interaction of estuarine gradients, local conditions, climate and litter quality. Litter quality is thereby a key parameter driving litter decomposition along the estuary. The recalcitrant nature of rooibos, leads to reduced mass loss under frequent flooding, while the more labile green tea experiences enhanced mass loss. The chemical composition of local native litter, particularly the lignin content, drove its decomposition along the estuarine gradients. Seasonal variation in litter decomposition was affected by estuarine gradients, with optimal conditions in less frequently flooded areas of the brackish and freshwater marsh during summer, while simultaneously salt marshes exhibited low decomposition rates due to high salinity and dry soil. Salinity also strongly shaped the prokaryotic community involved in decomposition, affecting both community structure and diversity. With this the estuarine gradient indirectly influence litter decomposition, particularly the foreign tea litter. The prokaryotic soil community demonstrated a strong overlap with the community associated with native litter, suggesting an adaptation to the local vegetation. Based on our findings, climate change could have substantial effects on OM decomposition dynamics in estuarine marshes but predicting the potential effects is challenging due to the numerous interacting factors. The impact of climate change on litter decomposition will be determined by the complex interplay of salinity, flooding, temperature, soil conditions and litter quality. Warmer temperatures may lead to higher litter decomposition but only as long as sufficient soil water is available. This highlights the necessity for further research to consider this complexity to fully comprehend litter decomposition dynamics in estuarine ecosystems.

Acknowledgements

This study was funded by the *Deutsche Forschungsgemeinschaft* (DFG, German Research Foundation) within the Research Training Group 2530: “Biota-mediated effects on Carbon cycling in Estuaries” (project number 407270017; contribution to *Universität Hamburg* and *Leibniz-Institut für Gewässerökologie und Binnenfischerei im Forschungsverbund Berlin e.V.*) and further supported by the DFG Research Infrastructure NGS_CC (project 407495230) as part of the Next Generation Sequencing Competence Network (project 423957469). We thank Volker Kleinschmidt, Deborah Harms, Sumita Rui, Annika Naumann, Julian Mittmann-Goetsch, Fay Lexmond and all involved student assistants for their help during field and lab

work, as well as technical support. We further thank all persons involved in the planning, establishment and maintenance of the RTG2530 marsh research facilities.

Author contributions

Conceptualization, F.N., L.G., A.E., W.R.S., J.N.B.; Formal Analysis, F.N., L.G.; Investigation, F.N., L.G., M.W., K.J.; Writing – original draft, F.N.; Writing – review & editing, L.G., A.E., M.W., W.R.S., K.J., J.N.B.; Visualization, F.N., L.G.; Project administration, F.N., J.N.B.; Resources, A.E., W.R.S., K.J.; Supervision, A.E., W.R.S., K.J., J.N.B.; Funding acquisition, A.E., W.R.S., K.J.

Chapter 5

Synthesis

This synthesis is structured in two sections. In the first section, I discuss the findings from the previous three manuscript chapters (Chapters 2 - 4), emphasizing key concepts such as environmental gradients, carbon cycling processes and the composition of microbial communities. In the second section, I draw conclusions and provide directions for future research.

Environmental gradients

Within this thesis, I highlighted the importance of environmental gradients (e.g., salinity, redox conditions, proximity to roots) in shaping microbial communities and processes. Both small-scale and large-scale gradients have been considered. Along the course of a river, large environmental gradients arise due to the distance from the sea and the tidal dynamics within estuarine marshes. In contrast, within the rhizosphere, similarly steep environmental gradients can also occur on a very small scale (Koop-Jakobsen et al., 2018). The release of oxygen from roots creates oxygen-rich microsites in an otherwise strictly anaerobic environment (Cook & Knight, 2003). Similarly, the release of organic root exudates, such as amino acids or defense compounds, follows the same pattern in the soil (Canarini et al., 2019). My findings show that both microbial community composition and functional gene expression tightly co-vary along these large-scale and small-scale environmental gradients.

Chapter 2 and 4 investigate microbial dynamics in the tidal marshes of the Elbe estuary (Chapter 2, Figure 1; Chapter 4, Figure 1). Chapter 2 primarily focuses on how various environmental parameters correlate with the abundance of dark CO_2-fixing pathways. For this, not only spatial gradients like the distance-to-sea, surface-elevation and soil-depth gradients were considered, but also a variety of environmental soil parameters were measured and compared to the

abundance of key genes and transcripts of dark CO_2-fixing pathways. The results show that organic matter and reduction both covary with the soil-depth gradient (Chapter 2, Table 2), and that reducing soil conditions are strongly associated with the transcript abundance of the CO_2-fixing Wood-Ljungdahl pathway (WLP) (Chapter 2, Table 3). Chapter 4 uses the estuarine gradients to investigate how varying abiotic factors influence litter decomposition and microbial community dynamics in the marsh soils. Chapter 4 shows a negative correlation of reduction with the rate of litter decomposition (see Chapter 4, Figure 7). Combining the findings on reduction effects from this chapter with those from chapter 2, where WLP transcript abundance correlates positively with reduction (see Chapter 2, Table 3), it can be concluded that in highly reduced soils, where litter decomposition is slow, microbes adapted to anaerobic environments are not displaced by microbes with a more energy-efficient metabolism, namely litter decomposition, when new substrates are added.

Unlike chapters 2 and 4, chapter 3 focuses on a small-scale rhizosphere gradient. Despite being smaller in spatial scale, biochemical gradients inside rhizospheres are not necessarily weaker (Koop-Jakobsen et al. 2018). The two extremes – high root exudate influence versus no root exudate influence – were compared to assess the impact of root exudates on the transcriptomic activity of the microbial community and led to the conclusion that root exudates strongly promote a wide array of microbial pathway groups, particularly those related to motility, infection and stress response.

Carbon cycling processes

Chapters 2 - 4 collectively address various aspects of carbon cycling, such as CO_2 fixation, litter decomposition and responses of soil microbes to plant inputs of labile carbon compounds from roots (i.e., exudates). The investigation of these aspects covers both the role of microorganisms in the carbon cycle and the role of biotic interactions, in this case focusing on plant-microbe interactions.

By examining the abundance and transcription of key genes involved in dark CO_2 fixation pathways, I demonstrate how different environmental conditions along steep estuarine gradients influence the abundance of these microbial pathways.

My results show that the Calvin cycle was present in niches high in organic matter, nitrate availability correlated positively with the reductive tricarboxylic acid cycle (rTCA cycle), and the WLP was present in highly reduced soil environments (Chapter 2, Table 3). Now that the niches for dark CO_2 fixation in tidal wetlands have been described in more detail, we are not yet ready to make statements about the carbon balance of the individual metabolic pathways,

but we have a much better understanding of where we can find dark CO_2 fixation in nature. The results from chapter 3 also confirm the high transcript abundance of one of the CO_2-fixing metabolic pathways, the WLP, which appears to be one of the key players in the investigated anaerobic soils (Chapter 3, Figure 3).

Chapter 3 focuses on plant-microbe interactions at the molecular level through transcriptomic analysis. I investigated how root exudates influence the activity of specific microbial metabolic pathways that can strongly impact soil and sediment carbon dynamics (Ren et al., 2022). By combining $^{13}CO_2$ pulse-labeling and metatranscriptomics in a novel methodological approach, I identified a particularly strong upregulation of pathways related to infection, stress response and motility. This highlights the direct response mechanisms and adaptations of microorganisms to plant stimuli, allowing for a deeper understanding of plant-microbe dynamics in the carbon cycle of wetlands.

Chapter 4 also addresses plant-microbe interactions by examining the decomposition process of plant litter and comparing it to microbial data in estuarine marshes along the Elbe estuary. It highlights the important role of litter decomposition in carbon storage within coastal wetlands.

Microbial community composition

I examined microbial community composition within the context of varying environmental conditions. The phyla Pseudomonadota, Bacteroidota, Chloroflexota, Bacillota, Actinomycetotaota, Acidobacteriota and Desulfobacterota were the main players in the ecosystems investigated.

In chapter 2, I evaluated the microbial community behind dark CO_2 fixation pathways in estuarine wetlands and found that the bacterial phyla Desulfobacterota, Methylomirabilota, Nitrospirota, Chloroflexota and Pseudomonadota were the primary players. Regarding the assignment of taxonomy to transcripts, I was able to compare the community of active dark CO_2 fixation (Chapter 2) and the community responding to root exudates (Chapter 3). Apart from the large phylum Pseudomonadota, there were only taxonomic overlaps with the phylum Nitrospirota. On the one hand, the original composition of the communities in the Elbe estuarine tidal marshes and in the salt marsh located at the Hamburger Hallig differ clearly. On the other hand, the active community studied in chapter 2 focuses only on dark CO_2 fixation, while chapter 3 examined the entirety of functional gene transcripts. Chapter 3 emphasized shifts in the active microbial community based on taxonomic assignment of transcripts. These shifts were characterized by increased relative abundances of specific bacterial phyla such as Betaproteobacteria, Campylobacterota, Kiritimatiellota, Lentisphaerota and Verrucomicrobiota.

These results demonstrate the influence of interactions between plants and microbes on the composition of microbial communities in the rhizosphere. When taxonomy is analyzed on the basis of transcripts, we see stronger shifts in the community than when taxonomy is based on the 16S fragment. This is because the reactions at the transcript level are much faster to detect than the reactions at the DNA level, which often require long term incubations to see clear differences (De Vrieze et al., 2016).

Chapter 4 observed a decrease in microbial diversity from soil via native litter to standardized tea litter, emphasizing that different substrates support different plant-derived microbial communities. The strong overlap between soil and native litter microbial communities indicates that soil microbes are well adapted to the local vegetation (Chapter 4, Figure 5). Research for chapters 2 and 4 was carried out in the same study areas, the marshes of the Elbe estuary. Despite seasonal differences (Chapter 2: September sampling, Chapter 4: June sampling), both studies report almost identical soil community distributions with Pseudomonadota, Bacteroidota, Chloroflexota, Acidobacteriota and Desulfobacterota as the most abundant phyla. In an estuarine environment, salinity is probably the strongest driver for changes in microbial community composition, but also pH and oxygen availability for example shape the composition of microbes in the environment (Bernhard et al., 2005; Crump et al., 2004; Herlemann et al., 2011). If community shifts are compared along the estuarine gradients studied in chapters 2 and 4, it becomes evident that salinity is also the strongest driver here (Figure 1 and Chapter 4, Figure 5).

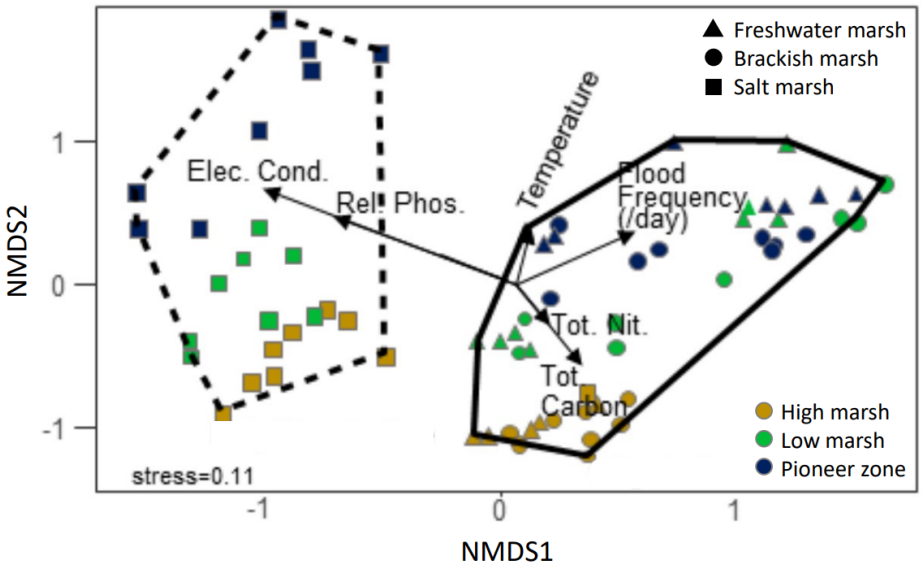

Figure 1. Nonmetric multidimensional scaling ordination of the Elbe estuary soil 16S microbial communities. At least two distinct communities, one salt marsh and one brackish/freshwater marsh community can be identified in the soil microbial samples. Underlying sequence data are the same as presented in chapter 2 (Source: Branoff, Grüterich et al. 2024).

The key findings of chapters 2 - 4 are visualized in figure 3. Green arrows point to the locations, where the highest transcript abundance of the respective CO_2-fixing pathways was observed (Chapter 2). Pathway groups that are highly upregulated as response to root exudates (located below the plant in figure 3) and pathways that were highly upregulated independent of the influence of root exudates are highlighted in blue. Pink arrows indicate the marsh locations with the highest microbial diversity.

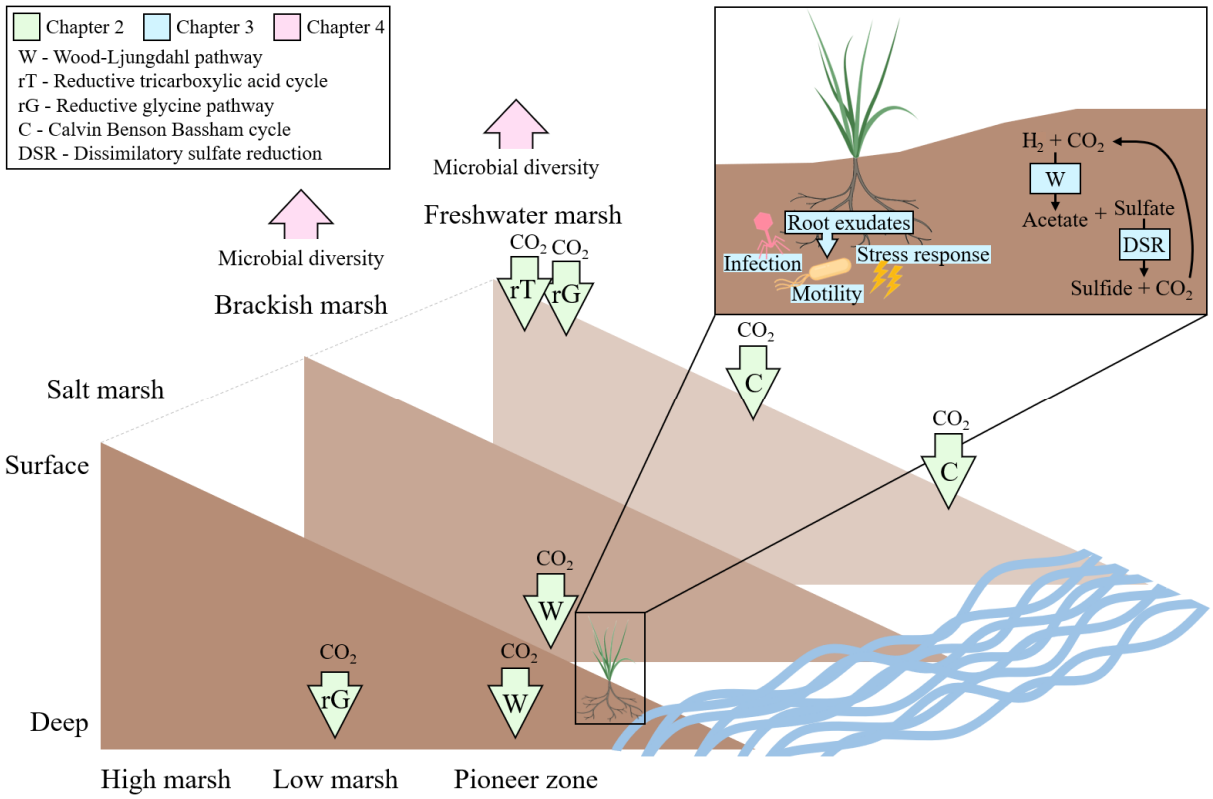

Figure 3. Summary of the key findings of chapters 2 (green), 3 (blue) and 4 (pink) in an environmental context. The localization of microbial metabolic pathways and properties in tidal marshes are visualized.

Conclusion and future research perspectives

My work identifies environmental niches for dark CO_2 fixation (Chapter 2), describes how soil microbes respond to plant root exudates (Chapter 3) and reveals the microbial communities colonizing different types of plant litter material (Chapter 4).

The results presented in **chapter 4**, which relate to the microbial community composition, show that both estuarine gradients and litter material shape microbial community diversity and composition. In order to further investigate the role of the microbial community on litter decomposition in future studies, it would be useful to add metagenome and metatranscriptome

analyses to the rRNA amplicon analysis, which only provides information on the community composition, in order to be able to say something about the functional capacity of the communities. Targeted enzymatic assays can also provide further information about the actual activity of the microbes in the soil, which is related to litter decomposition.

Chapter 3 uncovered the transcriptomic responses of soil microbes on *Spartina anglica* root exudates and emphasize the role of plant-soil interactions on microbial community dynamics and metabolic processes in tidal wetlands. For a broader applicability of these findings, further studies should work with more than a single plant species and also vary the origin or type of soil in order to compare the transcriptomic response differences between variable environmental settings. On a molecular biological level, the experimental approach used in chapter 3 investigates microbial responses to exudates beyond their use as a carbon source, in contrast to RNA-SIP (RNA-stable isotope probing), which focuses on uptake and metabolism. This new approach was chosen because microbes can sense and respond to exudates without metabolizing them. A limitation of the method used for the research in chapter 3 is that exudate effects cannot be clearly distinguished from other root processes. To fully capture microbial responses to exudates and isolate them from background effects, future research will require combined approaches of both tracking root exudates and RNA-SIP.

The results presented in **chapter 2** improve our understanding of the environmental conditions that promote dark CO_2 fixation. These findings allow us to identify environments for screening CO_2-fixing microorganisms, which can then be enriched and cultured in the laboratory for biotechnological applications. In addition, the knowledge gained about the niche preferences of these metabolic pathways can help to optimize the cultivation conditions of these microbes. For example, I showed in chapter 2 that a high organic matter content facilitates high transcript abundance of the Calvin cycle, the rTCA cycle occurs in niches with high nitrate concentration and the WLP is favored by highly reducing conditions (Chapter 2, Table 3). The high transcript abundance of the WLP key genes in anaerobic, reduced soils was also confirmed by the results of chapter 3, where the WLP together with dissimilatory sulfate reduction (DSR) showed the highest transcript abundances (Chapter 3, Figure 3). In order to bring dark CO_2 fixation into the laboratory, it is also useful to understand the syntrophic networks in nature in order to keep these metabolic pathways vital for biotechnological applications. In chapter 3, it is shown that the WLP and DSR are interconnected or mutually beneficial pathways, because the end product of the WLP, acetate, can flow into the DSR as carbon and energy source (Capone & Kiene, 1988). Conversely, the DSR end-product, CO_2, can serve as carbon source in the WLP (Chapter 3, Figure 1A). From an ecosystem perspective, the findings improve our understanding of dark

CO_2 fixation in wetland soils and draw attention to the potential of microbial CO_2 fixation on ecosystem-level greenhouse gas (GHG) dynamics.

While this study provides valuable insights into the ecological niches that support dark CO_2 fixation, there is considerable potential for further research. Introducing a temporal component could improve our understanding of the dynamics of dark CO_2 fixation pathways. This would allow us to investigate how seasonal variations on the large temporal scale and tidal cycles on the smaller temporal scale affect the dark CO_2 fixation potential of soils. Furthermore, additional biogeochemical analyses, such as flux rate measurements of GHGs, which are combined with omics analyses, could help to quantify the role of dark CO_2 fixation in ecosystem CO_2 budgets. Furthermore, modeling approaches that integrate dark CO_2 fixation in ecosystem process models might be useful to more accurately predict biosphere-atmosphere interactions in terms of CO_2 exchange fluxes.

Take-Home Messages

Chapter 2 "Assessing Environmental Gradients in Relation to Dark CO_2 Fixation in Estuarine Wetland Microbiomes"

- Marsh soils of the Elbe estuary show a high diversity of microorganisms, indicating a considerable metabolic potential.
- Several pathways of dark CO_2 fixation have been identified in the marsh soils, including the Calvin cycle, the Wood-Ljungdahl pathway (WLP), the reductive glycine pathway and the reductive tricarboxylic acid cycle.
- Environmental factors that strongly correlate with the transcription of CO_2 fixation pathways are oxygen availability, salinity and nitrate concentration.
- Functional gene regulation is more crucial for the response to environmental gradients than the simple presence of certain microbial groups.
- Knowledge of where CO_2-fixing metabolic pathways occur in the environment enables targeted screening (based on deep DNA and RNA sequencing combined with enrichment cultures) to refine cultivation conditions and optimize the efficiency of microbial CO_2 fixation in the laboratory.

Chapter 3 "Transcriptomic Response of Wetland Microbes to Root Influence"

- Significant transcriptional changes occur in wetland soil microbes in response to plant root exudates in diverse pathways, highlighting complex interactions between plants and microbes.
- Root exudates enhance microbial metabolic pathways related to infection, stress response and motility, indicating a strong influence on microbial behavior and interactions.
- The predominant metabolic pathways operating in the background of anoxic wetland soils include the WLP and dissimilatory sulfate reduction (DSR), which are primarily driven by the microbial groups Deltaproteobacteria and Thermodesulfobacteriota.

Chapter 4 "Litter Decomposition and Prokaryotic Decomposer Communities along Estuarine Gradients"

- Plant litter decomposition rates decrease with increasing salinity and elevation, with higher salinity leading to greater litter stabilization and flooding reducing it.

- The composition of local vegetation and microbial diversity have a significant influence on plant litter decomposition rates, with native litter overlapping with soil microbial communities, suggesting adaptation to local vegetation.
- Substrate type influences microbial community composition and diversity, as soil, native litter and tea litter harbor distinct microbial communities, with selective colonization of tea litter by certain microbial taxa highlighting substrate-specific characteristics.

Supplementary Material

Supplement (Chapter 2)

Table S1. Environmental parameters along special gradients of the Elbe estuary. The table shows the measured values of chloride, organic matter, acetate, pyruvate, isocitrate, nitrate, sulfate and reduction index at each of the 18 sampling sites.

Salinity	Elevation	Depth	Chloride [mg/L]	Organic Matter [g OM/g DW]	Acetate [µM]	Pyruvate [µM]	Isocitrate [µM]	Nitrate [mg/L]	Sulfate [mg/L]	Reduction Index
Salt	High marsh	Surface	2482.49	0.07	65.41	7.39	40.36	34.57	284.30	0.06
Salt	High marsh	Deep	7174.34	0.05	33.55	3.29	22.23	59.77	929.74	0.18
Salt	Low marsh	Surface	2706.68	0.08	26.27	27.95	32.18	42.69	336.76	0.09
Salt	Low marsh	Deep	2356.34	0.04	0.00	103.85	24.09	34.99	391.24	0.21
Salt	Pioneer Zone	Surface	5140.63	0.07	28.83	29.15	15.56	63.66	669.92	0.03
Salt	Pioneer Zone	Deep	5977.01	0.04	0.00	156.09	33.05	41.89	716.18	0.49
Brackish	High marsh	Surface	128.73	0.12	40.43	13.24	23.76	162.43	74.92	0.04
Brackish	High marsh	Deep	264.92	0.01	1.63	3.38	14.47	44.13	122.64	0.22
Brackish	Low marsh	Surface	715.92	0.12	25.29	5.85	51.04	40.83	279.14	0.07
Brackish	Low marsh	Deep	476.69	0.04	0.00	48.69	35.08	29.06	82.47	0.80
Brackish	Pioneer Zone	Surface	419.26	0.11	21.75	11.99	22.92	31.69	88.95	0.08
Brackish	Pioneer Zone	Deep	302.37	0.06	0.00	211.14	16.32	78.20	109.07	0.70
Fresh	High marsh	Surface	268.75	0.07	74.68	31.18	34.01	125.85	179.40	0.02
Fresh	High marsh	Deep	188.40	0.02	9.33	37.12	48.83	58.63	132.29	0.36
Fresh	Low marsh	Surface	219.46	0.15	35.07	45.50	63.32	44.94	228.65	0.02
Fresh	Low marsh	Deep	176.31	0.04	40.90	124.49	146.57	42.46	80.76	0.65
Fresh	Pioneer Zone	Surface	157.39	0.13	67.44	134.37	72.08	37.36	145.30	0.08
Fresh	Pioneer Zone	Deep	185.95	0.09	137.82	136.41	84.06	46.80	69.22	0.83

Text S1. Identification of dark CO_2 fixation in marsh soils

In the process of aiming to characterize the diversity of dark CO_2-fixing pathways in sediments of the Elbe estuary we identified a number of limitations to previous approaches. Of these was the acknowledgement that many of the enzymes involved in these pathways are distinguishable from genes involved in heterotrophic processes (namely TCA cycle) or other processes including maintenance of cellular homeostasis. It is therefore necessary to use genes that, if not exclusive, are for the most part strongly associated with a single pathway. Berg et al. (2010a) previously described a number of 'key genes' that can be used as indicators for the presence of individual dark CO_2-fixing pathways within the genomes of bacteria and archaea. Whilst these genes might be strong indicators of these dark CO_2-fixing pathways, developing our approach we were made aware that these genes alone are insufficient. We should also acknowledge that our genome-centric metagenome approach, also has limitations in that the recovery of complete metagenome assembled genomes (MAGs) is also limited. More specifically, pathways may

appear incomplete due to genes that are otherwise present, but appear to be missing due to differences in assembly and binning.

To this end we sought to develop a pipeline that leverages multiple genes, genomic context and taxonomic information to assess the completion of dark CO_2 fixation pathways. Our pipeline generally consisted of:

1. Identifying genomes containing key genes involved in dark CO_2 fixation (Table 1).
2. Validating the occurrence of these pathways by checking for additional genes/enzymes that are critical for the pathway.
3. Resolving conflicts between CO_2-fixing pathways where one or more genes are shared
4. Validation by comparing pathway completeness for closely related genomes (genus/species)
5. Literature review to resolve missing genes for known dark CO_2-fixing taxa and to confirm/validate identified pathways.

Only once we were confident that individual key gene orthologs were representative of an organism with the capacity to undertake dark CO_2 fixation we included the respective abundance estimations and subsequent analyses. Below we will outline in detail our selection criteria for each of the dark CO_2 fixation pathways and considerations we made at each stage.

Reductive tricarboxylic acid cycle (rTCA cycle)

The rTCA cycle, utilizes many of the enzymes involved in the TCA cycle making its identification difficult using bioinformatic analyses. Fortunately, we observe two enzymes that are markedly different between the forward and reverse cycles, namely the ATP-citrate lyase and the 2-oxoglutarate synthase. In the rTCA cycle the ATP-citrate lyase, replaces the citrate lyase, catalyzing the conversion of citrate to acetyl-CoA and oxaloacetate, consuming one molecule of ATP in the process. The ATP-citrate lyase operon comprises two genes, *aclA* and *aclB*, which encode the alpha and beta subunits, respectively. Similarly, the 2-oxoglutarate dehydrogenase, in the rTCA is replaced by the 2-oxoacid:ferredoxin oxidoreductase. Whilst the dehydrogenase utilizes NAD(H), under favorable oxidative conditions, the reverse reaction requires a reduced ferredoxin to overcome the energic constraints. The precise nature of this enzyme appears to differ amongst organisms capable of using the rTCA cycle with some organisms possessing either a 2-subunit or 4-subunit 2-oxoglutarate:ferredoxin oxidoreductase (OGOR, *korAB*(*CD*)), whilst others appear to leverage additional 4-subunit or 5-subunit

pyruvate:ferredoxin oxidoreductases (OPOR, *porABCD*(*E*)), with the 5-subunit form proposed to confer addition oxygen tolerance.

We started by identifying genomes containing the ATP-citrate lyase operon, considering genomes containing both the *aclA* and *aclB* genes. We initially identified 15 genomes, associated with six genera, containing either the *aclA* or *aclB* genes, including seven non-redundant *aclA* and seven non-redundant *aclB* orthologs. We identified two *aclA* and one *aclB* othologs amongst four genomes of the Gammaproteobacteria genus UBA9214. In one of the four genomes, we actually identified, both *aclA* orthologs, with one clustered alongside other rTCA genes and another embedded in genes associated with DNA replication. We considered this second ortholog to be erroneous and removed it. We identified three genera of Nitrospirota (*Nitrospira*_F, Palsa-1315 and an unclassified NS-4 family member) containg *aclAB* orthologs, with each of the three containing different non-redundant orthologs. The single NS-4 family genome contained both genes, of the three *Nitrospira*_F genomes only one contained both genes, although the individual genes were all homologous. We identified four Palsa-1315 genomes, with two originating from the same sample. These two genomes were assigned to the same genus, both contained both *aclA* and *aclB* but between these two genomes we detected different orthologs of these two genes. A third genome contained a single *aclA* gene which was homologous to one of the two previously mentioned, whereas the fourth genome contained a single *aclB* gene which was not similar to any of the aforementioned. We also detected a single *aclA* ortholog in the genome of a Desulfobacterota SM23-61 and a single *aclB* ortholog in the genome of the Thermoproteota PALSA-986.

We next sought to validate these occurrences based on the presence of the 2-oxoacid/pyruvate ferredoxin oxidoreductases. We detected the presence of 2-oxoacid ferredoxin oxidoreductases in 432 genomes, mostly in the form of 2-subunit OGOR (*korAB*) but also as 4-subunit OPOR (*porABCD*). Of those genomes with *aclAB* we detected both 2-subunit OGOR and 4-subunit OPOR in the UBA9214, PALSA-986 and SM23-61 genomes. The SM23-61 genome was unique in many ways in that it contained many divergent *korAB* and *porABCD* copies with a pattern that was shared amongst other ATP-citrate lyase lacking Desulfobacterota genomes. This uncertainty, the lack of *aclB* was sufficient to exclude this organism from our subsequent analysis. We were unable to detect OGOR (*korAB*) genes amongst any of the Nitrospirota genomes, rather amongst these genomes we detected two to three clusters encoding three subunit OPOR (*porABC*) with at least one of these clusters containing *porD*. The potential of OPOR enzymes to perform OGOR activity has been previously reported for *Nitrospira marina* and giving us confidence that a similar process is likely occurring here. OPOR genes in

Nitrospira species were not present on the same contig as the ATP-citrate lyase operon, for a single *Nitrospira*_F genome we found a cluster encoding the ATP-citrate lyase, isocitrate dehydrogenase (*icd*) aconitate hydratase (*acnA*) and succinyl-CoA synthetase beta subunit (*sucC*) providing us confidence that these three *Nitrospira* taxa, similar to *Nitrospira marina* are capable of dark CO_2 fixation via the rTCA cycle. For exploration of gene copy number and transcript abundance we selected the *aclA* gene, representing five orthologs:

Table S4. List of *aclA* orthologs and taxonomic assignment.

***aclA* ortholog**	**Phylum**	**Class**	**Family/genus**
STRE22-1_MAGS_0000069813	Nitrospirota	Nitrospiria	f__NS-4
STRE22-1_MAGS_0000070550	Nitrospirota	Nitrospiria	g__Nitrospira_F
STRE22-1_MAGS_0000070440	Nitrospirota	Nitrospiria	g__Palsa-1315
STRE22-1_MAGS_0000070441	Nitrospirota	Nitrospiria	g__Palsa-1315
STRE22-1_MAGS_0000060863	Pseudomonadota	Gammaproteobacteria	g__UBA9214

Wood-Ljungdahl pathway (WLP)

The WLP involves two specific enzymes namely the Acetyl-CoA synthase (ACS) and a CO dehydrogenase (CODH) forming the CODH/ACS complex. The genes directing the assembly of these two enzyme complexes are often colocalized into a single operon with slight differences between archaea (*cdhA-E*) and bacteria (*acsA-E*). Bacteria encode for an additional THF-corrinoid methyltransferase (*acsE*) which forms part of the ACS module and archaea encode an additional small subunit (*chdB*) which binds FAD as a cofactor (Adam et al., 2018). We commenced our search by identifying genomes with genes encoding the large subunit of the CODH (*cooS/acsA*). This gene alone is not sufficient to identify confirm the presence of the ACS/CODH operon as its homolog *cooS*. Whilst both enzymes are capable of the reduction of CO_2 to CO or oxidation of CO to CO_2, the standalone *cooS* enzyme has been shown to be essential for growth on CO suggesting the reverse reaction is favored (Jain et al., 2022). We identified 47 unique *cooS/acsA* amongst 51 genomes. These genomes primarily represented Chloroflexota and Desulfobacterota but also included Myxococcota, Nitrospirota, Gammaproteobacteria and Acidobacteriota.

We attempted to confirm the presence of the complete *acs/cdh* operons in bacterial and archaeal genomes. The fragmented nature of our MAGs meant that it was not always possible to determine whether missing genes were a consequence of assembly or binning parameters. Incomplete *acs* operons have been demonstrated for instance in Dehalococcoides, where rather

than CO_2 fixation the pathway is involved in methyl-tetrahydrofolate recycling supporting methionine biosynthesis (Zhuang et al., 2014).

We confirmed the presence of an archaeal type *cdhA-E* operon (across two contigs) in the genome of Bathyarchaeota (g__PALSA-986), a complete bacterial type (*acsA-E*, 3 contigs) operon in the genome of Nitrospirota (g__JAAXXJ01), partial bacterial type (*acsACD*) in genome of Nitrospirota g__JACRPZ01, partial bacterial type (*ascBCDE*) in the genome of Desulfobacterota (g__BM002), partial bacterial type (*ascCDE*) in the genome of Desulfobacterota (g__BM002), partial bacterial type (*ascADE*) in the genome of Desulfobacterota (g__SM23-61), partial bacterial type (*ascABCE*) in the genome of Desulfobacterota (SM23-61), partial bacterial type (*ascBCE*) in two genomes of Desulfobacterota (g__JAHJIQ01), partial bacterial type (*ascABCE*) in five genomes of Desulfobacterota (g__BM004), partial bacterial type (*ascABE*) in the genome of Desulfobacterota (g__ g__UBA2230), partial bacterial type (*ascABCE*) in the genome of Desulfobacterota (g__UBA11574), partial bacterial type (*ascABCE*) in the genome of Desulfobacterota (g__ g__JAAXQD01), partial bacterial type (*ascABCE*) in 5 genomes of Desulfobacterota (g__DSXZ01), partial bacterial type (*ascABCE*) in the genome of Desulfobacterota (g__4484-190-2), partial bacterial type (*ascACDE*) in the genome of Desulfobacterota (g__ g__ partial bacterial type (*ascABCE*) in the genome of Desulfobacterota (g__S015-6)), three genomes only *acsAC* g__SpSt-501.

Amongst the Desulfobacterota we observed a consistent pattern amongst the different taxa, specifically members of the Syntrophobacteria lacked *acsA*, SM23-61 lacked *acsB-C* and whereas other genomes consistently lacked *acsD*. The lack of *acsA* in amongst Syntrophobacteria is consistent with that of other potentially syntrophic bacteria e.g. Dehalococcoides which runs the WLP in reverse cleaving acetyl-CoA and leading to the accumulation of CO as an inhibitory by-product. For those lacking *acsD*, this included the Desulfobulbia which represent the enigmatic cable-bacteria. There is a general consensus for the presence of complete and functional WLP, with studies highlighting the capacity of Desulfobulbia to grow autotrophically in the absence of an organic carbon source. This discrepancy might arise due to differences in annotation approaches, with one study in particular noting that the WLP was incomplete when annotated with KEGG but then complete using UniProtKB annotation. Manual inspection of contigs containing all genes, except *acsD*, showed no evidence for an unannotated gene. Despite this, considering the overwhelming literature evidence in support of autotrophic growth amongst Desulfobulbia we concluded this

consistent lack of an annotated *acsD* was insufficient to discount that there is a high likelihood that the WLP is active in these genomes.

For exploration of gene copy number and transcript abundance we considered which of the four genes shared between archaea and bacteria would be suitable. We immediately discounted *acsD*/*cdhD* as it was absent from the genomes of Desulfobulbia. We also ruled out *acsA*/*cdhA* as its homology with *cooS* meant it was often duplicated within the genome. Ultimately, we chose *acsC*/*cdhE* as it was nearly always exclusively present at single copy in those organisms with a near complete operon and was well conserved amongst closely related genomes.

This resulted in 13 *acsC*/*cdhE* orthologs that we used for subsequent analyses:

Table S5. List of *acsC/cdhE* orthologs and taxonomic assignment.

***acsC/cdhE* ortholog**	**Phylum**	**Class**	**Family/genus**
STRE22-1_MAGS_0000172077	Desulfobacterota	DSM-4660	g__4484-190-2
STRE22-1_MAGS_0000171191	Desulfobacterota	DSM-4660	g__DSXZ01
STRE22-1_MAGS_0000173103	Desulfobacterota	Desulfobacteria	g__JAAXQD01
STRE22-1_MAGS_0000173477	Desulfobacterota	Desulfobacteria	g__SpSt-501
STRE22-1_MAGS_0000173498	Desulfobacterota	Desulfobacteria	g__SpSt-501
STRE22-1_MAGS_0000172741	Desulfobacterota	Desulfobacteria	g__UBA11574
STRE22-1_MAGS_0000167657	Desulfobacterota	Desulfobulbia	g__BM004
STRE22-1_MAGS_0000167616	Desulfobacterota	Desulfobulbia	g__BM004
STRE22-1_MAGS_0000167621	Desulfobacterota	Desulfobulbia	g__BM004
STRE22-1_MAGS_0000172603	Desulfobacterota	Desulfobulbia	g__JABDQA01
STRE22-1_MAGS_0000154618	Desulfobacterota	Desulfobulbia	g__JAHJIQ01
STRE22-1_MAGS_0000173451	Nitrospirota	UBA9217	g__JAAXXJ01
STRE22-1_MAGS_0000144585	Thermoproteota	Bathyarchaeia	g__PALSA-986

Calvin cycle

The Calvin cycle represents the mechanism for inorganic carbon fixation by all photosynthetic organisms. RuBisCO is the central enzyme in this catalyzing the carboxylation of ribose-1,5-bisphophsate with CO_2. We identified 99 MAGs containing the gene encoding the RuBisCO large subunit (*rbcL*) and 86 MAGs which contained, in addition, the gene encoding the RuBisCO small subunit (*rbcS*). Considering only Type I RuBisCO possesses the small subunit, compared to type II-III which also perform carbon fixation (Asplund-Samuelsson & Hudson, 2021), we did not consider absence of *rbcS* as disqualifying. Therefore, we also considered additional genes, specifically we insisted that the phosphoribulokinase (*prkB*) was present in addition to both *rbc* genes. In instances where *prkB* or one of the *rbc* genes was absent we additional checked for other genes in the Calvin cycle specifically phosphoglycerate kinase (*pgk*) and ribose 5-phosphate isomerase (*rpiAB*).

We did not detect any photosynthetic genes (*puf* operon) in the genomes of those organisms with *rbcL* suggesting that the Calvin cycle is not driven by photosynthesis. Rather we detected sulfur oxidizing genes in the form of either thiosulfate dehydrogenase (*tsd*) or sulfur oxidizing protein SoxZ in the genomes of nearly all *rbcL* positive genomes. We also identified bacterioferritin gene (*bfd*/*bfr*) in a number of *rbcL* positive genomes, but also those lacking *rbcL*. What was more interesting is that for a number of genomes (e.g. UBA9214) bacterioferritin was colocalized with *rbcL*/*S* on the genome. In contrast, we did not detect a strong association of Fe(II) oxidizing or ammonium oxidizing pathways in the *rbcL* positive genomes.

In contrast to other pathways, we identified multiple distinct copies of the *rbcL*, *rbcS* and *prkB* genes. Ultimately, we decided to retain *rbcL* abundances for downstream analyses. In a few cases we detected more than distinct copy of the *rbcL* gene per genome, with one clearly colocalized with *rbcS* and other carbon fixing genes. In these few instances we retained only the colocalized *rbcL* copy.

This resulted in 38 *rbcL* orthologs that we used for subsequent analyses:

Table S6. List of *rbcL* orthologs and taxonomic assignment.

***rbcL* ortholog**	**Phylum**	**Class**	**Family/genus**
STRE22-1_MAGS_0000139357	Acidobacteriota	Vicinamibacteria	
STRE22-1_MAGS_0000187619	Chloroflexota	Anaerolineae	
STRE22-1_MAGS_0000129077	Chloroflexota	Limnocylindria	g__CF-167
STRE22-1_MAGS_0000132891	Methylomirabilota	Methylomirabilia	g__Methylomirabilis
STRE22-1_MAGS_0000133626	Methylomirabilota	Methylomirabilia	g__Methylomirabilis
STRE22-1_MAGS_0000133639	Methylomirabilota	Methylomirabilia	g__Methylomirabilis
STRE22-1_MAGS_0000134692	Myxococcota_A	UBA9160	
STRE22-1_MAGS_0000146838	Pseudomonadota	Alphaproteobacteria	g__JADFVY01
STRE22-1_MAGS_0000133783	Pseudomonadota	Alphaproteobacteria	g__R-RK-3
STRE22-1_MAGS_0000128945	Pseudomonadota	Gammaproteobacteria	
STRE22-1_MAGS_0000129166	Pseudomonadota	Gammaproteobacteria	
STRE22-1_MAGS_0000158893	Pseudomonadota	Gammaproteobacteria	
STRE22-1_MAGS_0000131940	Pseudomonadota	Gammaproteobacteria	g__CADEEN01
STRE22-1_MAGS_0000132721	Pseudomonadota	Gammaproteobacteria	g__Ga0077527
STRE22-1_MAGS_0000122682	Pseudomonadota	Gammaproteobacteria	g__Gallionella
STRE22-1_MAGS_0000130040	Pseudomonadota	Gammaproteobacteria	g__GCA-001735895
STRE22-1_MAGS_0000145946	Pseudomonadota	Gammaproteobacteria	g__GCA-001735895
STRE22-1_MAGS_0000148759	Pseudomonadota	Gammaproteobacteria	g__GCA-001735895
STRE22-1_MAGS_0000141422	Pseudomonadota	Gammaproteobacteria	g__JAABQT01
STRE22-1_MAGS_0000151976	Pseudomonadota	Gammaproteobacteria	g__JAACFB01
STRE22-1_MAGS_0000158726	Pseudomonadota	Gammaproteobacteria	g__JAACFE01
STRE22-1_MAGS_0000158436	Pseudomonadota	Gammaproteobacteria	g__JABDPF01
STRE22-1_MAGS_0000128793	Pseudomonadota	Gammaproteobacteria	g__RPQJ01
STRE22-1_MAGS_0000128062	Pseudomonadota	Gammaproteobacteria	g__SG8-30

STRE22-1_MAGS_0000142226	Pseudomonadota	Gammaproteobacteria	g__SG8-39
STRE22-1_MAGS_0000129882	Pseudomonadota	Gammaproteobacteria	g__SM1-46
STRE22-1_MAGS_0000127155	Pseudomonadota	Gammaproteobacteria	g__Sulfuricaulis
STRE22-1_MAGS_0000129631	Pseudomonadota	Gammaproteobacteria	g__Sulfuricaulis
STRE22-1_MAGS_0000143834	Pseudomonadota	Gammaproteobacteria	g__Sulfuricaulis
STRE22-1_MAGS_0000157466	Pseudomonadota	Gammaproteobacteria	g__SZUA-36
STRE22-1_MAGS_0000158405	Pseudomonadota	Gammaproteobacteria	g__SZUA-36
STRE22-1_MAGS_0000146986	Pseudomonadota	Gammaproteobacteria	g__Thiogranum
STRE22-1_MAGS_0000155953	Pseudomonadota	Gammaproteobacteria	g__UBA1847
STRE22-1_MAGS_0000127856	Pseudomonadota	Gammaproteobacteria	g__UBA6901
STRE22-1_MAGS_0000131669	Pseudomonadota	Gammaproteobacteria	g__UBA9214
STRE22-1_MAGS_0000145819	Pseudomonadota	Gammaproteobacteria	g__UBA9214
STRE22-1_MAGS_0000146716	Pseudomonadota	Gammaproteobacteria	g__UBA9214
STRE22-1_MAGS_0000146998	Pseudomonadota	Gammaproteobacteria	g__UBA9214

Reductive glycine pathway (rGlyP)

The rGlyP commences in a similar manner to the WLP with the reduction of CO_2 to formate, however following the reduction of formate rather than CO, condensation of a second CO_2 occurs giving rise to glycine. The critical enzymes in this step are the methyenyl-THF cyclohydrolase (MTHFD) involved in the reduction of formate, glycine cleavage/synthase (*glr*) which performs the condensation reaction of the second CO_2 molecule to give rise to glycine and the glycine reductase (*grd*) which converts glycine to acetyl-P.

The glycine reductase complex is only partially specific to the reductive glycine pathway, in that homologs are also known to act to reduce also sarcosine and betaine. The enzyme complex comprises four subunits with *grdA*, *grdC* and *grdD* involved in none specific reactions, however *grdB*/*E* and its paralogs *grdF*/*G* and *grdH*/*I* confer specificity of the different substrates. As for other pathways we sought to establish the presence of the *grd* operon in genomes also containing the MTHFD and glycine cleavage/synthase module. In total we identified 14 *grdB* orthologs. Of these four did not occur alongside other *grdB* genes, the MTHFD or *glr* genes. Eight of the remaining ten orthologous *grdB* copies represented four pairs of co-occurring and often adjacent genes, consisting of a > 1000 bp gene and a ~230-250 bp gene. The combined size of these two fragments were consistent with database and literature searches for this gene. These genes were situated between the *grdA* and a gene annotated as glycine C-acetyltransferase consistent with the function of *grdC*. It was not clear what contributed to this cleavage, however we opted to select in each case the larger fragment for quantification.

Table S7. List of *rbcL* orthologs and taxonomic assignment.

***grdB* ortholog**	**Phylum**	**Class**	**Family/genus**
STRE22-1_MAGS_0000296067	Pseudomonadota	Alphaproteobacteria	g__
STRE22-1_MAGS_0000303920	Chloroflexota	Anaerolineae	g__J095

STRE22-1_MAGS_0000306728	Methylomirabilota	Methylomirabilia	g__
STRE22-1_MAGS_0000311329	Desulfobacterota_B	Binatia	g__JACPFE01

Hydroxybutarate cycles (DC/4-HB cycle, 3-HP/4-HB cycle, 3-HP-bicycle)

The decarboxylative 4-hydroxybutarate and 3-hydroxypropinoate/4-hydroxyburate cycles share a number of common enzymes, specifically involved in the regeneration of acetyl-CoA from succinyl-CoA via 4-HB-CoA, crotonoyl-CoA intermediates. The pathways specifically diverge with the DC/HB-cycle mirroring the rTCA cycle with the carboxylation of acetyl-CoA to pyruvate and reduction via malate and fumarate intermediates. In contrast, the 3-HP/4-HB cycle mirrors the 3-HP bicycle with carboxylation of acetyl-CoA to a malonyl-CoA intermediate which is reduced via 3-HP, 3-HP-CoA and methylmalonyl-CoA intermediates.

Considering the number of shared genes/enzymes between these pathways, their overlap with other carbon-fixing pathways and the potential redundancy of genes with other metabolic pathways, ultimately proving the functionality of these pathways from metagenome data is tenuous. Despite this we still sought to identify genomes, where these pathways are present and use this data to explore their ecological significance.

We commenced our search by identifying 94 genomes containing the gene encoding the 4-hydroxybutyryl-CoA dehydratase (*abfD*). These 94 genomes included Chloroflexota, Desulfobacterota, Myxococcota as well as Gamma- and Alphaproteobacteria and comprised 60 unique *abfD* orthologs. We next expanded our search to include additional genes involved in the 3-HP/4-HB cycle namely the methylmalonyl-CoA mutase (MUT) which is also present in the 3-HP bicycle and the 3-methylcrotonyl-CoA carboxylase which is also shared by the DC/4-HB cycle. We only identified three genomes, belonging to the Alphaproteobacterial genus WHUA01 which contained all three of these genes. We did not detect either the phosphoenolpyruvate (PEP) carboxylase (*ppc*), which would be necessary for a functional DC/HB cycle. However, when we expanded our search to also include genes involved in 3-HP metabolism we were surprised to find a complete lack of critical genes. Most notably enzymes (ec:6.4.1.2, ec:1.2.1.75, ec:1.1.1.298, ec:6.2.1.36) involved in carboxylation of acetyl-CoA to propionyl-CoA via 3-HP were completely absent from the dataset excluding (ec:4.2.1.116 and ec:1.3.1.84), which occurred in a handful of genomes with no overlap.

Based on the complete absence of these enzymes from any genome we considered that both the 3-HP/4-HB cycle and the 3-HP bicycle were completely absent from genomes in our samples.

We next refined our list of *abfD* containing genomes to those that do contain the PEP carboxylase as a means for identifying those organisms utilizing the DC/4-HB cycle. We identified seven genomes belonging to the Gammaprotoebacterial genus g__CADEEN01, one

genome from an unclassified Desulfuromonadia (STRE22-1_SAMEA110292004_MAG_00000068), one genome from the Desulfobacterota g__S015-6, one genome from an *Acidimicrobiia* genus UBA4744 that contained both *abfD* and *ppc* genes. However, despite containing the *abfD* and *ppc* genes, we were unable to detect the presence of critical enzymes in any of these genomes, that would allow for the reduction of succinyl-CoA to acetyl-CoA via 4-HB. Specifically, we did not identify any succinyl-CoA reductases, succinate semialdehyde reductases, or enoyl-reductases. This strongly suggests that despite the diversity of *abfD* genes in our dataset very few are involved directly in dark CO_2-fixing pathways.

A recent analysis examining the occurrence of dark CO_2-fixing pathways across several thousand MAGs suggested that the DC/4-HB cycle appears to be restricted to archaea, specifically Sulfolobales and Thermoproteales, whereas the 3-HP/4-HB cycle occurs in both archaea as well as Alpha- and Gammaproteobacteria. 3-HP bicycle genes were first described for Chloroflexota but were also found in Gammaproteobacteria and Gemmatimonadota. 3-HP CO_2 fixation pathways (3-HP/4-HB and 3-HP bicycle) were generally limited to photosynthetic bacteria with pathways for bacteriochlorophyll biosynthesis, an aspect which was also lacking from any of our sequenced genomes (Garritano et al., 2022).

Supplement (Chapter 3)

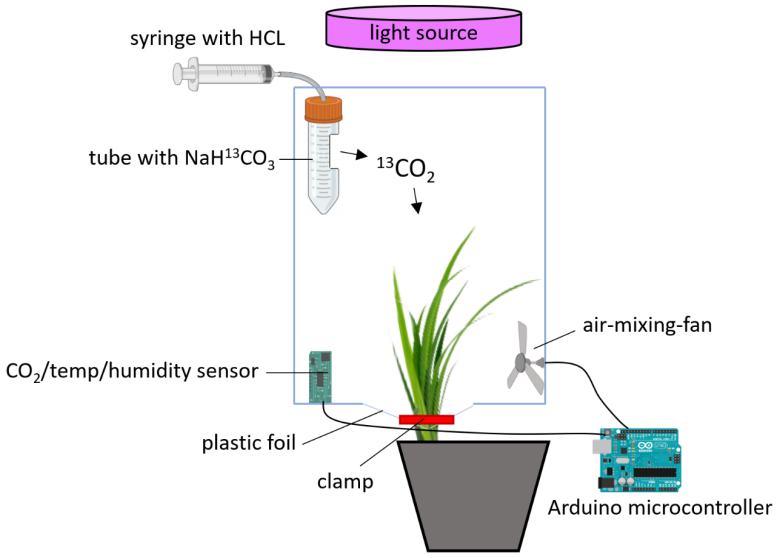

Figure S1. Schematic of $^{13}CO_2$ labeling chamber. Aboveground biomass is illuminated with an LED light source and exposed to $^{13}CO_2$ circulated in the transparent PVC chamber. Direct contact of labeled CO_2 with the soil was prevented by sealing the aboveground biomass at the shoot base using plastic film and clamps. A tight seal was accomplished and damage to shoots minimized by placing foam pads between clamp and shoots.

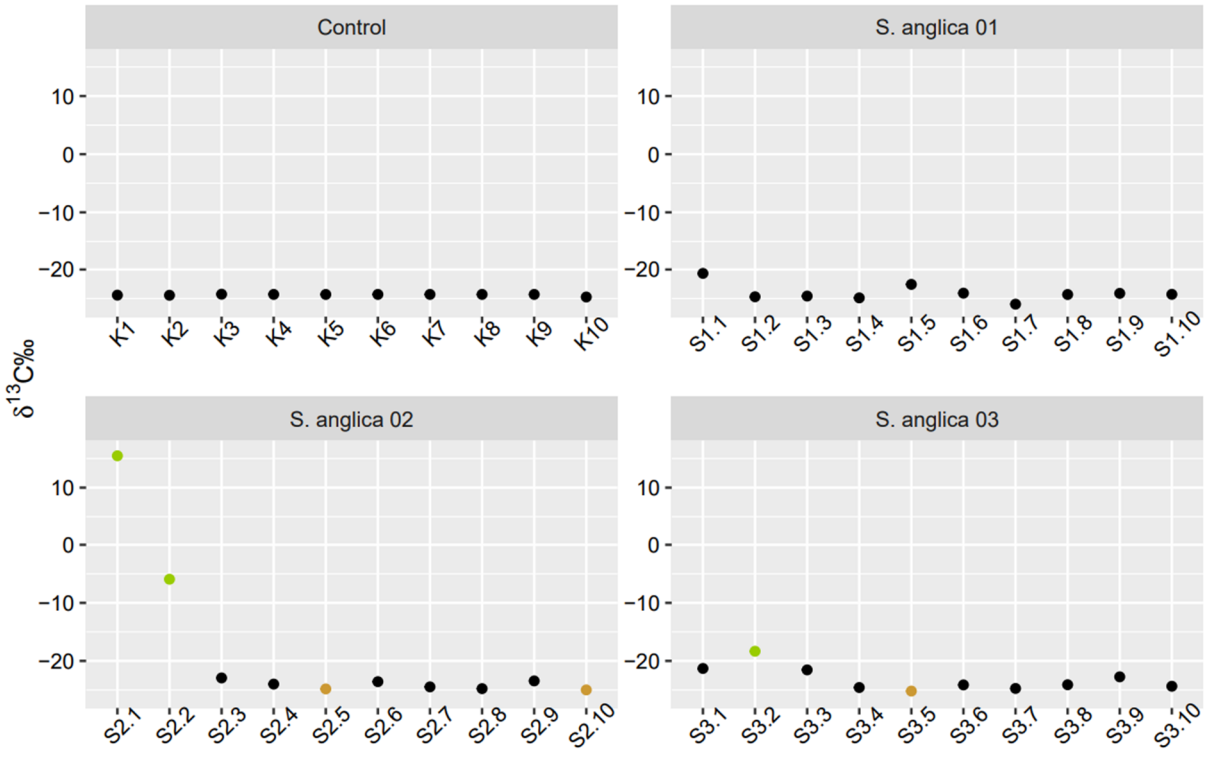

Figure S2. Scatterplot of delta ^{13}C signal in 40 soil samples after pulse-labelling. Colored are the samples used for metatranscriptomic sequencing. Soil samples with high ^{13}C signatures (i.e. rhizosphere soil) are in green; samples with low ^{13}C signatures (i.e. bulk soil) in brown.

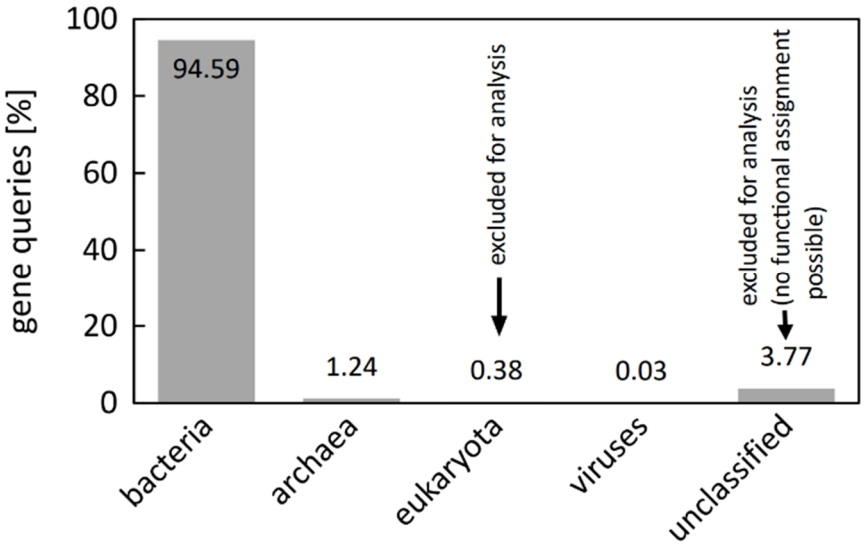

Figure S3. Taxonomic distribution of gene queries.
Percentage of gene queries assigned to bacteria, archaea, eukaryota, viruses and genes that could not taxonomically be assigned (unclassified). Arrows indicate groups that were excluded for analysis.

Table S1. Bioinformatic output summary of the metagenome (metaG) that consists of a co-assembly of the metagenome 'NoRoot' and 'Root'.

	NoRoot	Root	co-assembled metaG
Total_Reads	74,148,310	80,603,444	37,965,400
Mapped reads	19,202,660	20,994,728	
Mapped [%]	25.90	26.05	
Num_of_scaffolds			80,894
Num_of_contigs			87,362
Contig [bp]			237,020,000
Gap [%]			0.145
N50			14,475
L50			3,372
N90			64,632
L90			1,217
N_Predicted_Genes			269,428
MAGs (compl. 70-99.8%)			13

Table S2. Bioinformatic output of metatranscriptomic reads (metaT) mapped to coassembled contigs.

	S2_1_high metaT	S2_2_high metaT	S3_2_high metaT	S2_7_low metaT	S3_6_low metaT	S3_10_low metaT
Total_Reads	11,926,662	20,677,854	13,468,226	16,843,094	27,279,520	5,420,742
mapped_Reads	828,063	1,421,828	1,031,738	1,046,490	1,721,926	387,670
Mapped [%]	6.94	6.88	7.66	6.21	6.31	7.15

Table S3. Bioinformatic output of mapped metatranscriptomic reads to the SILVA database.

	S2_1_high metaT	S2_2_high metaT	S3_2_high metaT	S2_7_low metaT	S3_6_low metaT	S3_10_low metaT
Total_Reads	59,183,872	92,628,710	66,058,376	71,013,190	106,000,000	20,247,024
mapped_Reads	33,114,620	50,674,333	38,172,098	33,699,450	49,910,414	9,508,265
Mapped [%]	55.95	54.71	57.79	47.46	47.03	46.96

Supplement (Chapter 4)

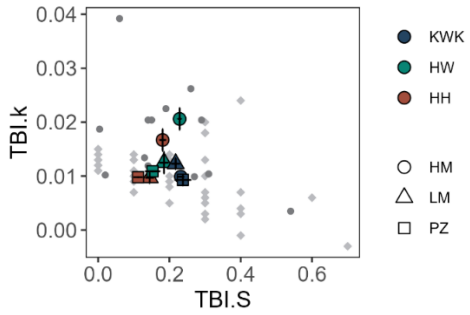

Figure S1. (A) Annual means of decomposition rates k_{TBI} versus stabilization factor S_{TBI} of tea litter along the salinity and flooding gradient of the Elbe estuary. Light grey diamonds indicate global marshes taken from Mueller et al. (2018), darker grey dots indicate global data taken from Keuskamp et al. (2013). Whiskers indicate standard error of the mean based on five pairs of tea bags and four seasons at each site.

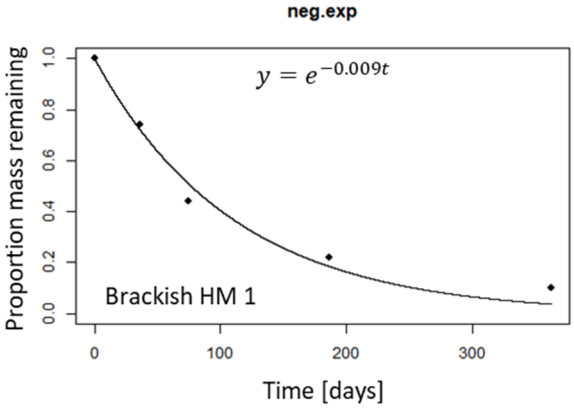

Figure S2. Example model fit (negative exponential) using the R package "litterfitter". Based on relative remaining mass over five time steps.

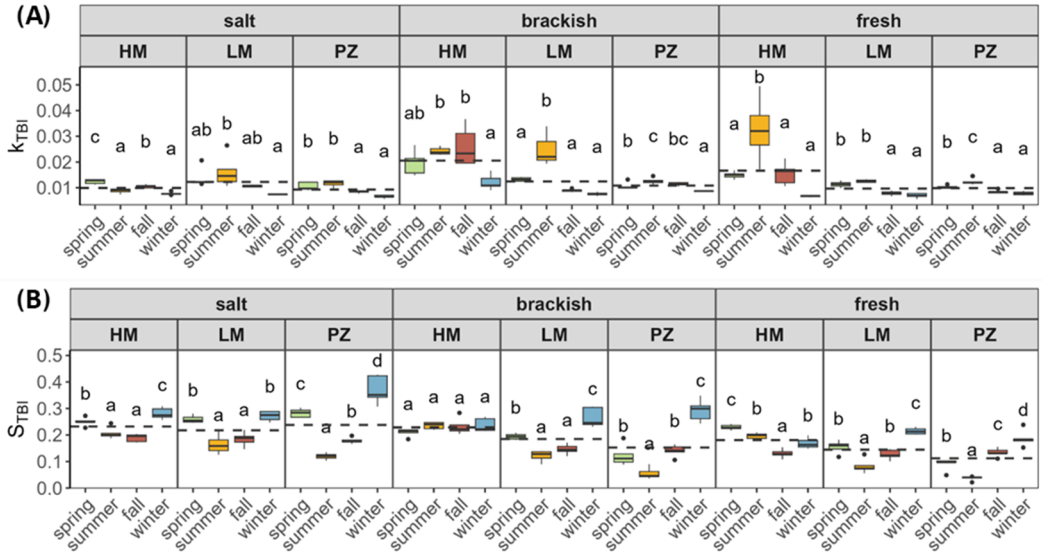

Figure S3. Seasonal variation in (A) decomposition rate k_{TBI} and (B) stabilization factor S_{TBI} of tea litter along the salinity (salt marsh, brackish marsh, freshwater marsh) and flooding gradient (HM = high marsh, LM = low marsh, PZ = pioneer zone) of the Elbe estuary (n = 5). Lowercase letters indicate significant differences ($p < 0.05$) derived from linear mixed effect model applied on each marsh location separately (n = 5). Dashed lines indicate mean annual decomposition rate k_{TBI} or stabilization factor S_{TBI}.

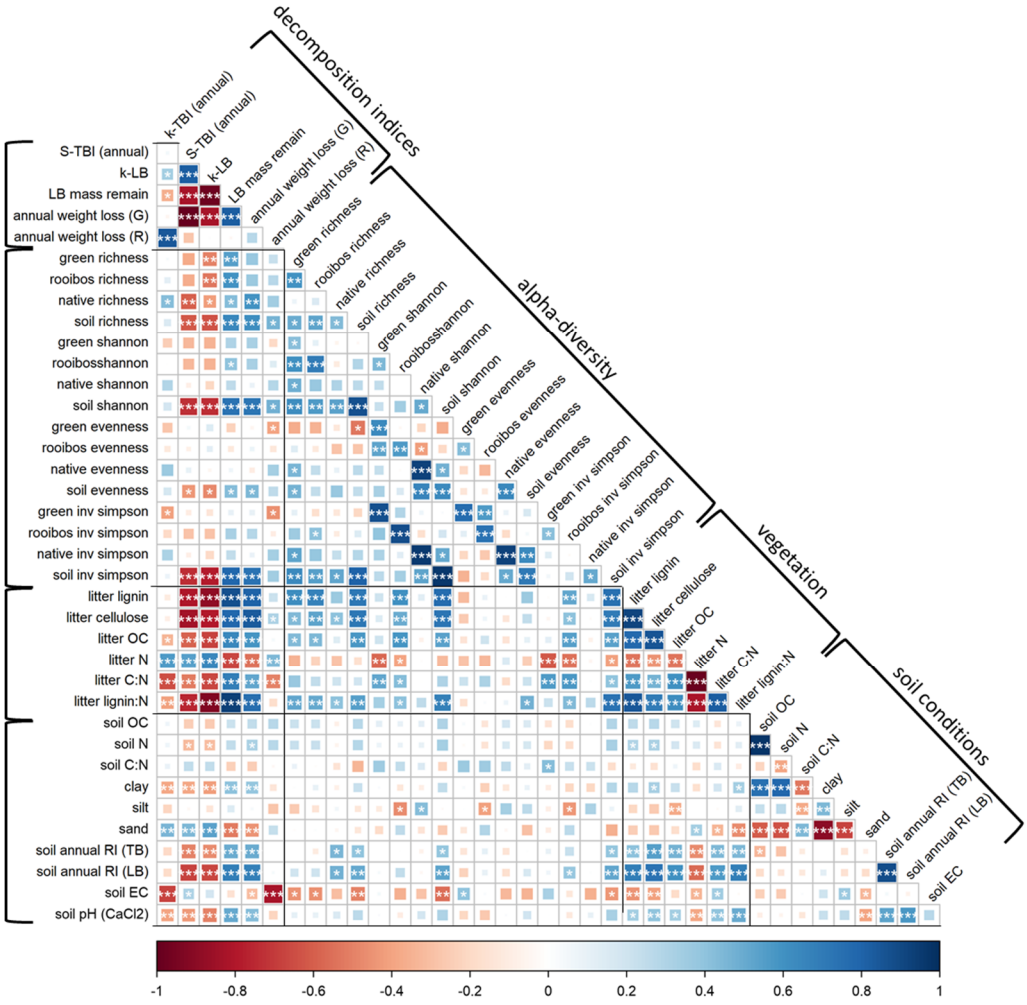

Figure S4. Spearman correlation matrix between litter decomposition indices and selected site characteristics. Asterisk indicate significant correlation at: * $p < 0.05$, ** $p < 0.005$ and *** $p < 0.001$.

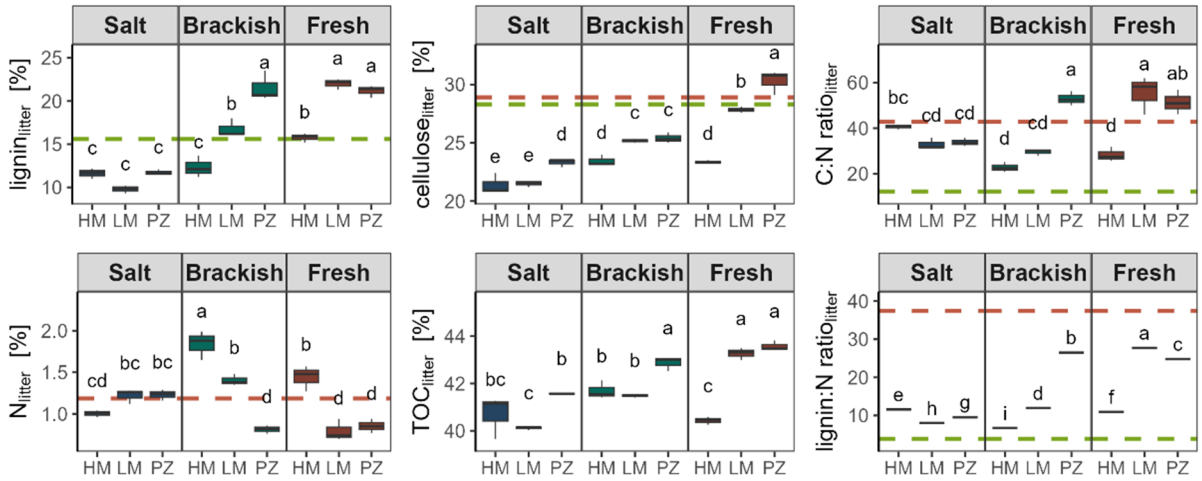

Figure S5. Litter quality indices along the salinity (salt marsh, brackish marsh, freshwater marsh) and flooding gradient (HM = high marsh, LM = low marsh, PZ = pioneer zone) of the Elbe estuary (n = 3). Lowercase letters indicate significant differences ($p < 0.05$) derived from ANOVA with TukeyHSD post-hoc comparison. Dashed horizontal lines indicate values for green tea (green) and rooibos tea (red) based on values in Keuskamp et al. 2013.

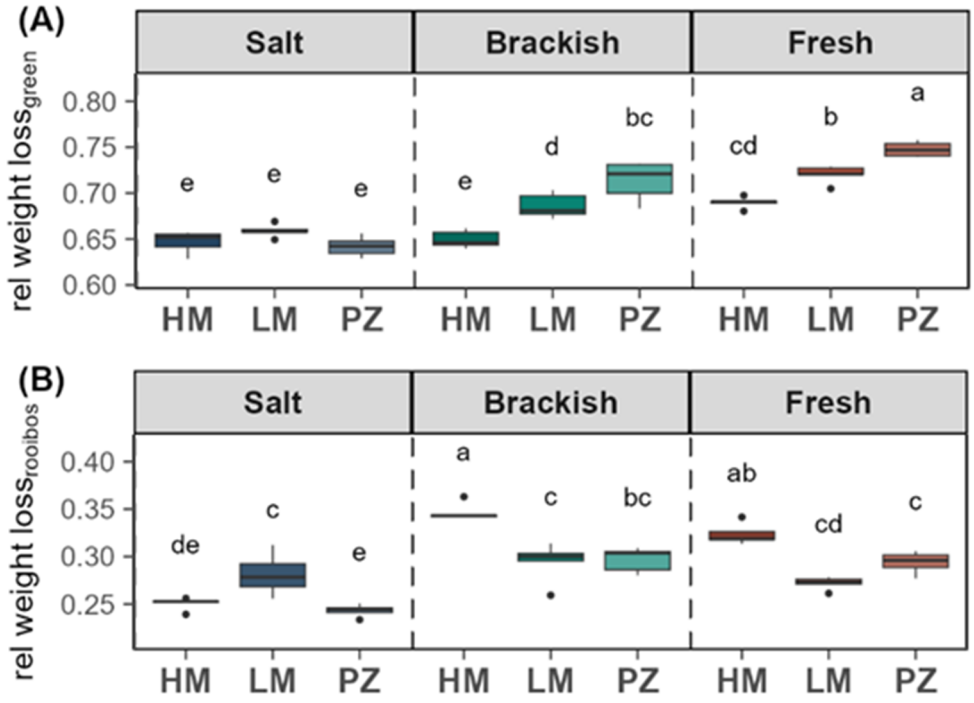

Figure S6. Annual weight loss of (A) green tea and (B) rooibos tea along the salinity (salt marsh, brackish marsh, freshwater marsh) and flooding gradient (HM = high marsh, LM = low marsh, PZ = pioneer zone) of the Elbe estuary (n = 5). Lowercase letters indicate significant differences ($p < 0.05$) derived from ANOVA with TukeyHSD post-hoc comparison.

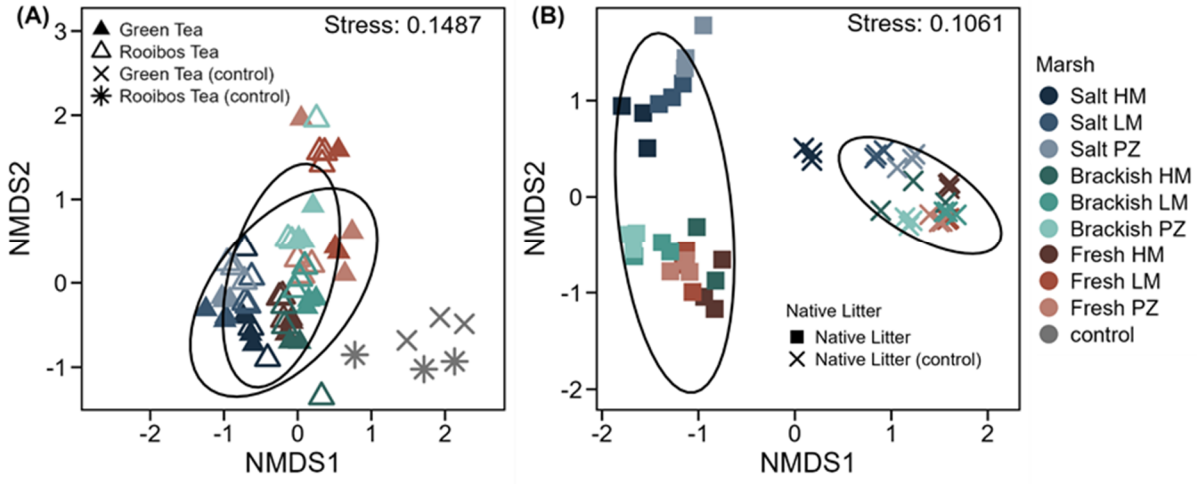

Figure S7. NMDS based on Bray-Curtis dissimilarity of the prokaryotic community associated with (A) tea litter and (B) native litter at genus level along the salinity (salt marsh, brackish marsh, freshwater marsh) and flooding gradient (HM = high marsh, LM = low marsh, PZ = pioneer zone) of the Elbe estuary and their non-incubated controls. Ellipses indicate 90% confidence area per litter type.

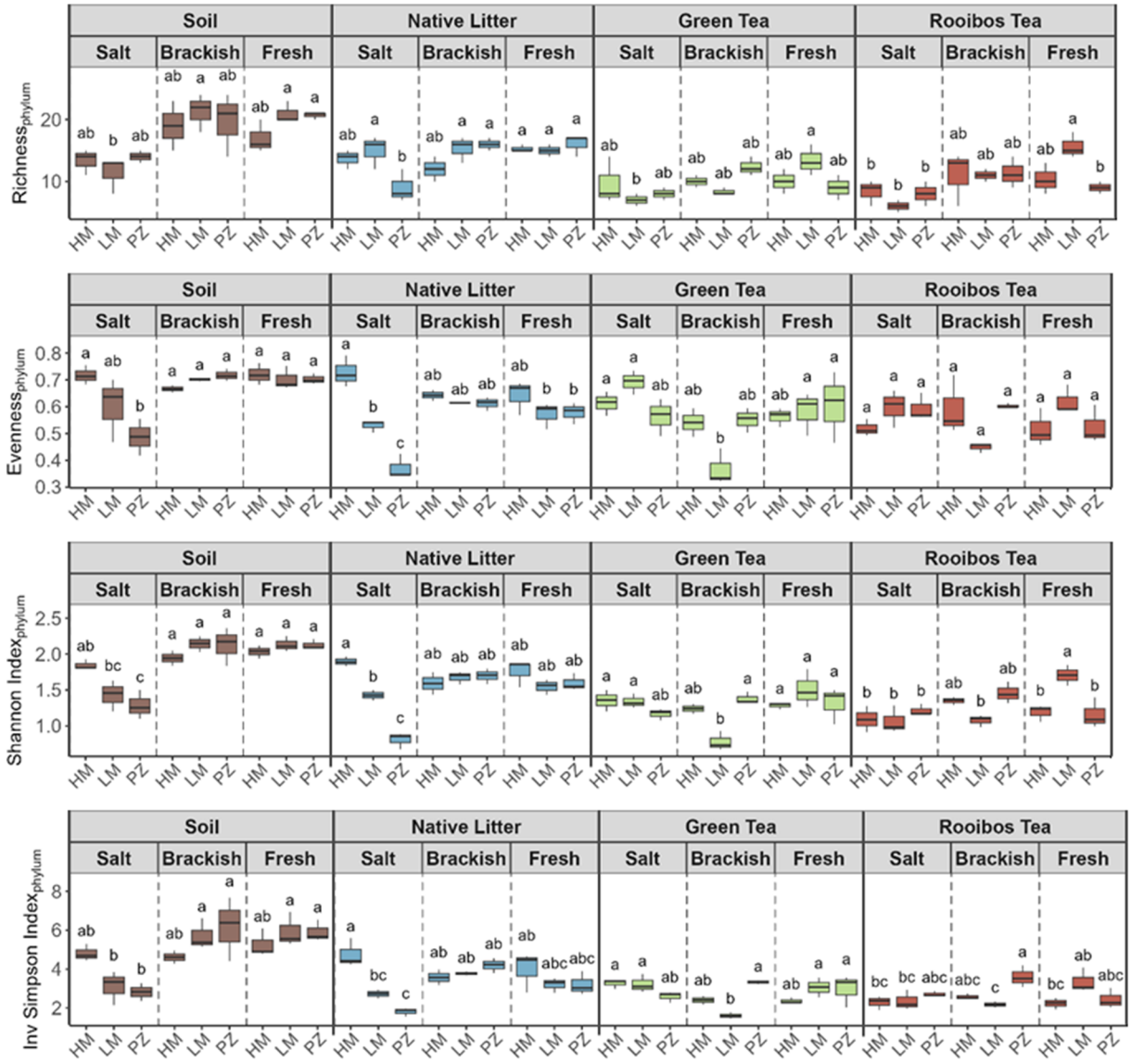

Figure S8. Alpha diversity (richness, evenness, Shannon Diversity Index and Inverse Simpson Index) of the prokaryotic community at phylum level in the different substrate types along the salinity (salt marsh, brackish marsh, freshwater marsh) and flooding gradient (HM = high marsh, LM = low marsh, PZ = pioneer zone) of the Elbe estuary (n = 3). Lowercase letters indicate significant differences ($p < 0.05$) derived from ANOVA with TukeyHSD post-hoc comparison applied on each substrate type separately.

Table S1. Decomposition indices of tea and native litter along the salinity and flooding gradient of the Elbe estuary.

Salinity Gradient	Flooding Gradient	Season	Tea litter								Native litter			
			k (TBI)		S (TBI)		rel weight loss (G)		rel weight loss (R)		k (LB)		rel mass remaining (LB)	
			mean	sde	mean	sde	mean	sde	mean	sde	mean	sde	mean	sde
Salt Marsh	HM	spring	0.012	± 0.0004	0.25	± 0.01	0.63	± 0.01	0.28	± 0.01				
		summer	0.009	± 0.0004	0.21	± 0.01	0.67	± 0.01	0.24	± 0.01				
		fall	0.011	± 0.0003	0.19	± 0.01	0.68	± 0.01	0.28	± 0.00				
		winter	0.008	± 0.0003	0.28	± 0.01	0.61	± 0.01	0.21	± 0.00				
		annual	0.010	± 0.0000	0.23	± 0.01	0.65	± 0.01	0.25	± 0.01	0.006	± 0.00	0.24	± 0.01
	LM	spring	0.014	± 0.0017	0.26	± 0.01	0.62	± 0.01	0.28	± 0.02				
		summer	0.016	± 0.0028	0.17	± 0.02	0.70	± 0.01	0.34	± 0.02				
		fall	0.011	± 0.0002	0.18	± 0.01	0.69	± 0.01	0.28	± 0.00				
		winter	0.007	± 0.0001	0.27	± 0.01	0.61	± 0.01	0.20	± 0.00				
		annual	0.012	± 0.0010	0.22	± 0.01	0.66	± 0.01	0.28	± 0.01	0.011	± 0.00	0.13	± 0.01
	PZ	spring	0.011	± 0.0007	0.28	± 0.01	0.60	± 0.01	0.25	± 0.01				
		summer	0.012	± 0.0006	0.12	± 0.01	0.74	± 0.00	0.32	± 0.01				
		fall	0.008	± 0.0002	0.18	± 0.01	0.69	± 0.00	0.24	± 0.00				
		winter	0.007	± 0.0003	0.37	± 0.02	0.53	± 0.02	0.16	± 0.01				
		annual	0.009	± 0.0010	0.24	± 0.02	0.64	± 0.02	0.24	± 0.01	0.008	± 0.00	0.20	± 0.02
Brackish Marsh	HM	spring	0.020	± 0.0021	0.21	± 0.01	0.67	± 0.01	0.36	± 0.01				
		summer	0.024	± 0.0007	0.24	± 0.01	0.64	± 0.00	0.37	± 0.00				
		fall	0.026	± 0.0034	0.23	± 0.01	0.65	± 0.01	0.38	± 0.01				
		winter	0.012	± 0.0013	0.24	± 0.01	0.64	± 0.01	0.28	± 0.02				
		annual	0.021	± 0.0020	0.23	± 0.01	0.65	± 0.00	0.35	± 0.01	0.009	± 0.00	0.12	± 0.03
	LM	spring	0.013	± 0.0003	0.19	± 0.00	0.68	± 0.00	0.30	± 0.00				
		summer	0.025	± 0.0034	0.12	± 0.01	0.74	± 0.01	0.44	± 0.02				
		fall	0.009	± 0.0002	0.15	± 0.01	0.72	± 0.01	0.27	± 0.00				
		winter	0.008	± 0.0003	0.27	± 0.02	0.62	± 0.01	0.19	± 0.01				
		annual	0.012	± 0.0020	0.18	± 0.01	0.69	± 0.01	0.30	± 0.02	0.004	± 0.00	0.38	± 0.02
	PZ	spring	0.011	± 0.0006	0.12	± 0.02	0.74	± 0.01	0.32	± 0.01				
		summer	0.013	± 0.0006	0.06	± 0.01	0.80	± 0.01	0.35	± 0.01				
		fall	0.011	± 0.0003	0.14	± 0.01	0.72	± 0.01	0.31	± 0.01				
		winter	0.009	± 0.0001	0.29	± 0.02	0.60	± 0.02	0.21	± 0.01				
		annual	0.011	± 0.0000	0.15	± 0.02	0.71	± 0.02	0.30	± 0.01	0.002	± 0.00	0.54	± 0.01
Fresh-water Marsh	HM	spring	0.015	± 0.0006	0.23	± 0.00	0.65	± 0.00	0.31	± 0.01				
		summer	0.033	± 0.0060	0.20	± 0.01	0.68	± 0.00	0.42	± 0.02				
		fall	0.016	± 0.0019	0.13	± 0.01	0.73	± 0.01	0.36	± 0.02				
		winter	0.007	± 0.0001	0.17	± 0.01	0.70	± 0.01	0.21	± 0.00				
		annual	0.017	± 0.0020	0.18	± 0.01	0.69	± 0.01	0.32	± 0.02	0.004	± 0.00	0.32	± 0.03
	LM	spring	0.011	± 0.0005	0.15	± 0.01	0.71	± 0.01	0.30	± 0.01				
		summer	0.013	± 0.0003	0.08	± 0.01	0.77	± 0.01	0.34	± 0.00				
		fall	0.008	± 0.0004	0.13	± 0.01	0.74	± 0.01	0.25	± 0.01				
		winter	0.007	± 0.0004	0.21	± 0.01	0.66	± 0.00	0.20	± 0.01				
		annual	0.010	± 0.0010	0.14	± 0.01	0.72	± 0.01	0.27	± 0.01	0.002	± 0.00	0.61	± 0.02
	PZ	spring	0.010	± 0.0003	0.09	± 0.01	0.77	± 0.01	0.32	± 0.01				
		summer	0.012	± 0.0006	0.04	± 0.00	0.81	± 0.00	0.36	± 0.01				
		fall	0.008	± 0.0003	0.13	± 0.01	0.73	± 0.01	0.26	± 0.01				
		winter	0.008	± 0.0003	0.19	± 0.01	0.68	± 0.01	0.22	± 0.00				
		annual	0.010	± 0.0000	0.11	± 0.01	0.75	± 0.01	0.29	± 0.01	0.002	± 0.00	0.58	± 0.01

Table S2. Plant species with area coverage [%] and Ellenberg Indicator Values for salinity (EIV-S) (Ellenberg et al., 1991) along the salinity and flooding gradient of the Elbe estuary in July 2022.

Salt High Marsh	[%]	**Brackish High Marsh**	[%]	**Fresh High Marsh**	[%]
Agrostis stolonifera	<0.1	*Agrostis stolonifera*	0.1	*Agrostis stolonifera*	0.8
Aster tripolium	13.4	*Berula erecta*	0.3	*Calystegia sepium*	7.2
Atriplex littoralis	0.2	*Calystegia sepium*	28.3	*Equisetum palustre*	0.1
Atriplex prostrata	15.8	*Dactylis glomerata*	<0.1	*Phalaris arundinacea*	7.6
Elymus athericus	62.3	*Epilobium hirsutum*	24.1	*Phragmites australis*	54.0
Salicornia europaea	<0.1	*Galeopsis sp.*	<0.1	*Urtica dioica*	21.1
Suaeda maritima	0.5	*Galium palustre*	0.2	*Valeriana officinalis*	0.6
		Phalaris arundinacea	4.9		
		Phragmites australis	10.9		
		Poa trivalis	0.2		
		Rosa sp.	2.3		
		Urtica dioica	6.7		
		Valeriana officinalis	<0.1		
		Vicia cracca	0.3		
EIV-S: 5.4		EIV-S: 0.3		EIV-S: 0.0	
Salt Low Marsh	[%]	**Brackish Low Marsh**	[%]	**Fresh Low Marsh**	[%]
Agrostis stolonifera	0.2	*Agrostis stolonifera*	0.2	*Bidens sp.*	0.1
Aster tripolium	18.2	*Berula erecta*	6.9	*Caltha palustris*	0.1
Atriplex littoralis	<0.1	*Caltha palustris*	0.3	*Myosotis palustris*	0.1
Atriplex prostrata	5.6	*Calystegia sepium*	9.5	*Nasturtium officinale*	0.1
Elymus athericus	<0.1	*Lycopus europaeus*	0.9	*Phragmites australis*	92.6
Festuca rubra	8.3	*Phragmites australis*	73.0		
Halimione portulacoides	1.4				
Plantago maritima	<0.1				
Puccinellia maritima	40.8				
Salicornia europaea	1.7				
Spartina anglica	2.3				
Spergularia media	0.1				
Suaeda maritima	3.4				
Triglochin maritima	13.2				
EIV-S: 7.0		EIV-S: 0.1		EIV-S: 0.0	
Salt Pioneer Zone	[%]	**Brackish Pioneer Zone**	[%]	**Fresh Pioneer Zone**	[%]
Aster tripolium	3.2	*Bolboschoenus maritimus*	73.5	*Alisma plantago-aquatica*	1.8
Atriplex prostrata	2.0	*Nasturtium officinale*	0.2	*Caltha palustris*	16.0
Halimione portulacoides	0.01			*Mentha aquatica*	0.1
Puccinellia maritima	4.1			*Myosotis palustris*	0.1
Salicornia europaea	<0.1			*Typha angustifolia*	46.0
Spartina anglica	59.1				
Suaeda maritima	2.6				
Triglochin maritima	0.8				
EIV-S: 7.8		EIV-S: 2.0		EIV-S: 0.7	

Table S3. Selected soil properties of the different marsh types along the salinity (salt marsh, brackish marsh, freshwater marsh) and flooding gradient (HM = high marsh, LM = low marsh, PZ = pioneer zone) of the Elbe estuary (mean ± standard error, n = 5). Mean of five replicates.

Marsh type & zone		Depth [cm]	SOC [%]	pH_{CaCl_2}	EC *[µS/cm]*	clay *[%]*	silt *[%]*	sand *[%]*
Salt Marsh	HM	0 - 10	2.9 ± 0.6	7.2 ± 0.3	2606 ± 1081	21.1 ± 4.3	68.1 ± 3.5	10.8 ± 6.1
	LM	0 - 10	1.6 ± 0.2	7.2 ± 0.1	2093 ± 418	14.5 ± 5.1	54.4 ± 7.0	31.1 ± 10.8
	PZ	0 - 10	1.8 ± 0.3	7.2 ± 0.1	2494 ± 387	20.0 ± 7.8	48.4 ± 4.5	31.6 ± 6.4
Brackish Marsh	HM	0 - 10	3.8 ± 1.0	7.1 ± 0.1	292 ± 87	10.4 ± 6.2	18.2 ± 6.4	71.4 ± 12.5
	LM	0 - 10	2.7 ± 0.4	7.3 ± 0.1	704 ± 96	24.4 ± 4.1	63.4 ± 1.2	12.2 ± 3.5
	PZ	0 - 10	0.2 ± 0.0	7.3 ± 0.1	456 ± 39	3.4 ± 0.9	37.5 ± 3.3	59.2 ± 3.7
Freshwater Marsh	HM	0 - 10	5.2 ± 0.6	7.1 ± 0.0	330 ± 79	26.4 ± 1.7	63.3 ± 1.1	10.2 ± 1.6
	LM	0 - 10	5.8 ± 0.7	7.2 ± 0.0	1074 ± 436	39.8 ± 5.7	53.6 ± 4.6	6.6 ± 1.9
	PZ	0 - 10	4.6 ± 0.2	7.4 ± 0.1	1053 ± 188	39.9 ± 12.5	57.4 ± 11.4	2.8 ± 2.1

Table S4. Mean volumetric water content (VWC) of the soil profile at freshwater marsh (HM = high marsh, LM = low marsh, PZ = pioneer zone) corresponding to the incubation periods of the tea bags (n = 1).

Marsh type & zone		Depth [cm]	VWC_{spring} *[%]*	VWC_{summer} *[%]*	VWC_{fall} *[%]*	VWC_{winter} *[%]*
Freshwater Marsh	HM	10	41.9	27.4	43.0	55.5
	LM	10	59.6	56.9	59.6	60.9
	PZ	10	70.1	72.7	75.4	76.1

References

Adam, P. S., Borrel, G., & Gribaldo, S. (2018). Evolutionary history of carbon monoxide dehydrogenase/acetyl-CoA synthase, one of the oldest enzymatic complexes. Proceedings of the National Academy of Sciences, 115(6), E1166-E1173.

Aerts, R. (1997). Climate, Leaf Litter Chemistry and Leaf Litter Decomposition in Terrestrial Ecosystems: A Triangular Relationship. Oikos, 79(3), 439.

Agethen, S., Sander, M., Waldemer, C., & Knorr, K.-H. (2018). Plant rhizosphere oxidation reduces methane production and emission in rewetted peatlands. Soil Biology and Biochemistry, 125, 125-135.

Akinyede, R., Taubert, M., Schrumpf, M., Trumbore, S., & Küsel, K. (2022). Dark CO_2 fixation in temperate beech and pine forest soils. Soil Biology and Biochemistry, 165, 108526.

Aoshima, M., Ishii, M., & Igarashi, Y. (2004). A novel biotin protein required for reductive carboxylation of 2-oxoglutarate by isocitrate dehydrogenase in Hydrogenobacter thermophilus TK-6. Molecular Microbiology, 51(3), 791-798.

Appel, A. M., Bercaw, J. E., Bocarsly, A. B., Dobbek, H., DuBois, D. L., Dupuis, M., Ferry, J. G., Fujita, E., Hille, R., & Kenis, P. J. (2013). Frontiers, opportunities, and challenges in biochemical and chemical catalysis of CO_2 fixation. Chemical Reviews., 113(8), 6621-6658.

Asplund-Samuelsson, J., & Hudson, E. P. (2021). Wide range of metabolic adaptations to the acquisition of the Calvin cycle revealed by comparison of microbial genomes. PLOS Computational Biology, 17(2), e1008742.

Bährle, R., Böhnke, S., Englhard, J., Bachmann, J., & Perner, M. (2023). Current status of carbon monoxide dehydrogenases (CODH) and their potential for electrochemical applications. Bioresources and Bioprocessing, 10(1), 84.

Bais, H. P., Park, S.-W., Weir, T. L., Callaway, R. M., & Vivanco, J. M. (2004). How plants communicate using the underground information superhighway. Trends in Plant Science, 9(1), 26-32.

Bais, H. P., Weir, T. L., Perry, L. G., Gilroy, S., & Vivanco, J. M. (2006). The role of root exudates in rhizosphere interactions with plants and other organisms. Annual Review of Plant Biology, 57, 233-266.

Baker, B. J., Lazar, C. S., Teske, A. P., & Dick, G. J. (2015). Genomic resolution of linkages in carbon, nitrogen, and sulfur cycling among widespread estuary sediment bacteria. Microbiome, 3, 14.

Balch, W. E., Schoberth, S., Tanner, R. S., & Wolfe, R. (1977). Acetobacterium, a new genus of hydrogen-oxidizing, carbon dioxide-reducing, anaerobic bacteria. International Journal of Systematic and Evolutionary Microbiology, 27(4), 355-361.

Banda, D. M., Pereira, J. H., Liu, A. K., Orr, D. J., Hammel, M., He, C., Parry, M. A., Carmo-Silva, E., Adams, P. D., & Banfield, J. F. (2020). Novel bacterial clade reveals origin of form I Rubisco. Nature Plants, 6(9), 1158-1166.

Basile-Doelsch, I., Balesdent, J., & Pellerin, S. (2020). Reviews and syntheses: The mechanisms underlying carbon storage in soil. Biogeosciences, 17(21), 5223-5242.

Bauer, M., Kube, M., Teeling, H., Richter, M., Lombardot, T., Allers, E., Würdemann, C. A., Quast, C., Kuhl, H., Knaust, F., Woebken, D., Bischof, K., Mussmann, M., Choudhuri, J. V., Meyer, F., Reinhardt, R., Amann, R. I., & Glöckner, F. O. (2006). Whole genome analysis of the marine Bacteroidetes'Gramella forsetii' reveals adaptations to degradation of polymeric organic matter. Environmental Microbiology, 8(12), 2201-2213.

Becker, J. N., & Kuzyakov, Y. (2018). Teatime on Mount Kilimanjaro: Assessing climate and land-use effects on litter decomposition and stabilization using the Tea Bag Index. Land Degradation & Development, 29(8), 2321-2329.

Beer, J., & Blodau, C. (2007). Transport and thermodynamics constrain belowground carbon turnover in a northern peatland. Geochimica et Cosmochimica Acta, 71(12), 2989-3002.

Benner, R., Maccubbin, A., & Hodson, R. E. (1984). Anaerobic biodegradation of the lignin and polysaccharide components of lignocellulose and synthetic lignin by sediment microflora. Applied and Environmental Microbiology, 47(5), 998-1004.

Berg, I. A. (2011). Ecological aspects of the distribution of different autotrophic CO_2 fixation pathways. Applied and Environmental Microbiology, 77(6), 1925-1936.

Berg, I. A., Kockelkorn, D., Buckel, W., & Fuchs, G. (2007). A 3-hydroxypropionate/4-hydroxybutyrate autotrophic carbon dioxide assimilation pathway in Archaea. Science, 318(5857), 1782-1786.

Berg, I. A., Kockelkorn, D., Ramos-Vera, W. H., Say, R., Zarzycki, J., & Fuchs, G. (2010a). Autotrophic Carbon Fixation in Biology: Pathways, Rules, and Speculations. In Carbon Dioxide as Chemical Feedstock, M. Aresta (Ed.), pp. 33-53.

Berg, I. A., Kockelkorn, D., Ramos-Vera, W. H., Say, R. F., Zarzycki, J., Hügler, M., Alber, B. E., & Fuchs, G. (2010b). Autotrophic carbon fixation in archaea. Nature Reviews Microbiology, 8(6), 447-460.

Berg, I. A., Ramos-Vera, W. H., Petri, A., Huber, H., & Fuchs, G. (2010c). Study of the distribution of autotrophic CO_2 fixation cycles in Crenarchaeota. Microbiology, 156(1), 256-269.

Berg, J. S., Ahmerkamp, S., Pjevac, P., Hausmann, B., Milucka, J., & Kuypers, M. M. M. (2022). How low can they go? Aerobic respiration by microorganisms under apparent anoxia. FEMS Microbiology Reviews, 46(3).

Bernhard, A. E., Colbert, D., McManus, J., & Field, K. G. (2005). Microbial community dynamics based on 16S rRNA gene profiles in a Pacific Northwest estuary and its tributaries. FEMS Microbiology Ecology, 52(1), 115-128.

Bezemer, T. M., Fountain, M. T., Barea, J. M., Christensen, S., Dekker, S. C., Duyts, H., van Hal, R., Harvey, J. A., Hedlund, K., Maraun, M., Mikola, J., Mladenov, A. G., Robin, C., Ruiter, P. C. d., Scheu, S., Setälä, H., Smilauer, P., & van der Putten, W. H. (2010). Divergent composition but similar function of soil food webs of individual plants: plant species and community effects. Ecology, 91(10), 3027–3036.

Bezerra, R. H. S., Sousa-Souto, L., Santana, A. E. G., & Ambrogi, B. G. (2021). Indirect plant defenses: volatile organic compounds and extrafloral nectar. Arthropod-Plant Interactions, 15(4), 467-489.

Bianchi, T. S. (2007). Biogeochemistry of estuaries. Oxford University Press.

Bierschenk, A. M., Savage, C., Townsend, C. R., & Matthaei, C. D. (2012). Intensity of Land Use in the Catchment Influences Ecosystem Functioning Along a Freshwater-Marine Continuum. Ecosystems, 15(4), 637-651.

Blöchl, E., Rachel, R., Burggraf, S., Hafenbradl, D., Jannasch, H. W., & Stetter, K. O. (1997). *Pyrolobus fumarii*, gen. and sp. nov., represents a novel group of archaea, extending the upper temperature limit for life to 113°C. Extremophiles, 1, 14-21.

Boehlich, M. J., & Strotmann, T. (2008). The Elbe Estuary. Die Küste, 74(1), 288-306.

Borges, F. O., Santos, C. P., Paula, J. R., Mateos-Naranjo, E., Redondo-Gomez, S., Adams, J. B., Caçador, I., Fonseca, V. F., Reis-Santos, P., & Duarte, B. (2021). Invasion and extirpation potential of native and invasive Spartina species under climate change. Frontiers in Marine Science, 8, 696333.

Bowen, J. L., Morrison, H. G., Hobbie, J. E., & Sogin, M. L. (2012). Salt marsh sediment diversity: a test of the variability of the rare biosphere among environmental replicates. The ISME Journal, 6(11), 2014-2023.

Branoff, B. B., Grüterich, L., Wilson, M., Tobias-Hunefeldt, S. P., Saadaoui, Y., Mittmann-Goetsch, J., Neiske, F., Lexmond, F., Becker, J. N., Grossart, H.-P., Porada, P., Streit, W. R., Eschenbach, A., Kutzbach, L., & Jensen, K. (2024). Partitioning biota along the Elbe River estuary: where are the community transitions? bioRxiv, 10.1101/2024.05.13.593883.

Brevik, E. C., & Homburg, J. A. (2004). A 5000 year record of carbon sequestration from a coastal lagoon and wetland complex, Southern California, USA. Catena, 57(3), 221-232.

Buchfink, B., Reuter, K., & Drost, H.-G. (2021). Sensitive protein alignments at tree-of-life scale using DIAMOND. Nature Methods, 18(4), 366-368.

Büttner, D. (2016). Behind the lines–actions of bacterial type III effector proteins in plant cells. FEMS Microbiology Reviews, 40(6), 894-937.

Butzeck, C., Eschenbach, A., Gröngröft, A., Hansen, K., Nolte, S., & Jensen, K. (2015). Sediment Deposition and Accretion Rates in Tidal Marshes Are Highly Variable Along Estuarine Salinity and Flooding Gradients. Estuaries and Coasts, 38(2), 434-450.

Cai, M., Yin, X., Tang, X., Zhang, C., Zheng, Q., & Li, M. (2022). Metatranscriptomics reveals different features of methanogenic archaea among global vegetated coastal ecosystems. Science of the Total Environment, 802, 149848.

Callahan, B. J., McMurdie, P. J., Rosen, M. J., Han, A. W., Johnson, A. J. A., & Holmes, S. P. (2016). DADA2: High-resolution sample inference from Illumina amplicon data. Nature Methods, 13(7), 581–583.

Canarini, A., Kaiser, C., Merchant, A., Richter, A., & Wanek, W. (2019). Root Exudation of Primary Metabolites: Mechanisms and Their Roles in Plant Responses to Environmental Stimuli. Frontiers in Plant Science, 10(157).

Cantalapiedra, C. P., Hernández-Plaza, A., Letunic, I., Bork, P., & Huerta-Cepas, J. (2021). eggNOG-mapper v2: functional annotation, orthology assignments, and domain prediction at the metagenomic scale. Molecular Biology and Evolution, 38(12), 5825-5829.

Capone, D. G., & Kiene, R. P. (1988). Comparison of microbial dynamics in marine and freshwater sediments: Contrasts in anaerobic carbon catabolism. Limnology and Oceanography, 33(4part2), 725-749.

Carrasco-Barea, L., Llorens, L., Romaní, A. M., Gispert, M., & Verdaguer, D. (2022). Litter decomposition of three halophytes in a Mediterranean salt marsh: Relevance of litter quality, microbial activity and microhabitat. The Science of the Total Environment, 838(Pt 1), 155743.

Carvalhais, L. C., Dennis, P. G., Tyson, G. W., & Schenk, P. M. (2013). Rhizosphere metatranscriptomics: challenges and opportunities. Molecular Microbial Ecology of the Rhizosphere, 1, 1137-1144.

Castenson, K. L., & Rabenhorst, M. C. (2006). Indicator of reduction in soil (IRIS) evaluation of a new approach for assessing reduced conditions in soil. Soil Science Society of America Journal, 70(4), 1222-1226.

Chaumeil, P.-A., Mussig, A. J., Hugenholtz, P., & Parks, D. H. (2020). GTDB-Tk: a toolkit to classify genomes with the Genome Taxonomy Database. Bioinformatics, 36(6), 1925-1927.

Chen, Y. T., Wang, Y., & Yeh, K. C. (2017). Role of root exudates in metal acquisition and tolerance. Current opinion in plant biology, 39, 66-72.

Chen, H., Ma, K., Huang, Y., Fu, Q., Qiu, Y., & Yao, Z. (2022). Significant response of microbial community to increased salinity across wetland ecosystems. Geoderma, 415, 115778.

Chiang, S. M., & Schellhorn, H. E. (2012). Regulators of oxidative stress response genes in Escherichia coli and their functional conservation in bacteria. Archives of Biochemistry and Biophysics, 525(2), 161-169.

Chmura, G. L., Anisfeld, S. C., Cahoon, D. R., & Lynch, J. C. (2003). Global carbon sequestration in tidal, saline wetland soils. Global Biogeochemical Cycles, 17(4).

Chowdhury, T. R., & Dick, R. P. (2013). Ecology of aerobic methanotrophs in controlling methane fluxes from wetlands. Applied Soil Ecology, 65, 8-22.

Claassens, N. J., Sousa, D. Z., dos Santos, V. A., De Vos, W. M., & van der Oost, J. (2016). Harnessing the power of microbial autotrophy. Nature Reviews Microbiology, 14(11), 692-706.

Conrad, R. (2020). Importance of hydrogenotrophic, aceticlastic and methylotrophic methanogenesis for methane production in terrestrial, aquatic and other anoxic environments: a mini review. Pedosphere, 30(1), 25-39.

Cook, F., & Knight, J. (2003). Oxygen transport to plant roots: modeling for physical understanding of soil aeration. Soil Science Society of America Journal, 67(1), 20-31.

Corzo, A., Jiménez-Arias, J. L., Torres, E., García-Robledo, E., Lara, M., & Papaspyrou, S. (2018). Biogeochemical changes at the sediment–water interface during redox transitions in an acidic reservoir: exchange of protons, acidity and electron donors and acceptors. Biogeochemistry, 139, 241-260.

Craft, C. (2007). Freshwater input structures soil properties, vertical accretion, and nutrient accumulation of Georgia and U.S tidal marshes. Limnology and Oceanography, 52(3), 1220-1230.

Craft, C., Clough, J., Ehman, J., Joye, S., Park, R., Pennings, S., Guo, H., & Machmuller, M. (2009). Forecasting the effects of accelerated sea-level rise on tidal marsh ecosystem services. Frontiers in Ecology and the Environment, 7(2), 73-78.

Crump, B. C., Hopkinson, C. S., Sogin, M. L., & Hobbie, J. E. (2004). Microbial biogeography along an estuarine salinity gradient: combined influences of bacterial growth and residence time. Applied and Environmental Microbiology, 70(3), 1494-1505.

Crump, B. C., Peranteau, C., Beckingham, B., & Cornwell, J. C. (2007). Respiratory succession and community succession of bacterioplankton in seasonally anoxic estuarine waters. Applied and Environmental Microbiology, 73(21), 6802-6810.

Daebeler, A., Petrová, E., Kinz, E., Grausenburger, S., Berthold, H., Sandén, T., & Angel, R. (2022). Pairing litter decomposition with microbial community structures using the Tea Bag Index (TBI). SOIL, 8(1), 163–176.

Daims, H., Lebedeva, E. V., Pjevac, P., Han, P., Herbold, C., Albertsen, M., Jehmlich, N., Palatinszky, M., Vierheilig, J., & Bulaev, A. (2015). Complete nitrification by *Nitrospira* bacteria. Nature, 528(7583), 504-509.

Day, F. P., & Megonigal, J. P. (1993). The relationship between variable hydroperiod, production allocation, and belowground organic turnover in forested wetlands. Wetlands, 13(2), 115-121.

De Vrieze, J., Regueiro, L., Props, R., Vilchez-Vargas, R., Jáuregui, R., Pieper, D. H., Lema, J. M., & Carballa, M. (2016). Presence does not imply activity: DNA and RNA patterns differ in response to salt perturbation in anaerobic digestion. Biotechnology for Biofuels, 9, 1-13.

Dijkstra, F. A., Carrillo, Y., Pendall, E., & Morgan, J. A. (2013). Rhizosphere priming: a nutrient perspective. Frontiers in Microbiology, 4, 216.

Dijkstra, F. A., Zhu, B., & Cheng, W. (2021). Root effects on soil organic carbon: a double-edged sword. New Phytologist, 230, 60-65.

Djukic, I., Kepfer-Rojas, S., Schmidt, I. K., Larsen, K. S., Beier, C., Berg, B., & Verheyen, K. (2018). Early stage litter decomposition across biomes. The Science of the Total Environment, 628, 1369-1394.

Dörries, M., Wöhlbrand, L., & Rabus, R. (2016). Differential proteomic analysis of the metabolic network of the marine sulfate-reducer Desulfobacterium autotrophicum HRM2. Proteomics, 16(22), 2878-2893.

Drake, H. L. (1994). Acetogenesis, acetogenic bacteria, and the acetyl-CoA "Wood/Ljungdahl" pathway: past and current perspectives. In Acetogenesis, Drake, H. L. (Ed.), pp. 3-60

Drake, H. L., Gößner, A. S., & Daniel, S. L. (2008). Old acetogens, new light. Annals of the New York Academy of Sciences, 1125(1), 100-128.

Duarte, C. M., & Cebrián, J. (1996). The fate of marine autotrophic production. Limnology and oceanography, 41(8), 1758-1766.

Duarte, C. M., Losada, I. J., Hendriks, I. E., Mazarrasa, I., & Marbà, N. (2013). The role of coastal plant communities for climate change mitigation and adaptation. Nature Climate Change, 3(11), 961-968.

Duarte, C. M., Middelburg, J. J., & Caraco, N. (2005). Major role of marine vegetation on the oceanic carbon cycle. Biogeosciences, 2(1), 1-8.

Dusenge, M. E., Duarte, A. G., & Way, D. A. (2019). Plant carbon metabolism and climate change: elevated CO_2 and temperature impacts on photosynthesis, photorespiration and respiration. New Phytologist, 221(1), 32-49.

Eisenhauer, N., Lanoue, A., Strecker, T., Scheu, S., Steinauer, K., Thakur, M. P., & Mommer, L. (2017). Root biomass and exudates link plant diversity with soil bacterial and fungal biomass. Scientific Reports, 7(1), 44641.

el Zahar Haichar, F., Santaella, C., Heulin, T., & Achouak, W. (2014). Root exudates mediated interactions belowground. Soil Biology and Biochemistry, 77, 69-80.

Ellenberg, H., Weber, H. E., & Düll, R. (1991). Zeigerwerte von Pflanzen in Mitteleuropa. Scripta Geobotanica, 18, 1-248.

Ellis, R. J. (1979). The most abundant protein in the world. Trends in Biochemical Sciences, 4(11), 241-244.

Engels, J. G., & Jensen, K. (2009). Patterns of wetland plant diversity along estuarine stress gradients of the Elbe (Germany) and Connecticut (USA) Rivers. Plant Ecology & Diversity, 2(3), 301-311.

Erb, T. J. (2011). Carboxylases in natural and synthetic microbial pathways. Applied and Environmental Microbiology, 77(24), 8466-8477.

Eren, A. M., Esen Ö, C., Quince, C., Vineis, J. H., Morrison, H. G., Sogin, M. L., & Delmont, T. O. (2015). Anvi'o: an advanced analysis and visualization platform for 'omics data. PeerJ, 3, e1319.

Evans, M., Buchanan, B. B., & Arnon, D. I. (1966). A new ferredoxin-dependent carbon reduction cycle in a photosynthetic bacterium. Proceedings of the National Academy of Sciences, 55(4), 928-934.

Falkowski, P. G. (1994). The role of phytoplankton photosynthesis in global biogeochemical cycles. Photosynthesis Research, 39(3), 235-258.

Fanin, N., Bezaud, S., Sarneel, J. M., Cecchini, S., Nicolas, M., & Augusto, L. (2020). Relative Importance of Climate, Soil and Plant Functional Traits During the Early Decomposition Stage of Standardized Litter. Ecosystems, 23(5), 1004-1018.

Fontaine, F., Peterson, W., McCoy, E., Johnson, M. J., & Ritter, G. J. (1942). A new type of glucose fermentation by Clostridium thermoaceticum. Journal of Bacteriology, 43(6), 701-715.

Franzitta, G., Hanley, M. E., Airoldi, L., Baggini, C., Bilton, D. T., Rundle, S. D., & Thompson, R. C. (2015). Home advantage? Decomposition across the freshwater-estuarine transition zone varies with litter origin and local salinity. Marine Environmental Research, 110, 1-7.

Friedman, M. (2007). Overview of antibacterial, antitoxin, antiviral, and antifungal activities of tea flavonoids and teas. Molecular Nutrition & Food Research, 51(1), 116-134.

Frindte, K., Allgaier, M., Grossart, H. P., & Eckert, W. (2016). Redox stability regulates community structure of active microbes at the sediment-water interface. Environmental Microbiology Reports, 8(5), 798-804.

Fuchs, G. (1989). Alternative pathways of autotrophic CO_2 fixation. Autotrophic Bacteria.

Fuchs, G. (2011). Alternative pathways of carbon dioxide fixation: insights into the early evolution of life? Annual Review of Microbiology, 65(1), 631-658.

Fuchs, G., Stupperich, E., & Eden, G. (1980). Autotrophic CO_2 fixation in *Chlorobium limicola*. Evidence for the operation of a reductive tricarboxylic acid cycle in growing cells. Archives of Microbiology, 128, 64-71.

Gargallo-Garriga, A., Preece, C., Sardans, J., Oravec, M., Urban, O., & Peñuelas, J. (2018). Root exudate metabolomes change under drought and show limited capacity for recovery. Scientific reports, 8, 12696.

Garritano, A. N., Song, W., & Thomas, T. (2022). Carbon fixation pathways across the bacterial and archaeal tree of life. PNAS Nexus, 1(5), 226.

Geng, H., Wang, F., Yan, C., Ma, S., Zhang, Y., Qin, Q., Tian, Z., Liu, R., Chen, H., & Zhou, B. (2022). Rhizosphere microbial community composition and survival strategies in oligotrophic and metal (loid) contaminated iron tailings areas. Journal of Hazardous Materials, 436, 129045.

Granse, D., Titschack, J., Ainouche, M., Jensen, K., & Koop-Jakobsen, K. (2022). Subsurface aeration of tidal wetland soils: Root-system structure and aerenchyma connectivity in Spartina (Poaceae). Science of the Total Environment, 802, 149771.

Graves, S., Piepho, H.-P., & Selzer, M. L. (2015). Package 'multcompView'. Visualizations of Paired Comparisons, 451, 452.

Grüterich, L., Woodhouse, J. N., Mueller, P., Tiemann, A., Ruscheweyh, H. J., Sunagawa, S., Grossart, H. P., & Streit, W. R. (2024a). Assessing environmental gradients in relation to dark CO_2 fixation in estuarine wetland microbiomes. Applied and Environmental Microbiology, 10.1128/aem.02177-24

Grüterich, L., Wilson, M., Jensen, K., Streit, W., & Müller, P. (2024b). Transcriptomic response of wetland microbes to root influence. iScience, 10.1016/j.isci.2024.110890

Guo, G., Kong, W., Liu, J., Zhao, J., Du, H., Zhang, X., & Xia, P. (2015). Diversity and distribution of autotrophic microbial community along environmental gradients in grassland soils on the Tibetan Plateau. Applied Microbiology and Biotechnology, 99, 8765-8776.

Hanson, R. S., & Hanson, T. E. (1996). Methanotrophic bacteria. Microbiology Reviews, 60(2), 439-471.

Hartmann, A., Rothballer, M., & Schmid, M. (2008). Lorenz Hiltner, a pioneer in rhizosphere microbial ecology and soil bacteriology research. Plant and Soil, 312, 7-14.

Hättenschwiler, S., Tiunov, A. V., & Scheu, S. (2005). Biodiversity and Litter Decomposition in Terrestrial Ecosystems. Annual Review of Ecology, Evolution, and Systematics, 36(1), 191-218.

Hayer-Hartl, M., & Hartl, F. U. (2020). Chaperone machineries of rubisco–the most abundant enzyme. Trends in Biochemical Sciences, 45(9), 748-763.

Hemminga, M., De Leeuw, J., de Munek, W., & Koutstaal, B. (1991). Decomposition in estuarine salt marshes: the effect of soil salinity and soil water content. Vegetatio, 94, 25-33.

Herlemann, D. P., Labrenz, M., Jürgens, K., Bertilsson, S., Waniek, J. J., & Andersson, A. F. (2011). Transitions in bacterial communities along the 2000 km salinity gradient of the Baltic Sea. The ISME Journal, 5(10), 1571-1579.

Herter, S., Fuchs, G., Bacher, A., & Eisenreich, W. (2002). A bicyclic autotrophic CO_2 fixation pathway in Chloroflexus aurantiacus. Journal of Biological Chemistry, 277(23), 20277-20283.

Herz, K., Dietz, S., Gorzolka, K., Haider, S., Jandt, U., Scheel, D., & Bruelheide, H. (2018). Linking root exudates to functional plant traits. PloS One, 13(10), e0204128.

Hiltner, L. (1904). Über neuere Erfahrungen und Probleme auf dem Gebiete der Bodenbakteriologie unter besonderer Berücksichtigung der Gründüngung und Brache. Arbeiten der Deutschen Landwirtschaftlichen Gesellschaft, 98, 59-78.

Hirsch, A. M., Bauer, W. D., Bird, D. M., Cullimore, J., Tyler, B., & Yoder, J. I. (2003). Molecular signals and receptors: Controlling rhizosphere interactions between plants and other organisms. Ecology, 84(4), 858-868.

Holo, H. (1989). Chloroflexus aurantiacus secretes 3-hydroxypropionate, a possible intermediate in the assimilation of CO_2 and acetate. Archives of Microbiology, 151, 252-256.

Hothorn, T., Bretz, F., Westfall, P., Heiberger, R. M., Schuetzenmeister, A., Scheibe, S., & Hothorn, M. T. (2016). Package 'multcomp'. Simultaneous inference in general parametric models. Project for Statistical Computing, pp. 1-36

Hu, S.-I., Pezacka, E., & Wood, H. (1984). Acetate synthesis from carbon monoxide by *Clostridium thermoaceticum*. Purification of the corrinoid protein. Journal of Biological Chemistry, 259(14), 8892-8897.

Huang, H., Ullah, F., Zhou, D.-X., Yi, M., & Zhao, Y. (2019). Mechanisms of ROS regulation of plant development and stress responses. Frontiers in Plant Science, 10, 800.

Huang, Q., Huang, Y., Wang, B., Dippold, M. A., Li, H., Li, N., Jia, P., Zhang, H., An, S., & Kuzyakov, Y. (2022). Metabolic pathways of CO_2 fixing microorganisms determined C-fixation rates in grassland soils along the precipitation gradient. Soil Biology and Biochemistry, 172, 108764.

Huber, H., Gallenberger, M., Jahn, U., Eylert, E., Berg, I. A., Kockelkorn, D., Eisenreich, W., & Fuchs, G. (2008). A dicarboxylate/4-hydroxybutyrate autotrophic carbon assimilation cycle in the hyperthermophilic Archaeum Ignicoccus hospitalis. Proceedings of the National Academy of Sciences, 105(22), 7851-7856.

Hug, L. A., Castelle, C. J., Wrighton, K. C., Thomas, B. C., Sharon, I., Frischkorn, K. R., Williams, K. H., Tringe, S. G., & Banfield, J. F. (2013). Community genomic analyses constrain the distribution of metabolic traits across the Chloroflexi phylum and indicate roles in sediment carbon cycling. Microbiome, 1(1), 22.

Hulthe, G., Hulth, S., & Hall, P. O. J. (1998). Effect of oxygen on degradation rate of refractory and labile organic matter in continental margin sediments. Geochimica et Cosmochimica Acta, 62(8), 1319-1328.

Ivanovsky, R., Sintsov, N., & Kondratieva, E. (1980). ATP-linked citrate lyase activity in the green sulfur bacterium Chlorobium limicola forma thiosulfatophilum. Archives of Microbiology, 128, 239-241.

Jain, S., Katsyv, A., Basen, M., & Müller, V. (2022). The monofunctional CO dehydrogenase CooS is essential for growth of *Thermoanaerobacter kivui* on carbon monoxide. Extremophiles, 26, 1-12.

Jennerjahn, T. C., & Ittekkot, V. (2002). Relevance of mangroves for the production and deposition of organic matter along tropical continental margins. Naturwissenschaften, 89, 23-30.

Ji, C., Liang, Z., Cao, H., Chen, Z., Kong, X., Xin, Z., He, M., Wang, J., Wei, Z., & Xing, J. (2023). Transcriptome-based analysis of the effects of compound microbial agents on gene expression in wheat roots and leaves under salt stress. Frontiers in Plant Science, 14, 1109077.

Jiang, Q., Jing, H., Jiang, Q., & Zhang, Y. (2022). Insights into carbon-fixation pathways through metagonomics in the sediments of deep-sea cold seeps. Marine Pollution Bulletin, 176, 113458.

Jiang, Z., Lu, Y., Xu, J., Li, M., Shan, G., & Li, Q. (2019). Exploring the characteristics of dissolved organic matter and succession of bacterial community during composting. Bioresource Technology, 292, 121942.

Jones, D. L., Hodge, A., & Kuzyakov, Y. (2004). Plant and mycorrhizal regulation of rhizodeposition. New Phytologist, 163, 459-480.

Jørgensen, B., Findlay, A., & Pellerin, A. (2019). The biogeochemical sulfur cycle of marine sediments. Front Microbiol 10: 849. In.

Kanehisa, M. (2002). The KEGG database. In silico simulation of biological processes: Novartis Foundation Symposium, 247, 91-103.

Kang, D. D., Li, F., Kirton, E., Thomas, A., Egan, R., An, H., & Wang, Z. (2019). MetaBAT 2: an adaptive binning algorithm for robust and efficient genome reconstruction from metagenome assemblies. PeerJ, 7, e7359.

Karner, M. B., DeLong, E. F., & Karl, D. M. (2001). Archaeal dominance in the mesopelagic zone of the Pacific Ocean. Nature, 409(6819), 507-510.

Keiluweit, M., Wanzek, T., Kleber, M., Nico, P., & Fendorf, S. (2017). Anaerobic microsites have an unaccounted role in soil carbon stabilization. Nature Communications, 8(1), 1771.

Keuskamp, J. A., Dingemans, B. J. J., Lehtinen, T., Sarneel, J. M., & Hefting, M. M. (2013). Tea Bag Index: a novel approach to collect uniform decomposition data across ecosystems. Methods in Ecology and Evolution, 4(11), 1070-1075.

Khadem, A. F., Pol, A., Wieczorek, A., Mohammadi, S. S., Francoijs, K.-J., Stunnenberg, H. G., Jetten, M. S., & Op den Camp, H. J. (2011). Autotrophic methanotrophy in Verrucomicrobia: Methylacidiphilum fumariolicum SolV uses the Calvin-Benson-Bassham cycle for carbon dioxide fixation. Journal of Bacteriology, 193(17), 4438-4446.

Kieser, S., Brown, J., Zdobnov, E. M., Trajkovski, M., & McCue, L. A. (2020). ATLAS: a Snakemake workflow for assembly, annotation, and genomic binning of metagenome sequence data. BMC Bioinformatics, 21, 1-8.

Kloock, A., Bonsall, M. B., & King, K. C. (2020). Evolution and maintenance of microbe-mediated protection under occasional pathogen infection. Ecology and Evolution, 10(16), 8634-8642.

Koop-Jakobsen, K., Meier, R. J., & Mueller, P. (2021). Plant-mediated rhizosphere oxygenation in the native invasive salt marsh grass *Elymus athericus*. Frontiers in Plant Science, 12, 669751.

Koop-Jakobsen, K., Mueller, P., Meier, R. J., Liebsch, G., & Jensen, K. (2018). Plant-Sediment Interactions in Salt Marshes - An Optode Imaging Study of O_2, pH, and CO_2 Gradients in the Rhizosphere. Frontiers in Plant Science, 9(541).

Koschorreck, M., Knorr, K. H., & Teichert, L. (2022). Temporal patterns and drivers of CO_2 emission from dry sediments in a groyne field of a large river. Biogeosciences, 19(22), 5221-5236.

Kristensen, E., Ahmed, S. I., & Devol, A. H. (1995). Aerobic and anaerobic decomposition of organic matter in marine sediment: which is fastest? Limnology and oceanography, 40(8), 1430-1437.

Kuzyakov, Y., & Blagodatskaya, E. (2015). Microbial hotspots and hot moments in soil: concept & review. Soil Biology and Biochemistry, 83, 184-199.

Kuzyakov, Y., & Domanski, G. (2000). Carbon input by plants into the soil. Review. Journal of Plant Nutrition and Soil Science, 163(4), 421-431.

Kuzyakov, Y., & Razavi, B. S. (2019). Rhizosphere size and shape: Temporal dynamics and spatial stationarity. Soil Biology and Biochemistry, 135, 343-360.

Kuzyakov, Y., & Schneckenberger, K. (2004). Review of estimation of plant rhizodeposition and their contribution to soil organic matter formation. Archives of Agronomy and Soil Science, 50(1), 115-132.

Lehto, N., Glud, R. N., á Norði, G., Zhang, H., & Davison, W. (2014). Anoxic microniches in marine sediments induced by aggregate settlement: Biogeochemical dynamics and implications. Biogeochemistry, 119, 307-327.

Leigh, J., Mayer, F., & Wolfe, R. (1981). *Acetogenium kivui*, a new thermophilic hydrogen-oxidizing acetogenic bacterium. Archives of Microbiology, 129, 275-280.

Li, F., Angelini, C., Byers, J. E., Craft, C., & Pennings, S. C. (2022). Responses of a tidal freshwater marsh plant community to chronic and pulsed saline intrusion. Journal of Ecology, 110(7), 1508-1524.

Li, H. (2021). New strategies to improve minimap2 alignment accuracy. Bioinformatics, 37(23), 4572-4574.

Li, H., & Durbin, R. (2009). Fast and accurate short read alignment with Burrows-Wheeler transform. Bioinformatics, 25(14), 1754-1760.

Li, Y., Jing, H., Xia, X., Cheung, S., Suzuki, K., & Liu, H. (2018). Metagenomic insights into the microbial community and nutrient cycling in the western subarctic Pacific Ocean. Frontiers in Microbiology, 9, 623.

Limpens, J., Berendse, F., Blodau, C., Canadell, J., Freeman, C., Holden, J., Roulet, N., Rydin, H., & Schaepman-Strub, G. (2008). Peatlands and the carbon cycle: from local processes to global implications–a synthesis. Biogeosciences, 5(5), 1475-1491.

Lin, C. Y., Turchyn, A. V., Steiner, Z., Bots, P., Lampronti, G. I., & Tosca, N. J. (2018). The role of microbial sulfate reduction in calcium carbonate polymorph selection. Geochimica et Cosmochimica Acta, 237, 184-204.

Liu, B., Hou, L., Zheng, Y., Zhang, Z., Tang, X., Mao, T., Du, J., Bi, Q., Dong, H., & Yin, G. (2022). Dark carbon fixation in intertidal sediments: Controlling factors and driving microorganisms. Water Research, 216, 118381.

Liu, S., Plaza, C., Ochoa-Hueso, R., Trivedi, C., Wang, J., Trivedi, P., Zhou, G., Piñeiro, J., Martins, C. S. C., Singh, B. K., & Delgado-Baquerizo, M. (2023). Litter and soil biodiversity jointly drive ecosystem functions. Global Change Biology, 29(22), 6276-6285.

Liu, Z., Sun, Y., Zhang, Y., Feng, W., Lai, Z., Fa, K., & Qin, S. (2018). Metagenomic and 13C tracing evidence for autotrophic atmospheric carbon absorption in a semiarid desert. Soil Biology and Biochemistry, 125, 156-166.

Llorens-Marès, T., Yooseph, S., Goll, J., Hoffman, J., Vila-Costa, M., Borrego, C. M., Dupont, C. L., & Casamayor, E. O. (2015). Connecting biodiversity and potential functional role in modern euxinic environments by microbial metagenomics. The ISME Journal, 9(7), 1648-1661.

Lopes, M. L., Martins, P., Ricardo, F., Rodrigues, A. M., & Quintino, V. (2011). In situ experimental decomposition studies in estuaries: A comparison of Phragmites australis and Fucus vesiculosus. Estuarine, Coastal and Shelf Science, 92(4), 573-580.

Love, M. I., Huber, W., & Anders, S. (2014). Moderated estimation of fold change and dispersion for RNA-seq data with DESeq2. Genome Biology, 15, 1-21.

Lovley, D. R., Dwyer, D. F., & Klug, M. J. (1982). Kinetic analysis of competition between sulfate reducers and methanogens for hydrogen in sediments. Applied and Environmental Microbiology, 43(6), 1373-1379.

Lozupone, C. A., & Knight, R. (2007). Global patterns in bacterial diversity. Proceedings of the National Academy of Sciences of the United States of America, 104(27), 11436-11440.

Lu, Y., & Conrad, R. (2005). *In situ* stable isotope probing of methanogenic archaea in the rice rhizosphere. Science, 309(5737), 1088-1090.

Lücker, S., Wagner, M., Maixner, F., Pelletier, E., Koch, H., Vacherie, B., Rattei, T., Damsté, J. S. S., Spieck, E., & Le Paslier, D. (2010). A *Nitrospira* metagenome illuminates the physiology and evolution of globally important nitrite-oxidizing bacteria. Proceedings of the National Academy of Sciences, 107(30), 13479-13484.

Luther, G. W., Ferdelman, T. G., Kostka, J. E., Tsamakis, E. J., & Church, T. M. (1991). Temporal and spatial variability of reduced sulfur species (FeS_2, $S_2O_3^{2-}$) and porewater parameters in salt marsh sediments. Biogeochemistry, 14, 57-88.

Lyu, Z., Shao, N., Akinyemi, T., & Whitman, W. B. (2018). Methanogenesis. Current Biology, 28(13), R727-R732.

Ma, J., Wang, Z.-Y., Stevenson, B. A., Zheng, X.-J., & Li, Y. (2013). An inorganic CO_2 diffusion and dissolution process explains negative CO_2 fluxes in saline/alkaline soils. Scientific Reports, 3(1), 2025.

Macreadie, P. I., Anton, A., Raven, J. A., Beaumont, N., Connolly, R. M., Friess, D. A., Kelleway, J. J., Kennedy, H., Kuwae, T., Lavery, P. S., Lovelock, C. E., Smale, D. A., Apostolaki, E. T., Atwood, T. B., Baldock, J., Bianchi, T. S., Chmura, G. L., Eyre, B. D., Fourqurean, J. W.,…Duarte, C. M. (2019). The future of Blue Carbon science. Nature Communications, 10(1), 3998.

Makkonen, M., Berg, M. P., Handa, I. T., Hättenschwiler, S., van Ruijven, J., van Bodegom, P. M., & Aerts, R. (2012). Highly consistent effects of plant litter identity and functional traits on decomposition across a latitudinal gradient. Ecology Letters, 15(9), 1033-1041.

Mall, A., Sobotta, J., Huber, C., Tschirner, C., Kowarschik, S., Bačnik, K., Mergelsberg, M., Boll, M., Hügler, M., & Eisenreich, W. (2018). Reversibility of citrate synthase allows autotrophic growth of a thermophilic bacterium. Science, 359(6375), 563-567.

Marcé, R., Obrador, B., Gómez-Gener, L., Catalán, N., Koschorreck, M., Arce, M. I., Singer, G., & von Schiller, D. (2019). Emissions from dry inland waters are a blind spot in the global carbon cycle. Earth-Science Reviews, 188, 240-248.

Marley, A. R. G., Smeaton, C., & Austin, W. E. N. (2019). An Assessment of the Tea Bag Index Method as a Proxy for Organic Matter Decomposition in Intertidal Environments. Journal of Geophysical Research: Biogeosciences, 124(10), 2991-3004.

Maron, P.-A., Sarr, A., Kaisermann, A., Lévêque, J., Mathieu, O., Guigue, J., Karimi, B., Bernard, L., Dequiedt, S., Terrat, S., Chabbi, A., & Ranjard, L. (2018). High Microbial Diversity Promotes Soil Ecosystem Functioning. Applied and Environmental Microbiology, 84(9).

Martin, M. (2011). Cutadapt removes adapter sequences from high-throughput sequencing reads. EMBnet Journal, 17(1), 10-12.

Mateo, M.-Á., Sánchez-Lizaso, J.-L., & Romero, J. (2003). *Posidonia oceanica* 'banquettes': a preliminary assessment of the relevance for meadow carbon and nutrients budget. Estuarine, Coastal and Shelf Science, 56(1), 85-90.

Mcleod, E., Chmura, G. L., Bouillon, S., Salm, R., Björk, M., Duarte, C. M., Lovelock, C. E., Schlesinger, W. H., & Silliman, B. R. (2011a). A blueprint for blue carbon: toward an improved understanding of the role of vegetated coastal habitats in sequestering CO_2. Frontiers in Ecology and the Environment, 9(10), 552-560.

Megonigal, J. P., Hines, M., & Visscher, P. (2004). Anaerobic metabolism: linkages to trace gases and aerobic processes. In Biogeochemistry, W. H. Schlesinger (Ed.), pp. 317-424.

Meharg, A. A. (1994). A critical review of labelling techniques used to quantify rhizosphere carbon-flow. Plant and Soil, 166, 55-62.

Mendelssohn, I. A., Sorrell, B. K., Brix, H., Schierup, H.-H., Lorenzen, B., & Maltby, E. (1999). Controls on soil cellulose decomposition along a salinity gradient in a Phragmites australis wetland in Denmark. Aquatic Botany, 64(3-4), 381-398.

Milanese, A., Mende, D. R., Paoli, L., Salazar, G., Ruscheweyh, H.-J., Cuenca, M., Hingamp, P., Alves, R., Costea, P. I., & Coelho, L. P. (2019). Microbial abundance, activity and population genomic profiling with mOTUs2. Nature Communications, 10(1), 1014.

Miltner, A., Kopinke, F.-D., Kindler, R., Selesi, D., Hartmann, A., & Kästner, M. (2005). Non-phototrophic CO_2 fixation by soil microorganisms. Plant Soil, 269, 193-203.

Mittmann-Goetsch, J., Wilson, M., Jensen, K., & Mueller, P. (2024). Wetland roots as soil reducers–Insights from a Wadden Sea salt-marsh study. Research Square, 10.21203/rs.3.rs-3934063/v1

Miura, A., Kameya, M., Arai, H., Ishii, M., & Igarashi, Y. (2008). A soluble NADH-dependent fumarate reductase in the reductive tricarboxylic acid cycle of *Hydrogenobacter thermophilus* TK-6. Journal of Bacteriology, 190(21), 7170-7177.

Momper, L., Jungbluth, S. P., Lee, M. D., & Amend, J. P. (2017). Energy and carbon metabolisms in a deep terrestrial subsurface fluid microbial community. The ISME Journal, 11(10), 2319-2333.

Mori, T., Nakamura, R., & Aoyagi, R. (2022). Risk of misinterpreting the Tea Bag Index: Field observations and a random simulation. Ecological Research, 37(3), 381–389.

Morrissey, E. M., Gillespie, J. L., Morina, J. C., & Franklin, R. B. (2014). Salinity affects microbial activity and soil organic matter content in tidal wetlands. Global Change Biology, 20(4), 1351-1362.

Mueller, P., Granse, D., Nolte, S., Weingartner, M., Hoth, S., & Jensen, K. (2020a). Unrecognized controls on microbial functioning in Blue Carbon ecosystems: The role of mineral enzyme stabilization and allochthonous substrate supply. Ecology and Evolution, 10(2), 998-1011.

Mueller, P., Jensen, K., & Megonigal, J. P. (2016). Plants mediate soil organic matter decomposition in response to sea level rise. Global Change Biology, 22(1), 404-414.

Mueller, P., Mozdzer, T. J., Langley, J. A., Aoki, L. R., Noyce, G. L., & Megonigal, J. P. (2020b). Plant species determine tidal wetland methane response to sea level rise. Nature Communications, 11(1), 5154.

Mueller, P., Schile-Beers, L. M., Mozdzer, T. J., Chmura, G. L., Dinter, T., Kuzyakov, Y., Groot, A. V. d., Esselink, P., Smit, C., D'Alpaos, A., Ibáñez, C., Lazarus, M., Neumeier, U., Johnson, B. J., Baldwin, A. H., Yarwood, S. A., Montemayor, D. I., Yang, Z., Wu, J.,…Nolte, S. (2018). Global-change effects on early-stage decomposition processes in tidal wetlands – implications from a global survey using standardized litter. Biogeosciences, 15(10), 3189-3202.

Müller, H. W., Dohrmann, R., Klosa, D., Rehder, S., & Eckelmann, W. (2009). Comparison of two procedures for particle-size analysis: Köhn pipette and X-ray granulometry. Journal of Plant Nutrition and Soil Science, 172(2), 172-179.

Mundinger, A. B., Lawson, C. E., Jetten, M. S., Koch, H., & Lücker, S. (2019). Cultivation and transcriptional analysis of a canonical *Nitrospira* under stable growth conditions. Frontiers in Microbiology, 10, 1325.

Neiske, F., Seedtke, M., Eschenbach, A., Wilson, M., Jensen, K., & Becker, J. N. (2024). Soil organic carbon stocks and stabilization mechanisms in tidal marshes along estuarine gradients. bioRxiv, 10.1101/2024.05.18.594814.

Neumann, G. (2007). Root exudates and nutrient cycling. In Nutrient Cycling in Terrestrial Ecosystems. P. Marschner, Z. Rengel (Eds.), pp. 123-157.

Neumann, G., & Römheld, V. (2012). Rhizosphere chemistry in relation to plant nutrition. In Marschner's mineral nutrition of higher plants. P. Marschner (Ed.), pp. 347-368.

Nguyen, C. (2009). Rhizodeposition of organic C by plants: mechanisms and controls. Sustainable Agriculture, 97-123.

Nielsen, U. N., Ayres, E., Wall, D. H., & Bardgett, R. D. (2011). Soil biodiversity and carbon cycling: a review and synthesis of studies examining diversity–function relationships. European Journal of Soil Science, 62(1), 105–116.

Nuccio, E. E., Starr, E., Karaoz, U., Brodie, E. L., Zhou, J., Tringe, S. G., Malmstrom, R. R., Woyke, T., Banfield, J. F., & Firestone, M. K. (2020). Niche differentiation is spatially and temporally regulated in the rhizosphere. The ISME Journal, 14(4), 999-1014.

Nurk, S., Meleshko, D., Korobeynikov, A., & Pevzner, P. A. (2017). metaSPAdes: a new versatile metagenomic assembler. Genome Research, 27(5), 824-834.

Oburger, E., & Jones, D. (2009). Substrate mineralization studies in the laboratory show different microbial C partitioning dynamics than in the field. Soil Biology and Biochemistry, 41(9), 1951-1956.

Oburger, E., & Jones, D. L. (2018). Sampling root exudates–mission impossible? Rhizosphere, 6, 116-133.

Oksanen, J., Blanchet, F. G., Kindt, R., Legendre, P., Minchin, P. R., O'hara, R., Simpson, G. L., Solymos, P., Stevens, M. H. H., & Wagner, H. (2013). Package 'vegan'. Community Ecology Package, Version 2(9), 1-295.

Oremland, R. S., & Polcin, S. (1982). Methanogenesis and sulfate reduction: competitive and noncompetitive substrates in estuarine sediments. Applied and Environmental Microbiology, 44(6), 1270-1276.

Paoli, L., Ruscheweyh, H. J., Forneris, C. C., Hubrich, F., Kautsar, S., Bhushan, A., Lotti, A., Clayssen, Q., Salazar, G., Milanese, A., Carlström, C. I., Papadopoulou, C., Gehrig, D., Karasikov, M., Mustafa, H., Larralde, M., Carroll, L. M., Sánchez, P., Zayed, A. A.,…Sunagawa, S. (2022). Biosynthetic potential of the global ocean microbiome. Nature, 607(7917), 111-118.

Parks, D. H., Imelfort, M., Skennerton, C. T., Hugenholtz, P., & Tyson, G. W. (2015). CheckM: assessing the quality of microbial genomes recovered from isolates, single cells, and metagenomes. Genome Research, 25(7), 1043-1055.

Pausch, J., & Kuzyakov, Y. (2018). Carbon input by roots into the soil: quantification of rhizodeposition from root to ecosystem scale. Global Change Biology, 24(1), 1-12.

Peter, H., Beier, S., Bertilsson, S., Lindström, E. S., Langenheder, S., & Tranvik, L. J. (2011). Function-specific response to depletion of microbial diversity. The ISME Journal, 5(2), 351-361.

Petraglia, A., Cacciatori, C., Chelli, S., Fenu, G., Calderisi, G., Gargano, D., Abeli, T., Orsenigo, S., & Carbognani, M. (2019). Litter decomposition: effects of temperature driven by soil moisture and vegetation type. Plant and Soil, 435(1-2), 187-200.

Phillips, D. A., & Streit, W. (1996). Legume signals to rhizobial symbionts: a new approach for defining rhizosphere colonization. In Plant-Microbe Interactions, pp. 236-271.

Pierce, E., Xie, G., Barabote, R. D., Saunders, E., Han, C. S., Detter, J. C., Richardson, P., Brettin, T. S., Das, A., & Ljungdahl, L. G. (2008). The complete genome sequence of *Moorella thermoacetica* (f. *Clostridium thermoaceticum*). Environmental Microbiology, 10(10), 2550-2573.

Pioli, S., Sarneel, J., Thomas, H. J. D., Domene, X., Andrés, P., Hefting, M., Reitz, T., Laudon, H., Sandén, T., Piscová, V., Aurela, M., & Brusetti, L. (2020). Linking plant litter microbial diversity to microhabitat conditions, environmental gradients and litter mass loss: Insights from a European study using standard litter bags. Soil Biology and Biochemistry, 144, 107778.

Poffenbarger, H. (2010). Ruminant grazing of cover crops: Effects on soil properties and agricultural production. Journal of Natural Resources and Life Sciences Education, 39(1), 49-39.

Qiao, Y., Miao, S., Han, X., Yue, S., & Tang, C. (2017). Improving soil nutrient availability increases carbon rhizodeposition under maize and soybean in Mollisols. Science of the Total Environment, 603, 416-424.

Qu, W., Li, J., Han, G., Wu, H., Song, W., & Zhang, X. (2019). Effect of salinity on the decomposition of soil organic carbon in a tidal wetland. Journal of Soils and Sediments, 19(2), 609-617.

Quast, C., Pruesse, E., Yilmaz, P., Gerken, J., Schweer, T., Yarza, P., Peplies, J., & Glöckner, F. O. (2013). The SILVA ribosomal RNA gene database project: improved data processing and web-based tools. Nucleic Acids Research, 41(D1), D590-596.

Quintino, V., Sangiorgio, F., Ricardo, F., Mamede, R., Pires, A., Freitas, R., Rodrigues, A. M., & Basset, A. (2009). In situ experimental study of reed leaf decomposition along a full salinity gradient. Estuarine, Coastal and Shelf Science, 85(3), 497-506.

Rabenhorst, M. (2013). Using synthesized iron oxides as an indicator of reduction in soils. Methods in Biogeochemistry of Wetlands, 10, 723-740.

Rabenhorst, M. C. (2008). Protocol for using and interpreting IRIS tubes. Soil Survey Horizons, 49(3), 74-77.

Rabenhorst, M. C., & Burch, S. (2006). Synthetic iron oxides as an indicator of reduction in soils (IRIS). Soil Science Society of America Journal, 70(4), 1227-1236.

Ragsdale, S., Clark, J., Ljungdahl, L., Lundie, L., & Drake, H. (1983). Properties of purified carbon monoxide dehydrogenase from Clostridium thermoaceticum, a nickel, iron-sulfur protein. Journal of Biological Chemistry, 258(4), 2364-2369.

Ragsdale, S., & Wood, H. (1985). Acetate biosynthesis by acetogenic bacteria. Evidence that carbon monoxide dehydrogenase is the condensing enzyme that catalyzes the final steps of the synthesis. Journal of Biological Chemistry, 260(7), 3970-3977.

Ragsdale, S. W. (2008). Enzymology of the Wood–Ljungdahl pathway of acetogenesis. Annals of the New York Academy of Sciences, 1125(1), 129-136.

Ragsdale, S. W., & Pierce, E. (2008). Acetogenesis and the Wood–Ljungdahl pathway of CO_2 fixation. Biochimica et Biophysica Acta (BBA)-Proteins and Proteomics, 1784(12), 1873-1898.

Ramos-Vera, W. H., Berg, I. A., & Fuchs, G. (2009). Autotrophic carbon dioxide assimilation in Thermoproteales revisited. Journal of bacteriology, 191(13), 4286-4297.

Rasmann, S., & Turlings, T. C. (2016). Root signals that mediate mutualistic interactions in the rhizosphere. Current Opinion in Plant Biology, 32, 62-68.

Reis, P. C., Thottathil, S. D., & Prairie, Y. T. (2022). The role of methanotrophy in the microbial carbon metabolism of temperate lakes. Nature Communications, 13(1), 43.

Ren, L., Jensen, K., Porada, P., & Mueller, P. (2022). Biota-mediated carbon cycling-A synthesis of biotic-interaction controls on blue carbon. Ecology Letters, 25(2), 521-540.

Roache, M. C., Bailey, P. C., & Boon, P. I. (2006). Effects of salinity on the decay of the freshwater macrophyte, Triglochin procerum. Aquatic Botany, 84(1), 45-52.

Rolando, J., Kolton, M., Song, T., Liu, Y., Pinamang, P., Conrad, R., Morris, J., Konstantinidis, K., & Kostka, J. (2024). Sulfur oxidation and reduction are coupled to nitrogen fixation in the roots of the salt marsh foundation plant Spartina alterniflora. Nature Communications, 15(1), 3607.

Rolando, J. L., Kolton, M., Song, T., & Kostka, J. E. (2022). The core root microbiome of Spartina alterniflora is predominated by sulfur-oxidizing and sulfate-reducing bacteria in Georgia salt marshes, USA. Microbiome, 10(1), 37.

Rovira, A., & Harris, J. (1961). Plant root excretions in relation to the rhizosphere effect: v. The exudation of b-group vitamins. Plant and Soil, 14, 199-214.

Rudolph-Mohr, N., Tötzke, C., Kardjilov, N., & Oswald, S. E. (2017). Mapping water, oxygen, and pH dynamics in the rhizosphere of young maize roots. Journal of Plant Nutrition and Soil Science, 180(3), 336-346.

Rüger, L., Feng, K., Dumack, K., Freudenthal, J., Chen, Y., Sun, R., Wilson, M., Yu, P., Sun, B., & Deng, Y. (2021). Assembly patterns of the rhizosphere microbiome along the longitudinal root axis of maize (Zea mays L.). Frontiers in Microbiology, 12, 614501.

Ruscheweyh, H. J., Milanese, A., Paoli, L., Karcher, N., Clayssen, Q., Keller, M. I., Wirbel, J., Bork, P., Mende, D. R., Zeller, G., & Sunagawa, S. (2022). Cultivation-independent genomes greatly expand taxonomic-profiling capabilities of mOTUs across various environments. Microbiome, 10(1), 212.

Ruscheweyh, H. J., Milanese, A., Paoli, L., Sintsova, A., Mende, D. R., Zeller, G., & Sunagawa, S. (2021). mOTUs: profiling taxonomic composition, transcriptional activity and strain populations of microbial communities. Current Protocols, 1(8), e218.

Sakimoto, K. K., Wong, A. B., & Yang, P. (2016). Self-photosensitization of nonphotosynthetic bacteria for solar-to-chemical production. Science, 351(6268), 74-77.

Sakoula, D., Koch, H., Frank, J., Jetten, M. S., van Kessel, M. A., & Lücker, S. (2021). Enrichment and physiological characterization of a novel comammox *Nitrospira* indicates ammonium inhibition of complete nitrification. The ISME Journal, 15(4), 1010-1024.

Salazar, G., Paoli, L., Alberti, A., Huerta-Cepas, J., Ruscheweyh, H.-J., Cuenca, M., Field, C. M., Coelho, L. P., Cruaud, C., & Engelen, S. (2019). Gene expression changes and community turnover differentially shape the global ocean metatranscriptome. Cell, 179(5), 1068-1083. e1021.

Samaras, A., Kamou, N., Tzelepis, G., Karamanoli, K., Menkissoglu-Spiroudi, U., & Karaoglanidis, G. S. (2022). Root transcriptional and metabolic dynamics induced by the Plant Growth Promoting Rhizobacterium (PGPR) Bacillus subtilis Mbi600 on cucumber plants. Plants, 11(9), 1218.

Sánchez-Andrea, I., Guedes, I. A., Hornung, B., Boeren, S., Lawson, C. E., Sousa, D. Z., Bar-Even, A., Claassens, N. J., & Stams, A. J. (2020). The reductive glycine pathway allows autotrophic growth of *Desulfovibrio desulfuricans*. Nature Communications, 11(1), 1-12.

Šantrůčková, H., Kotas, P., Bárta, J., Urich, T., Čapek, P., Palmtag, J., Alves, R. J. E., Biasi, C., Diáková, K., & Gentsch, N. (2018). Significance of dark CO_2 fixation in arctic soils. Soil Biology and Biochemistry, 119, 11-21.

Sarneel, J. M., Hefting, M. M., Sandén, T., van den Hoogen, J., Routh, D., Adhikari, B. S., Alatalo, J. M., Aleksanyan, A., Althuizen, I. H. J., Alsafran, M. H. S. A., Atkins, J. W., Augusto, L., Aurela, M., Azarov, A. V., Barrio, I. C., Beier, C., Bejarano, M. D., Benham, S. E., Berg, B.,…Keuskamp, J. A. (2024). Reading tea leaves worldwide: Decoupled drivers of initial litter decomposition mass-loss rate and stabilization. Ecology Letters, 27(5), e14415.

Schlesinger, W. H. (1997). Biogeochemistry: an analysis of global change. Second edition.

Schmid, M. W., Hahl, T., van Moorsel, S. J., Wagg, C., De Deyn, G. B., & Schmid, B. (2019). Feedbacks of plant identity and diversity on the diversity and community composition of rhizosphere microbiomes from a long-term biodiversity experiment. Molecular Ecology, 28(4), 863-878.

Schreckinger, J., Mutz, M., Mendoza-Lera, C., & Frossard, A. (2021). Attributes of Drying Define the Structure and Functioning of Microbial Communities in Temperate Riverbed Sediment. Frontiers in Microbiology, 12, 676615.

Schuchmann, K., & Müller, V. (2013). Direct and reversible hydrogenation of CO_2 to formate by a bacterial carbon dioxide reductase. Science, 342(6164), 1382-1385.

Schulte Ostermann, T., Heuner, M., Fuchs, E., Temmerman, S., Schoutens, K., Bouma, T. J., & Minden, V. (2024). Identifying Key Plant Traits and Ecosystem Properties Affecting Wave Attenuation and the Soil Organic Carbon Content in Tidal Marshes. Estuaries and Coasts, 47(1), 144-161.

Seemann, T. (2014). Prokka: rapid prokaryotic genome annotation. Bioinformatics, 30(14), 2068-2069.

Seybold, C. A., Mersie, W., Huang, J., & McNamee, C. (2002). Soil redox, pH, temperature, and water-table patterns of a freshwater tidal wetland. Wetlands, 22(1), 149-158.

Sieber, C. M., Probst, A. J., Sharrar, A., Thomas, B. C., Hess, M., Tringe, S. G., & Banfield, J. F. (2018). Recovery of genomes from metagenomes via a dereplication, aggregation and scoring strategy. Nature Microbiology, 3(7), 836-843.

Simpson, M. J., Hjelmqvist, D., López-Alarcón, C., Karamehmedovic, N., Minehan, T. G., Yepremyan, A., Salehani, B., Lissi, E., Joubert, E., Udekwu, K. I., & Alarcon, E. I. (2013). Anti-peroxyl radical quality and antibacterial properties of rooibos infusions and their pure glycosylated polyphenolic constituents. Molecules, 18(9), 11264-11280.

Song, Y., Lee, J. S., Shin, J., Lee, G. M., Jin, S., Kang, S., Lee, J.-K., Kim, D. R., Lee, E. Y., & Kim, S. C. (2020). Functional cooperation of the glycine synthase-reductase and Wood–Ljungdahl pathways for autotrophic growth of *Clostridium drakei*. Proceedings of the National Academy of Sciences, 117(13), 7516-7523.

Spivak, A. C., Sanderman, J., Bowen, J. L., Canuel, E. A., & Hopkinson, C. S. (2019). Global-change controls on soil-carbon accumulation and loss in coastal vegetated ecosystems. Nature Geoscience, 12(9), 685-692.

Stagg, C. L., Baustian, M. M., Perry, C. L., Carruthers, T. J. B., & Hall, C. T. (2018). Direct and indirect controls on organic matter decomposition in four coastal wetland communities along a landscape salinity gradient. Journal of Ecology, 106(2), 655–670.

Starkey, R. L. (1966). Oxidation and reduction of sulfur compounds in soils. Soil Science, 101(4), 297-306.

Steffens, L., Pettinato, E., Steiner, T. M., Mall, A., König, S., Eisenreich, W., & Berg, I. A. (2021). High CO_2 levels drive the TCA cycle backwards towards autotrophy. Nature, 592(7856), 784-788.

Stevenel, P., Frossard, E., Abiven, S., Rao, I. M., Tamburini, F., & Oberson, A. (2019). Using a tri-isotope (^{13}C, ^{15}N, ^{33}P) labelling method to quantify rhizodeposition. Methods in Rhizosphere Biology Research, 169-195.

Storelli, N., Peduzzi, S., Saad, M. M., Frigaard, N.-U., Perret, X., & Tonolla, M. (2013). CO_2 assimilation in the chemocline of Lake Cadagno is dominated by a few types of phototrophic purple sulfur bacteria. FEMS Microbiology Ecology, 84(2), 421-432.

Strauss, G., & Fuchs, G. (1993). Enzymes of a novel autotrophic CO_2 fixation pathway in the phototrophic bacterium *Chloroflexus aurantiacus*, the 3-hydroxypropionate cycle. European Journal of Biochemistry, 215(3), 633-643.

Streit, W. R., Joseph, C. M., & Phillips, D. A. (1996). Biotin and other water-soluble vitamins are key growth factors for alfalfa root colonization by *Rhizobium meliloti* 1021. Molecular Plant-Microbe Interactions, 9(5), 330-338.

Studer, M. S., Siegwolf, R. T., & Abiven, S. (2014). Carbon transfer, partitioning and residence time in the plant-soil system: a comparison of two $^{13}CO_2$ labelling techniques. Biogeosciences, 11(6), 1637-1648.

Su, W., Ye, C., Zhang, Y., Hao, S., & Li, Q. Q. (2019). Identification of putative key genes for coastal environments and cold adaptation in mangrove Kandelia obovata through transcriptome analysis. Science of the Total Environment, 681, 191-201.

Sun, Y., Wang, C., Yang, J., Liao, J., Chen, H. Y., & Ruan, H. (2021). Elevated CO_2 shifts soil microbial communities from K-to r-strategists. Global Ecology and Biogeography, 30(5), 961-972.

Sunagawa, G. A., Séi, H., Shimba, S., Urade, Y., & Ueda, H. R. (2013). FASTER: an unsupervised fully automated sleep staging method for mice. Genes to Cells, 18(6), 502-518.

Sutton-Grier, A. E., Keller, J. K., Koch, R., Gilmour, C., & Megonigal, J. P. (2011). Electron donors and acceptors influence anaerobic soil organic matter mineralization in tidal marshes. Soil Biology and Biochemistry, 43(7), 1576-1583.

Tan, S., Yang, C., Mei, X., Shen, S., Raza, W., Shen, Q., & Xu, Y. (2013). The effect of organic acids from tomato root exudates on rhizosphere colonization of Bacillus amyloliquefaciens T-5. Applied Soil Ecology, 64, 15-22.

Tang, H., Nolte, S., Jensen, K., Rich, R., Mittmann-Goetsch, J., & Mueller, P. (2023). Warming accelerates belowground litter turnover in salt marshes – insights from a Tea Bag Index study. Biogeosciences, 20(10), 1925-1935.

Tebbe, D. A., Geihser, S., Wemheuer, B., Daniel, R., Schäfer, H., & Engelen, B. (2022). Seasonal and Zonal Succession of Bacterial Communities in North Sea Salt Marsh Sediments. Microorganisms, 10(5), 859.

Temmink, R. J. M., Lamers, L. P. M., Angelini, C., Bouma, T. J., Fritz, C., van de Koppel, J., Lexmond, R., Rietkerk, M., Silliman, B. R., Joosten, H., & van der Heide, T. (2022). Recovering wetland biogeomorphic feedbacks to restore the world's biotic carbon hotspots. Science, 376(6593), eabn1479.

Thauer, R. K. (2011). Anaerobic oxidation of methane with sulfate: on the reversibility of the reactions that are catalyzed by enzymes also involved in methanogenesis from CO_2. Current Opinion in Microbiology, 14(3), 292-299.

Timmusk, S., Paalme, V., Pavlicek, T., Bergquist, J., Vangala, A., Danilas, T., & Nevo, E. (2011). Bacterial distribution in the rhizosphere of wild barley under contrasting microclimates. PloS one, 6(3), e17968.

Tollerson, R., & Ibba, M. (2020). Translational regulation of environmental adaptation in bacteria. Journal of Biological Chemistry, 295(30), 10434-10445.

Trevathan-Tackett, S. M., Kepfer-Rojas, S., Engelen, A. H., York, P. H., Ola, A., Li, J., Kelleway, J. J., Jinks, K. I., Jackson, E. L., Adame, M. F., Pendall, E., Lovelock, C. E., Connolly, R. M., Watson, A., Visby, I., Trethowan, A., Taylor, B., Roberts, T. N. B., Petch, J.,…Macreadie, P. I. (2021). Ecosystem type drives tea litter decomposition and associated prokaryotic microbiome communities in freshwater and coastal wetlands at a continental scale. Science of the Total Environment, 782, 146819.

Valiela, I., Teal, J. M., Allen, S. D., van Etten, R., Goehringer, D., & Volkmann, S. (1985). Decomposition in salt marsh ecosystems: The phases and major factors affecting disappearance of above-ground organic matter. Journal of Experimental Marine Biology and Ecology, 89(1), 29-54.

Verhagen, F., Laanbroek, H., & Woldendrop, J. (1995). Competition for ammonium between plant roots and nitrifying and heterotrophic bacteria and the effects of protozoan grazing. Plant and Soil, 170, 241-250.

Vigneron, A., Cruaud, P., Aubé, J., Guyoneaud, R., & Goñi-Urriza, M. (2021). Transcriptomic evidence for versatile metabolic activities of mercury cycling microorganisms in brackish microbial mats. NPJ Biofilms Microbiomes, 7(1), 1-11.

Wang, M., Chen, J.-K., & LI, B. (2007). Characterization of Bacterial Community Structure and Diversity in Rhizosphere Soils of Three Plants in Rapidly Changing Salt Marshes Using 16S rDNA. Pedosphere, 17(5), 545–556.

Wang, N.-Q., Kong, C.-H., Wang, P., & Meiners, S. J. (2021). Root exudate signals in plant-plant interactions. Plant, Cell & Environment, 44(4), 1044-1058.

Wang, S., Huang, H., Kahnt, J., Mueller, A. P., Köpke, M., & Thauer, R. K. (2013). NADP-specific electron-bifurcating [FeFe]-hydrogenase in a functional complex with formate dehydrogenase in *Clostridium autoethanogenum* grown on CO. Journal of bacteriology, 195(19), 4373-4386.

Ward, N. L., Challacombe, J. F., Janssen, P. H., Henrissat, B., Coutinho, P. M., Wu, M., Xie, G., Haft, D. H., Sait, M., Badger, J., Barabote, R. D., Bradley, B., Brettin, T. S., Brinkac, L. M., Bruce, D., Creasy, T., Daugherty, S. C., Davidsen, T. M., DeBoy, R. T.,…Kuske, C. R. (2009). Three genomes from the phylum Acidobacteria provide insight into the lifestyles of these microorganisms in soils. Applied and environmental microbiology, 75(7), 2046–2056.

Wegner, C.-E., & Liesack, W. (2016). Microbial community dynamics during the early stages of plant polymer breakdown in paddy soil. Environmental microbiology, 18(9), 2825–2842.

Wickham, H., Chang, W., & Wickham, M. H. (2016). Package 'ggplot2'. Create Elegant Data Visualisations Using the Grammar of Graphics, Version 2(1), 1-189.

Wider, R. K., & Lang, G. E. (1982). A Critique of the Analytical Methods Used in Examining Decomposition Data Obtained From Litter Bags. Ecology, 63(6), 1636.

Wu, X., Bei, S., Zhou, X., Luo, Y., He, Z., Song, C., Yuan, H., Pivato, B., Liesack, W., & Peng, J. (2023). Metagenomic insights into genetic factors driving bacterial niche differentiation between bulk and rhizosphere soils. Science of the Total Environment, 891, 164221.

Wu, Y.-W., Simmons, B. A., & Singer, S. W. (2016). MaxBin 2.0: an automated binning algorithm to recover genomes from multiple metagenomic datasets. Bioinformatics, 32(4), 605-607.

Xiao, K.-Q., Nie, S.-A., Bao, P., Wang, F.-H., Bao, Q.-L., & Zhu, Y.-G. (2014). Rhizosphere effect has no effect on marker genes related to autotrophic CO_2 fixation in paddy soils? Journal of soils and sediments, 14, 1082-1087.

Xiao, K. Q., Ge, T. D., Wu, X. H., Peacock, C. L., Zhu, Z. K., Peng, J., Bao, P., Wu, J. S., & Zhu, Y. G. (2021). Metagenomic and 14C tracing evidence for autotrophic microbial CO_2 fixation in paddy soils. Environmental Microbiology, 23(2), 924-933.

Yamauchi, T., Shimamura, S., Nakazono, M., & Mochizuki, T. (2013). Aerenchyma formation in crop species: a review. Field Crops Research, 152, 8-16.

Yan, C., Zhao, S., Wu, H., Yang, D., Hou, Z., Shan, F., Yan, S., Lyu, X., Ma, C., & Gong, Z. (2024). Nitrogen release and microbial community characteristics during the decomposition of field-incorporated corn straw in Northeast China. Land Degradation & Development, 35(12), 3897-3910.

Yan, N., Marschner, P., Cao, W., Zuo, C., & Qin, W. (2015). Influence of salinity and water content on soil microorganisms. International Soil and Water Conservation Research, 3(4), 316-323.

Yang, J., Tam, N. F.-Y., & Ye, Z. (2014). Root porosity, radial oxygen loss and iron plaque on roots of wetland plants in relation to zinc tolerance and accumulation. Plant and Soil, 374, 815-828.

Yang, S., Liebner, S., Walz, J., Knoblauch, C., Bornemann, T. L., Probst, A. J., Wagner, D., Jetten, M. S., & in 't Zandt, M. H. (2021). Effects of a long-term anoxic warming scenario on microbial community structure and functional potential of permafrost-affected soil. Permafrost and Periglacial Processes, 32(4), 641-656.

Yang, Y., Moorhead, D. L., Craig, H., Luo, M., Chen, X., Huang, J., Olesen, J. E., & Chen, J. (2022). Differential Responses of Soil Extracellular Enzyme Activities to Salinization: Implications for Soil Carbon Cycling in Tidal Wetlands. Global Biogeochemical Cycles, 36(6). https://doi.org/10.1029/2021gb007285

Yang, Y., Yang, X., Gong, L., Ding, Z., Zhu, H., Tang, J., & Li, X. (2024). Changes in soil microbial carbon fixation pathways along the oasification process in arid desert region: A confirmation based on metagenome analysis. Catena, 239, 107955.

Yarwood, S. A. (2018). The role of wetland microorganisms in plant-litter decomposition and soil organic matter formation: a critical review. FEMS Microbiology ecology, 94(11).

Yilmaz, P., Parfrey, L. W., Yarza, P., Gerken, J., Pruesse, E., Quast, C., Schweer, T., Peplies, J., Ludwig, W., & Glöckner, F. O. (2013). The SILVA and "All-species Living Tree Project (LTP)" taxonomic frameworks. Nucleic Acids Research, 42(D1), D643-D648.

Zarzycki, J., Brecht, V., Müller, M., & Fuchs, G. (2009). Identifying the missing steps of the autotrophic 3-hydroxypropionate CO_2 fixation cycle in *Chloroflexus aurantiacus*. Proceedings of the National Academy of Sciences, 106(50), 21317-21322.

Zeikus, J. (1977). The biology of methanogenic bacteria. Bacteriological Reviews, 41(2), 514-541.

Zhang, D., Hui, D., Luo, Y., & Zhou, G. (2008). Rates of litter decomposition in terrestrial ecosystems: global patterns and controlling factors. Journal of Plant Ecology, 1(2), 85-93.

Zhang, G., Bai, J., Tebbe, C. C., Zhao, Q., Jia, J., Wang, W., Wang, X., & Yu, L. (2021). Salinity controls soil microbial community structure and function in coastal estuarine wetlands. Environmental Microbiology, 23(2), 1020-1037.

Zhang, X., Kuzyakov, Y., Zang, H., Dippold, M. A., Shi, L., Spielvogel, S., & Razavi, B. S. (2020). Rhizosphere hotspots: root hairs and warming control microbial efficiency, carbon utilization and energy production. Soil Biology and Biochemistry, 148, 107872.

Zhao, M., Tang, X., Sun, D., Hou, L., Liu, M., Zhao, Q., Klümper, U., Quan, Z., Gu, J.-D., & Han, P. (2021). Salinity gradients shape the nitrifier community composition in Nanliu River Estuary sediments and the ecophysiology of comammox *Nitrospira inopinata*. Science of the Total Environment, 795, 148768.

Zhuang, W.-Q., Yi, S., Bill, M., Brisson, V. L., Feng, X., Men, Y., Conrad, M. E., Tang, Y. J., & Alvarez-Cohen, L. (2014). Incomplete Wood–Ljungdahl pathway facilitates one-carbon metabolism in organohalide-respiring *Dehalococcoides mccartyi*. Proceedings of the National Academy of Sciences, 111(17), 6419-6424.

Zimmermann, M., Mayr, M., Bouffard, D., Eugster, W., Steinsberger, T., Wehrli, B., Brand, A., & Bürgmann, H. (2019). Lake overturn as a key driver for methane oxidation. bioRxiv, 10.1101/689182.

Acknowledgements

First of all, I would like to express my special thanks to Wolfgang Streit and Hans-Peter Grossart for their great supervision and constant support during my work.

I would also like to thank all my colleagues of the RTG2530 for the great teamwork and fun time we had together. In this regard, I would like to especially thank Kai Jensen, who always found a pragmatic solution to any problems that occurred.

Further, I want to thank my dearest colleagues of the AG Streit. You contributed to a positive and enjoyable working atmosphere and a memorable time.

Finally, I would like to thank my family and friends. In particular, my parents, brothers and Peter for their emotional support and constant encouragement.

Eidesstattliche Versicherung

Hiermit versichere ich an Eides statt, die vorliegende Dissertationsschrift selbst verfasst und keine anderen als die angegebenen Hilfsmittel und Quellen benutzt zu haben.

Sofern im Zuge der Erstellung der vorliegenden Dissertationsschrift generative Künstliche Intelligenz (gKI) basierte elektronische Hilfsmittel verwendet wurden, versichere ich, dass meine eigene Leistung im Vordergrund stand und dass eine vollständige Dokumentation aller verwendeten Hilfsmittel gemäß der Guten wissenschaftlichen Praxis vorliegt. Ich trage die Verantwortung für eventuell durch die gKI generierte fehlerhafte oder verzerrte Inhalte, fehlerhafte Referenzen, Verstöße gegen das Datenschutz- und Urheberrecht oder Plagiate.

Affidavit

I hereby declare and affirm that this doctoral dissertation is my own work and that I have not used any aids and sources other than those indicated.

If electronic resources based on generative artificial intelligence (gAI) were used in the course of writing this dissertation, I confirm that my own work was the main and value-adding contribution and that complete documentation of all resources used is available in accordance with good scientific practice. I am responsible for any erroneous or distorted content, incorrect references, violations of data protection and copyright law or plagiarism that may have been generated by the gAI.

Hamburg, 20.09.2024

Clara Luise Grüterich